MTR-7255

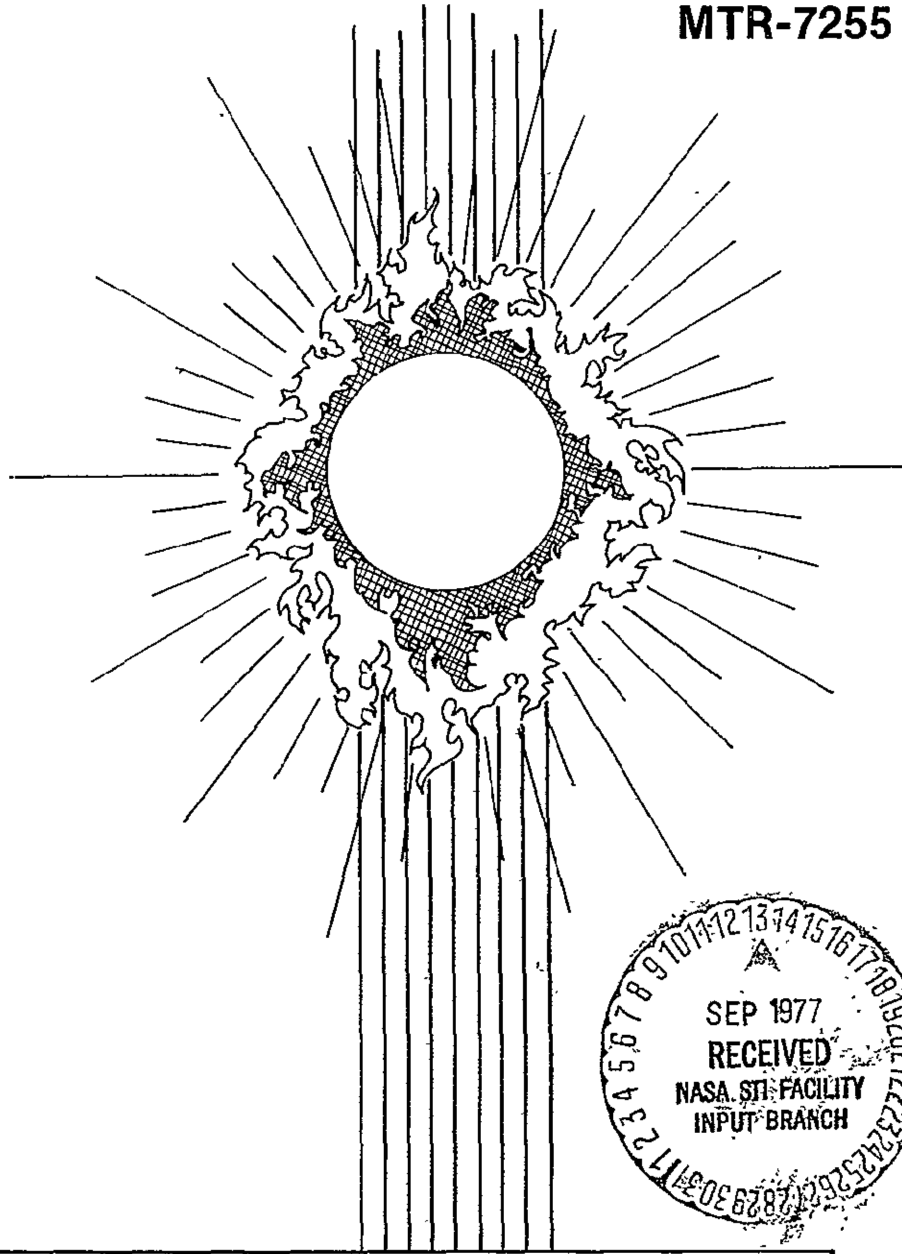

IN SITU PERFORMANCE MEASUREMENTS OF THE MITRE PHOTOVOLTAIC ARRAY

THE MITRE CORPORATION

AUGUST 1976

MTR-7255

IN SITU PERFORMANCE MEASUREMENTS OF THE MITRE PHOTOVOLTAIC ARRAY

A.S. Cherdak
Dr. G.M. Haas

Contract Sponsor: Jet Propulsion Laboratory
Contract Number: ERDA/JPL No. 954342
NASA Contract NAS 7-100
Project Number: 0620
Dept: W50

AUGUST 1976

MITRE Department
and Project Approval: ______________________

Richard S. Greeley
Technical Director
Energy Resources and

ABSTRACT

This report contains information prepared by The MITRE Corporation under Jet Propulsion Laboratory subcontract. Its content is not necessarily endorsed by the Jet Propulsion Laboratory, California Institute of Technology, or the National Aeronautics and Space Administration.

TABLE OF CONTENTS

LIST OF ILLUSTRATIONS

LIST OF TABLES

LIST OF TABLES
(Concluded)

EXECUTIVE SUMMARY

In 1974, The MITRE Corporation purchased a one-kilowatt photovoltaic array consisting of twenty 50-watt panels. During and after the first year of exposure to the environment, a variety of changes were noticed in many of the panels. MITRE, funded by the Jet Propulsion Laboratory, undertook to investigate these apparently degraded panels during the first quarter of 1976. A data acquisition system was designed and fabricated to make in-situ performance measurements of the panels and their constituent modules.

Current-voltage (I-V) curves measured in this program show that most of the panels now have lower power output and lower fill factors than their original ratings. Visual observations show significant deterioration of the packaging materials.

The Data Acquisition System

A system was designed and installed at MITRE to make in situ analog recordings of current and voltage measurements of the individual solar panels. It was felt that this approach would provide insight into the problem of making performance measurements in larger scale ERDA pilot and demonstration systems to be built in the future.

Table S-1 lists the data items measured for each of the 170 modules and panels in the array. Figure S-1 shows a functional block diagram of the system as configured. Figure S-2 shows a plot of available test time throughout the year. A minimum "window" of 1.5 hours exists if a minimum insolation level of 85 mW/cm^2 (100 mW/cm^2

TABLE S-1
DATA ITEMS

1. I-V Characteristic Curve
2. Solar Panel/Module Short Circuit Current
3. Solar Panel/Module Open Circuit Voltage
4. Panel Temperature
5. Standard Solar Cell Plot
6. Standard Solar Cell Short Circuit Currents (3)
7. Standard Solar Cell Temperature
8. Diffuse Illumination Value
9. Time of Day

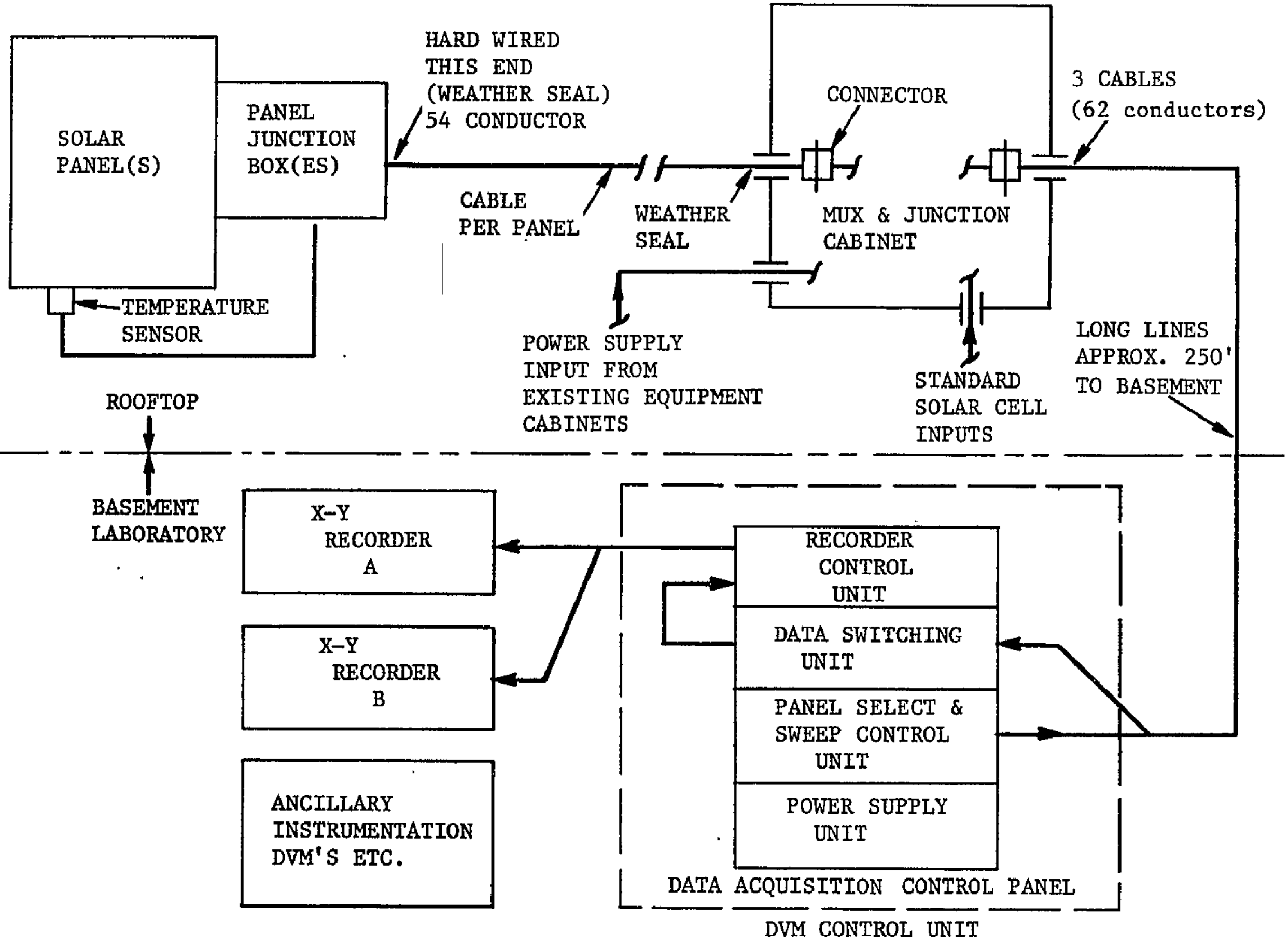

FIGURE S-1
FUNCTIONAL BLOCK DIAGRAM
SOLAR PANEL DATA ACQUISITION SYSTEM

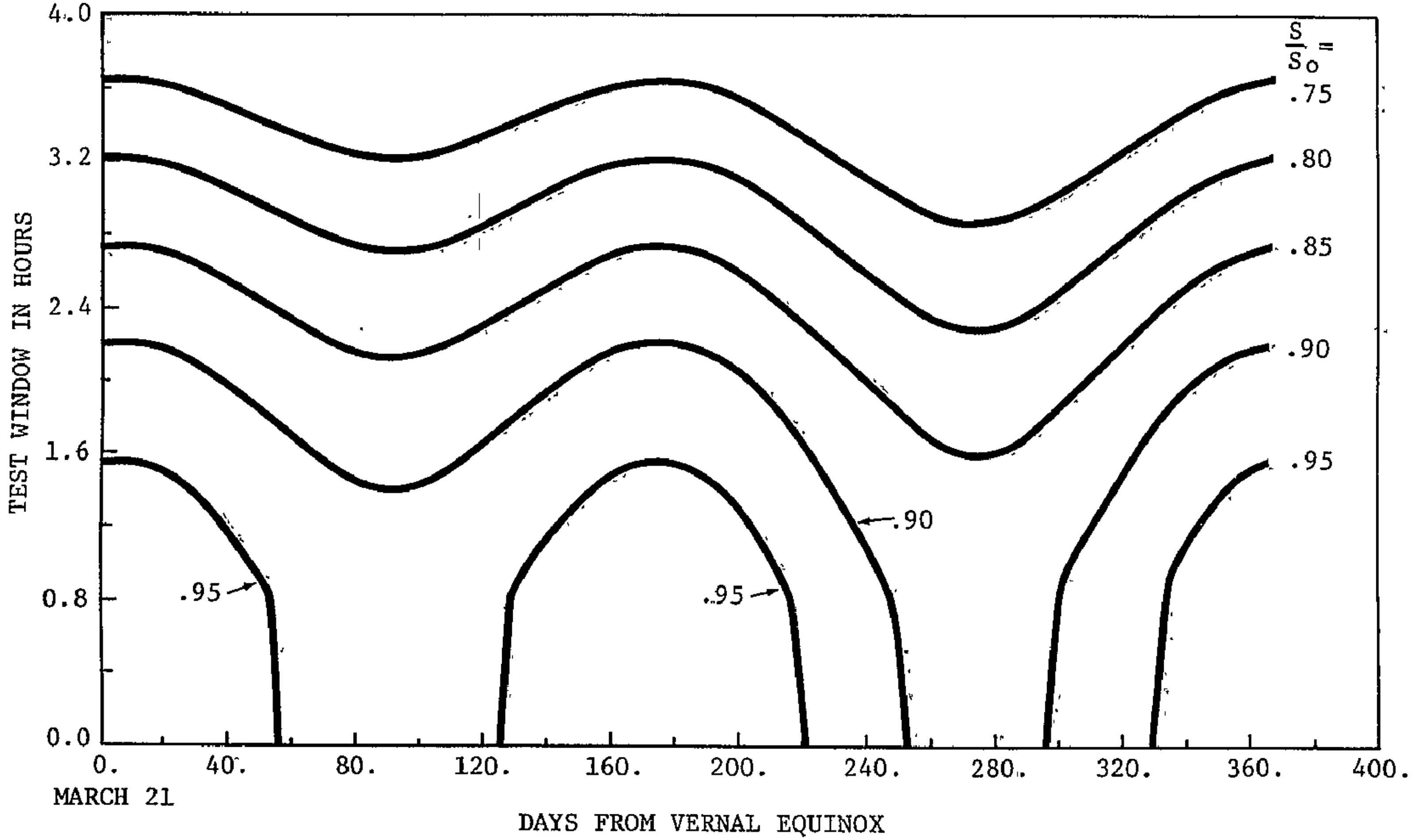

FIGURE S-2
MITRE SOLAR PANEL TEST WINDOW VS. TIME OF YEAR

taken as the maximum at solar noon) is required for accurate measurements. For the analog recording method chosen, five clear days were required to perform all the planned measurements.

An error analysis was made for the system and showed a maximum error range of +3.5 to -4.7 percent for absolute determination of the maximum power value of a solar panel or module.

Test Plan

A module or panel to be measured was selected in the laboratory and the resulting signals sent to the Multiplexor (MUX) on the roof. The MUX switched to the appropriate panel and transmitted the necessary signals to the laboratory for recording. Illumination was measured by pyranometer and standard solar cells in an assembly mounted on the roof in proximity to the array. This assembly was installed on the morning of the test day and removed when the test window elapsed.

The condition of most of the MITRE solar panels at the outset of the program was such that the usual techniques for I-V curve manipulation were not applicable. Deterioration of the panels led to very poor fill factors such that the measured I-V curves were far below normal. As a result, a qualitative approach to data analysis was adopted. The parameter of interest was the curve shape in the vicinity of the maximum power (Pmax) point of the I-V characteristic. By overlaying I-V curves taken from the same panel at different times, a qualitative understanding of changes is obtained.

Test Results

Table S-2 presents a comparison of original panel ratings and corrected data measured to date in this program. Because of the poor curve shape, accurate corrections cannot be made. However, the values in the table were derived based upon only small differences between the standard 100 mW/cm^2 and the observed conditions. Temperature corrections at the Pmax point were made on the basis of 0.5 percent per degree C. which should provide a conservative estimate.

- The power values are lower than those originally specified by the manufacturer, with the amount of change depending upon the specific manufacturer. This appears to represent a systematic difference and could be due to illumination measurement technique; to the temperature measurement technique or to the manufacturers quoting nominal data rather than measured power levels. It could also indicate some change in all panels due to weathering. Only further investigation can establish the nature of the difference.

- The difference between original specification and results obtained now is much larger for the Solarex panels than for any of the others and is considerably beyond anything that can be accounted for by variations in illumination or temperature effects. One must then conclude that these panels have exhibited substantial electrical performance degradation since their installation.

TABLE S-2

SOLAR PANEL POWER VALUES

Manufacturer	Manufacturer's Rating at 28°C, 100 mW/cm^2	Corrected, Measured Value 28°C, 100 mW/cm^2	Encapsulation
Solarex	50 watts 3/18/74	31 watts (average of 11 panels)	Silicone
Solar Power	52.5 watts 12/29/75	38 watts (single panel)	Silicone
Spectrolab	50 watts 1/25/74	38 watts (single panel)	Lexan/ silicone
OCLI	46.2 watts 1/23/74	45 watts (single panel)	Glass

- The results on the Solar Power panel are surprising, since this panel had only been installed about two months prior to measurement. The curve shape appears satisfactory, even though the maximum power is reduced. An I-V curve for this panel is shown in Figure S-3. The discontinuities in the curve result from inclusion of bypass diodes within the panel to preclude module voltage reversal during test.

- In general, the terrestrial cell panels which have been exposed to the weather for about two years show significantly lower fill factors than would be desirable. The panels with spacecraft-type cells show fill-factors which one would expect normally and are consistent with past measurements. Figure S-4 shows a typical I-V curve exhibiting a fill factor of 0.409.

- Sweeping an I-V curve of a full panel containing mismatched modules has caused the lower current modules to reverse in voltage. Figure S-5 shows two such curves for a pair of series-connected modules. Series-parallel interconnection of a number of modules would, of course, tend to reduce the voltage reversal problem as would inclusion of bypass diodes. However, the curve shape and short-circuit current variabilities still exist.

Conclusions on the Test Methods

- The analog recording approach taken in this program yielded adequate results for comparative data but not necessarily for absolute data.

- At the onset of this program, most of the solar panels in the MITRE array were apparently degraded beyond the point where conventional I-V curve shifting techniques are applicable. This necessitated a qualitative rather than quantitative assessment of performance changes over time. As far as can be determined, techniques for I-V curve shifting of poor solar panel characteristics have never been developed. Hopefully, the quality levels of products to come will eliminate the need for such tools in the future.

- Relative optical/spectral performance of illumination measurement standards was of concern here. Of the standards considered, the broadband, precision pyranometer was concluded to be the best available at this time.

- Visual inspection may be an effective adjunct to electrical performance measurement of terrestrial solar arrays. Photographic records offer advantages of comprehensive, permanent records which will not suffer inaccuracy due to inspector fatigue or discomfort.

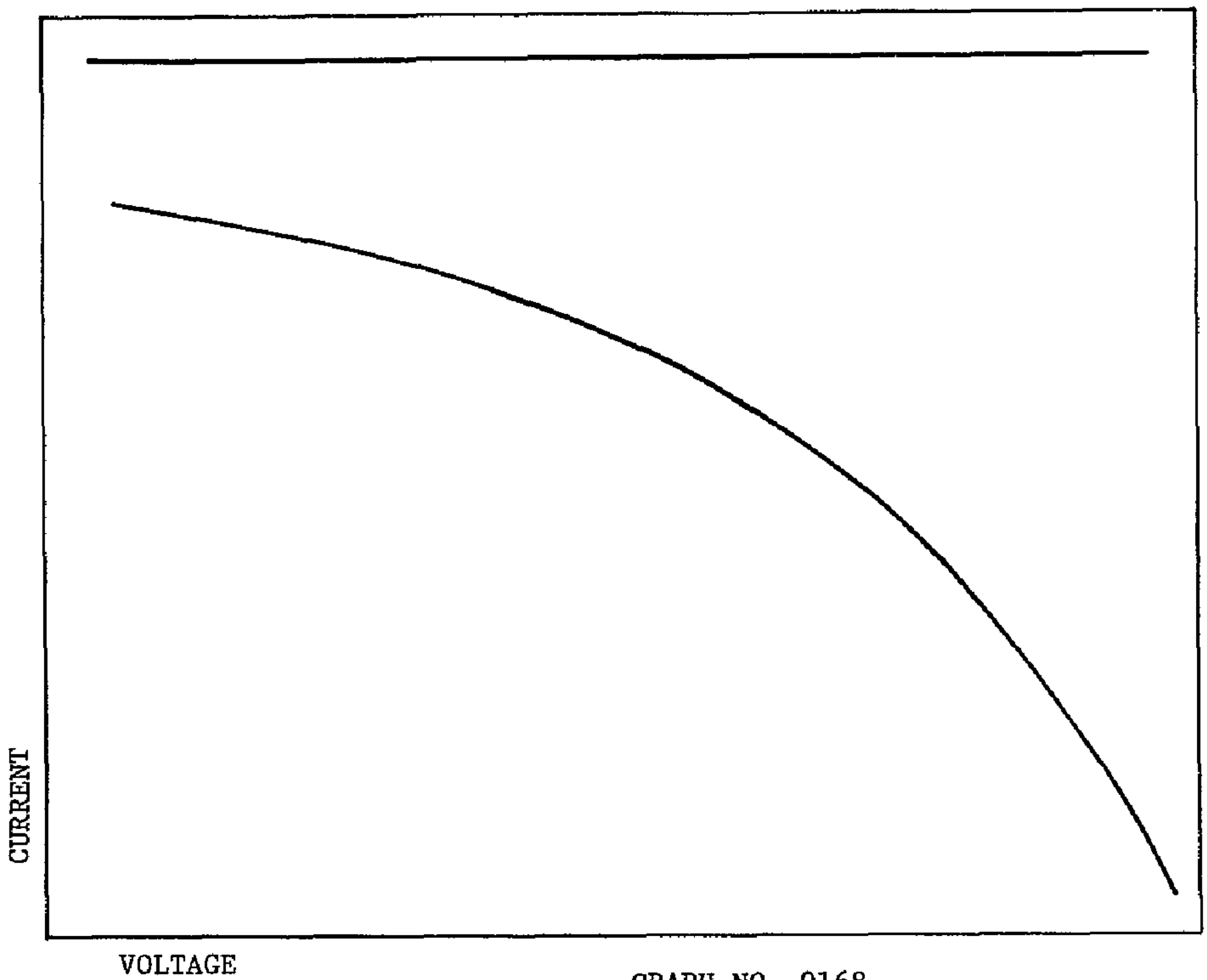

GRAPH NO. 0168
PANEL 16 MODULE 1
DATE 4/19/76

FIGURE S-3
TYPICAL I-V CURVE EXHIBITING A FILL FACTOR OF 0.409

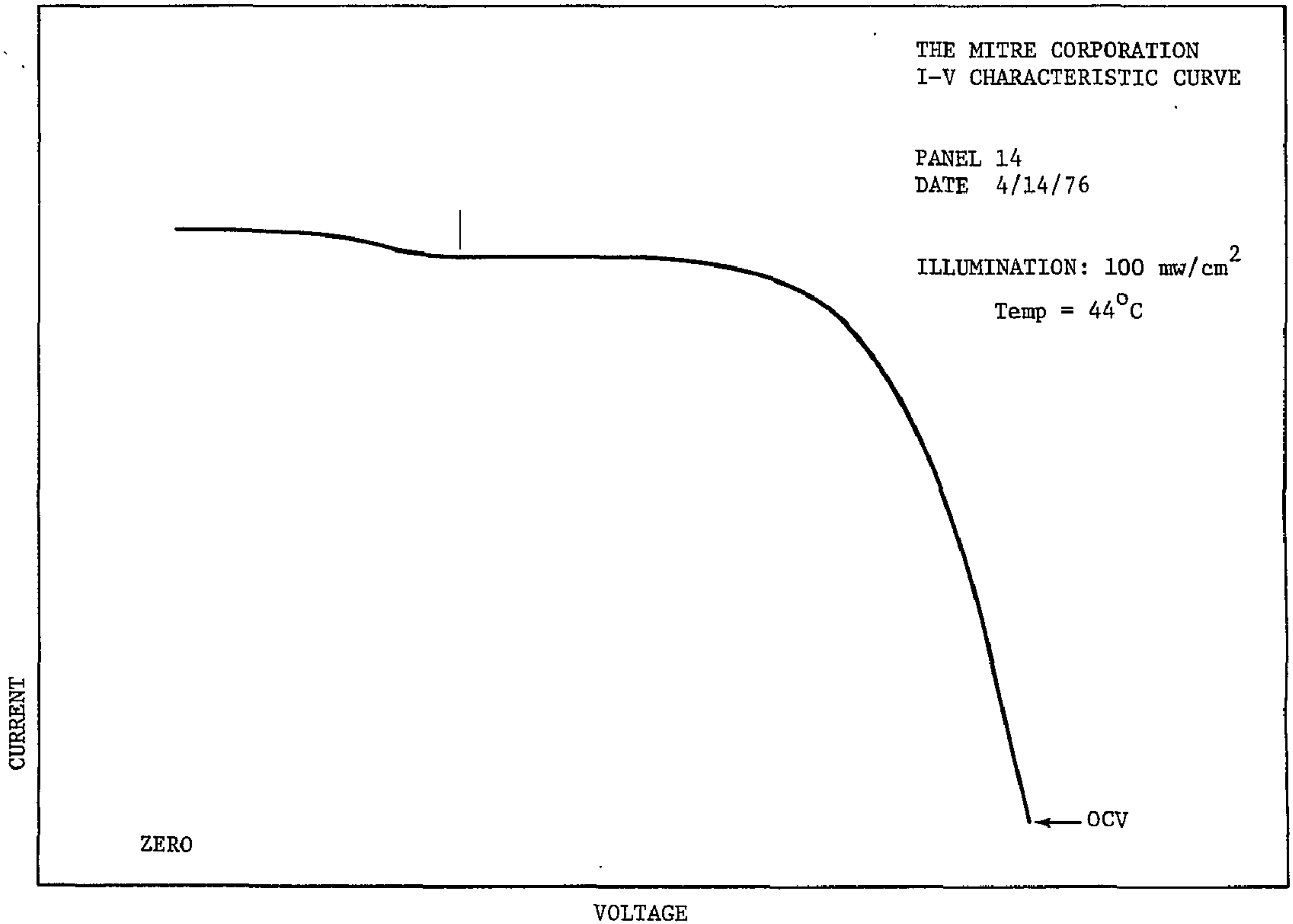

FIGURE S-4
I-V CURVE FOR PANEL 14 WITH VOLTAGE REVERSAL PROTECTION DIODES

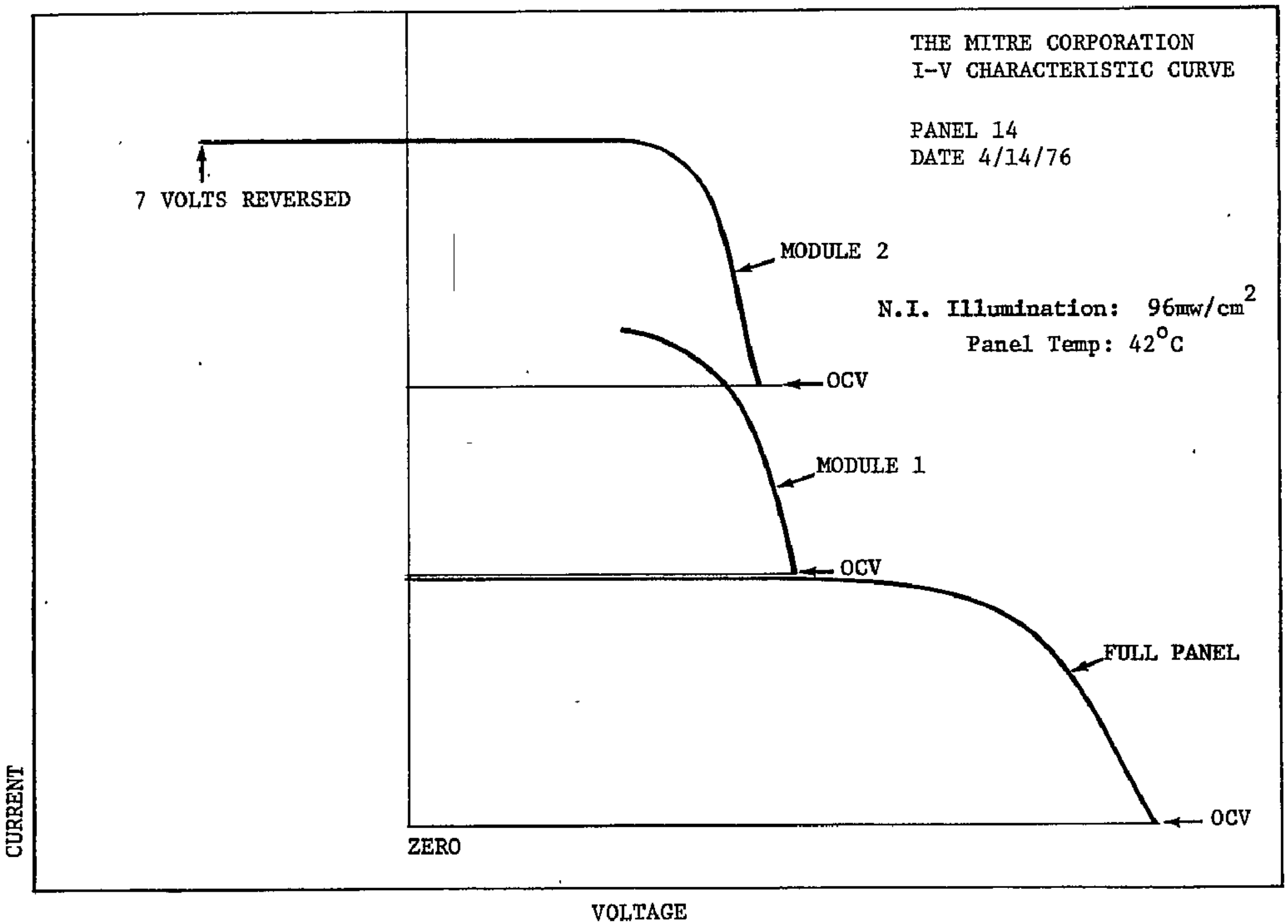

FIGURE S-5
I-V CURVES FOR SERIES CONNECTED, MISMATCHED MODULES

Conclusions Concerning the Solar Panels

- Solar panels of "terrestrial" cell composition have displayed very low-fill factors of the order of 0.5 and less. Earlier measurements indicate that these fill factors have undergone changes over the two-year period of environmental exposure. Panels of "spacecraft type" cells do not appear to have undergone any significant changes in this regard.

- Extensive packaging deterioration has occurred which may be responsible for the performance changes noted above. This deterioration is evidenced by delamination, entrapped moisture, corrosion of cell contacts, and apparent erosion of potting material surfaces. In addition, glass-epoxy substrates have begun to degrade. The epoxy binder at the surface of the material has been leached away by the weather and glass fibers are unravelling due to constant exposure to wind.

- Large variability in curve shape and in short circuit currents has been observed among most identically-rated panels made by the same manufacturer, as well as among similarly-rated panels made by different manufacturers. Economics may not permit more careful selection of panels and modules or application of diode bypass techniques for series electrical operation. However, this should be of concern to those who wish to design large arrays in the future.

- In addition, if such variability exists at the module level, greater variability might exist among cells within modules. This has serious ramifications in reliability considerations and in array economics in that module lifetime may be less than planned due to accompanying stresses.

1.0 INTRODUCTION

In 1974, the MITRE Corporation purchased, and installed on the roof of its building in McLean, Virginia, as part of an IR&D program, a 1-kilowatt peak photovoltaic array consisting of 20, 50-watt panels. These solar panels represented the state-of-the-art in terrestrial photovoltaics at the time. The primary purpose for establishing the MITRE photovoltaic array was to build a tool with which problems of designing, integrating, and operating photovoltaic power systems for terrestrial applications could be studied.

In view of the intended thrust of this program, little attention was paid initially to monitoring the array itself. During and after the first year of exposure to the environment, a variety of changes were noticed. Over four percent of the 136 modules of one type of panel had become open circuited, there were apparent decreases in short circuit currents, and fill factors* for some panels and modules had fallen as low as 0.46.

In August of 1975, a proposal was made to ERDA through the Jet Propulsion Laboratories (JPL) to make a more thorough investigation of these apparently degraded panels. MITRE provided a sample of a degraded module to JPL for detailed analysis. Under contract to JPL, MITRE proceeded to fabricate and install a data acquisition system to provide more accurate and consistent measurements of the 170 panels and modules in the array. An additional purpose for this program was to evolve some techniques for in situ measurement of photovoltaic panels of sufficient quality to permit evaluation of electrical performance over extended periods of several years or more.

---

*The fill factor is defined as the maximum panel output power divided by the product of open circuit voltage and short circuit current from the panel.

2.0 THE DATA ACQUISITION SYSTEM

2.1 Measurement Considerations

Because of the large number of measurements to be made and the desire on the part of MITRE to continue operating its Photovoltaic Demonstration System, it was concluded that all performance measurements would be made in situ. This approach would also provide some insight into the problems and technology involved in making in situ measurements which we feel is or will be of interest to the ERDA Photovoltaic Program as larger scale demonstration and testing programs get under way in the coming months and years.

The MITRE Solar Array consists of 20 panels from four manufacturers. Seventeen panels consist of eight modules of solar cells and one panel from each of three manufacturers has a variety of module structures. For uniformity, it was decided to provide facilities for measurement of eight modules per panel plus measurement of the full panel, although some panels had fewer than eight modules. This, then, resulted in a total of 170 I-V characteristics to be measured three or four times in the course of the year.

In order to determine the stability of performance of a photovoltaic array it is necessary to measure the current-voltage (I-V) characteristics of the array at several points over time and to carefully search these data for changes in electrical performance. Typically, solar panel I-V characteristics are measured under conditions of temperature and illumination which are as close to "standard" as possible. The resulting data are manipulated or "corrected" to bring them to standard, and comparisons are then made on a uniform basis. Data corrections must be as small as possible to minimize error in the results, since changes of no more than two or three percent in these short term data would indicate significant degradation in the solar array, over its lifetime.

Standard conditions of temperature and illumination for measurement of terrestrial photovoltaic arrays are generally accepted to be $28^{o}C \pm 2^{o}C$ and 100 mw/cm^2, respectively. These are most likely the conditions under which solar panel nameplate ratings are obtainable. They were adopted as the standard conditions for this program.

Measurements in the terrestrial environment are difficult to make at best due to ever changing weather conditions. Discussions with the Smithsonian Radiation Biology Laboratory, located only a few miles from MITRE, suggest that to get five good, clear days in our area will require a total time of 10 days at a minimum and 30-40 days, average. This depends, of course, upon the time of year. In addition, there is no consistency in the Washington, D. C., area from year-to-year. Indeed, five consecutive clear days are very rare.

On those rare clear days, it is desirable to make our I-V measurements as close to solar noon as possible and under conditions where clouds and haze offer minimal interference. An analysis was made to attempt to estimate the amount of testing time available in any single clear day. Neglecting diffuse radiation (which could amount to 20 percent additional illumination based upon measurements to date at MITRE) and considering only the direct solar radiation component, the equivalent, normally incident illumination on the MITRE solar panels was determined geometrically. Figure 1 shows the derivation of the angle between the panel normal and the solar vector. The normalized illumination intensity is given as the ratio of intensity on the panel surface to the intensity on a surface normally oriented to the solar vector and is equal to the cosine of θ. Assuming the solar vector intensity is 100 mw/cm^2 on a "good" day, the correction required in panel illumination is

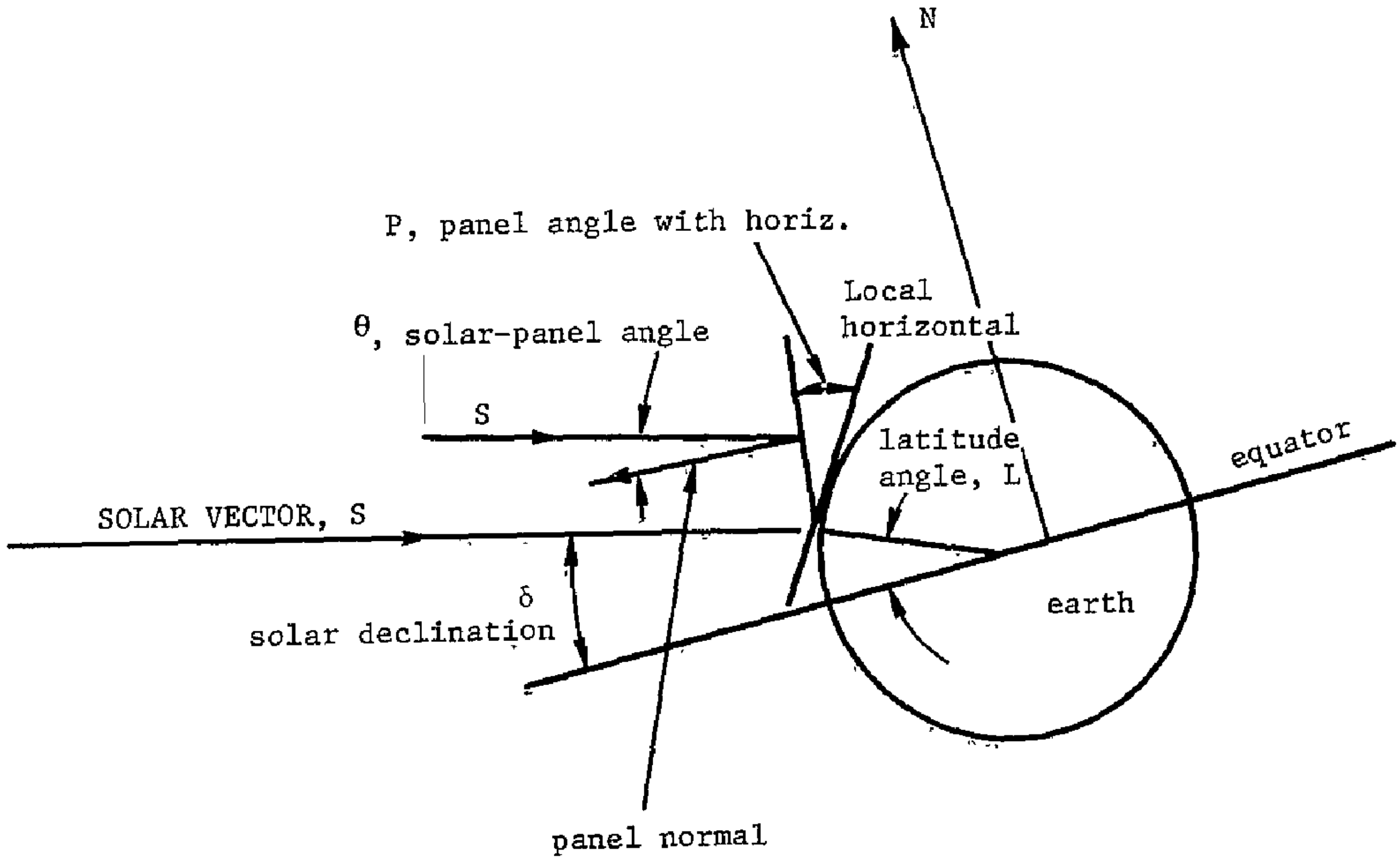

$$\theta = L - P - \delta$$

where $\delta = 23.5 \text{ Sin } \left(360. \frac{n}{365}\right)$

$n =$ number of days from vernal equinox

and $$\theta = L - P - 23.5 \text{ Sin } \left(\frac{360}{365} n\right) \text{ degrees.}$$

FIGURE 1
SOLAR VECTOR—PANEL ANGLE DETERMINATION

1./COSθ to bring the measured panel data to standard illumination conditions at solar noon.

At a time of day other than solar noon, an additional correction is required. The Earth's rotation causes the solar panel to rotate at a rate and through an angle identical with the Earth's. Figure 2 shows the derivation of illumination intensity variation due to this factor. The illumination intensity at solar noon was stated above as the cosine of the sun-panel angle at solar noon multiplied by So, the value of the solar vector. Making that substitution yields the expression for illumination intensity at a panel surface on any day at any time about solar noon as

$$S = So\ Cos\left[L-P-23.5^{o}Sin\ \left(\frac{360^{o}}{365}n\right)\right]Cos\ \left[90^{o}Sin\left(\frac{360^{o}}{24}t\right)\right]$$

The above expression was evaluated to determine the time periods about solar noon which would provide illumination intensities normal to the MITRE solar panels in excess of 75, 80, 85, 90 and 95 percent of the value of the solar vector. This period or Test Window is plotted in Figure 3.

From Figure 3 it is seen that the test windo- for 90 percent illumination drops to zero near day 250 and remains at zero until day 298 while the 85 percent illumination criterion yields at least an hour and a half at any time of year.

If the Solar Energy Laboratory computer was to be employed to measure solar panel I-V curves, all 170 sets of data could be measured in less than 30 minutes. However, the level of effort required to implement a computerized data acquisition system was found to be in

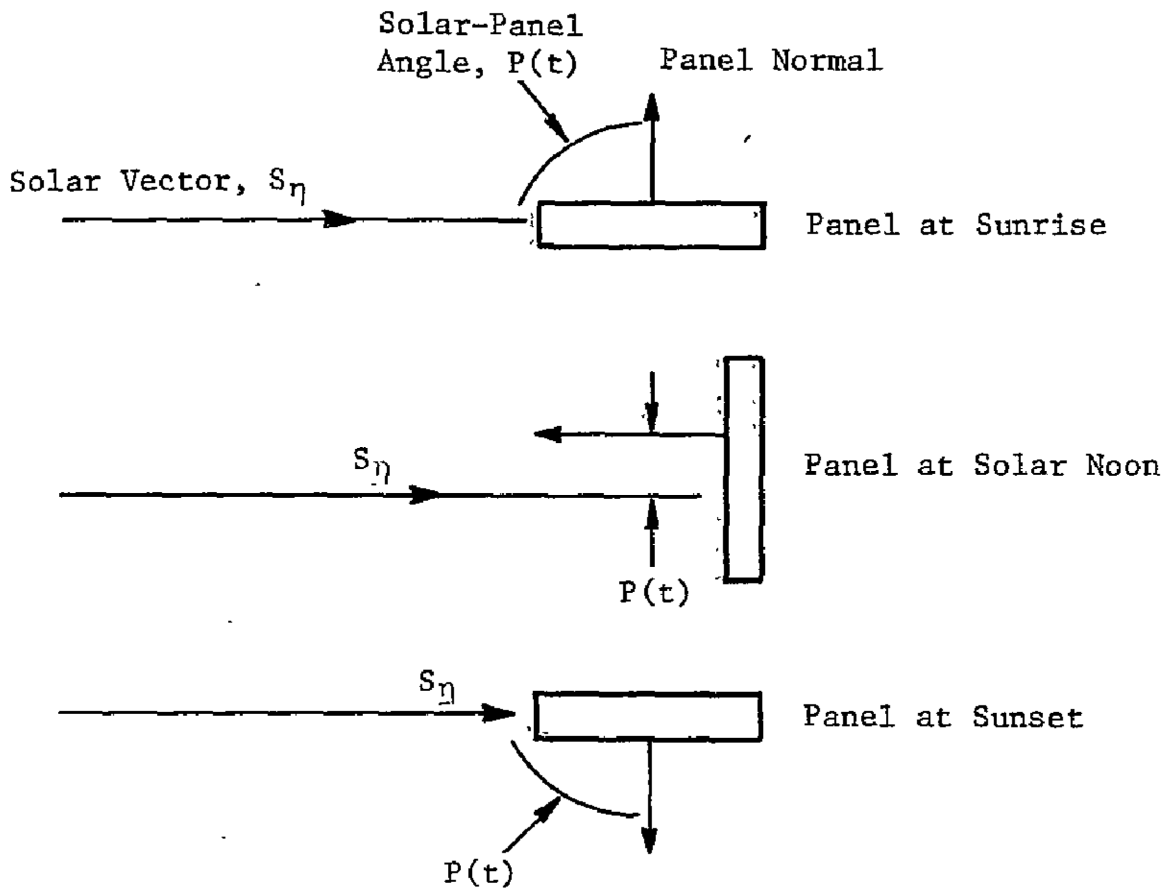

Projection of S_o on Solar Panel is

$S(t) = S_\eta \cos P(t)$

Where:

$P(t) = 90^\circ \sin\left(\frac{360t}{24}\right)$

t = time from solar noon

S_η = illumination intensity at solar noon

FIGURE 2
ILLUMINATION INTENSITY VARIATION WITH TIME OF DAY

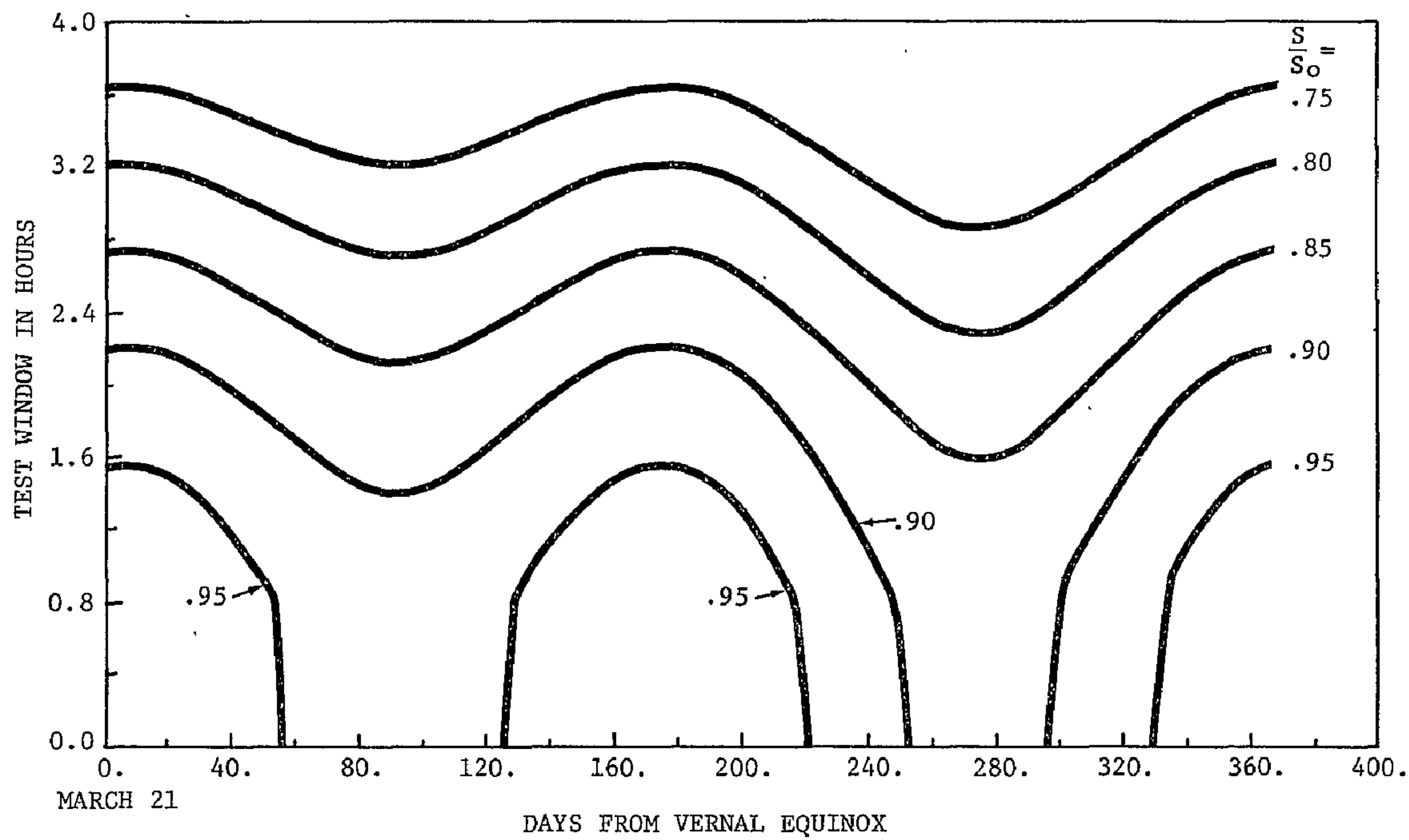

7

FIGURE 3
MITRE SOLAR PANEL TEST WINDOW VS. TIME OF YEAR

excess of both the MITRE Solar Laboratory and the JPL Program budgets at the time.

It would be desirable to make all 170 measurements in one test window to avoid variations in illumination, weather, and panel temperatures which might occur over a period of days or weeks. However, this does not seem possible without the computer or a fully automated system. The estimated time for measuring an I-V curve of a solar panel or module using an X-Y recorder is 2.5 minutes. This estimate is made assuming only a few seconds for switching instrumentation from panel to panel and for the actual I-V measurement. The bulk of the estimated time will be expended in changing recorder paper, zeroing the recorder pen(s), calibrating scales and measuring and recording data in support of the I-V curve. This corresponds with a total testing time of 7.1 hours for the 170 measurements. This, of course, does not include allowances for passing clouds and operator change-over. For a test window of 1.5 hours, a total of five days of clear weather would be required to perform the 170 sets of measurements. Additionally, manual data collection tasks would, of course, lengthen the entire procedure.

2.2 Data Types and Measurement Standards

Table I lists the data items to be recorded. The primary data item is the solar panel or module I-V characteristic curve. The remainder of the items are required to support analysis of the I-V characteristic.

TABLE I
DATA ITEMS

1. I-V Characteristic Curve
2. Solar Panel/Module Short Circuit Current
3. Solar Panel/Module Open Circuit Voltage
4. Panel Temperature
5. Standard Solar Cell Plot
6. Standard Solar Cell Short Circuit Currents (3)
7. Standard Solar Cell Temperature
8. Diffuse Illumination Value
9. Time of Day

The panel/module short circuit current and open circuit voltage are measured with a digital voltmeter to provide a more accurate and precise determination of these values than can be obtained with the X-Y recorders alone. Although the recorders will provide curve shape information, the DVM readings, together with the I-V plot, will enable more accurate determination of solar panel/module output power at any point on its I-V characteristic.

Solar panel temperature is necessary for purposes of shifting the resulting I-V characteristics to standard conditions of temperature and illumination in order to make the desired performance comparisons.

Standard solar cell and pyranometer data are commonly taken with I-V characteristics to provide a measure of illumination intensity. This is done here as well using three JPL Balloon Calibrated Standards and an Eppley Precision Pyranometer. We have introduced an additional measurement method. The pyranometer output is recorded in real time together with the I-V characteristic in order to provide for corrections of the characteristic for variations of illumination intensity which could occur during the I-V sweep. In order to expedite measurement of the large number of I-V characteristics required, it may be necessary to attempt data measurement on partially cloudy or hazy days or on days when high altitude winds and turbulence create rapidly varying illumination or spectral content levels at the solar panel locations. In cases such as this, we have observed on numerous occasions as much as 10-50 percent variation in illumination intensity in just a few seconds, the time required for an I-V sweep. These variations have occurred suddenly after many minutes of stable illumination levels (i.e - we equate stability with less than 0.5 percent of full scale variation in pyranometer output). These changes have been observed with a pyranometer and digital voltmeter as well as a chart recorder and appear to be smooth in transition without any jumps or discontinuities in the time scale used.

The pyranometer plot is made on the same graph sheet as the I-V characteristic using a two-pen X-Y plotter. In this way, the pyranometer output is plotted directly against panel or module voltage. Panel/module current and pyranometer/illumination intensity data pairs may then be read directly from a single graph for the correction process.

Standard cell temperature is measured and recorded with each set of measurements to provide a basis for correcting for standard cell temperature coefficients. This is necessary due to lack at this time of control means for standard cell temperature. Pyranometer temperature is considered to be the same as the standard cell temperature due to their physical proximity.

The pyranometer and the standard cells were not permanently installed on the roof in order to protect them (the cells) from adverse weather. They were mounted on the roof in the morning of the test day and removed after the test window had elapsed.

Selection of the JPL standard cells for illumination measurements was made primarily because these cells have become well established in the spacecraft industry as accurate, stable standards. A terrestrial standard cell was received from NASA-LERC but due to collimation requirements was not well suited for inclusion as a test standard in the present facility.

A point of concern which remains unresolved is the relative optical/spectral performance of the standards and the test panels. This yields some uncertainty as to the effects of shifting atmospheric conditions upon panel and standard cell indications. Although in theory a test could be devised to determine such relative behavior, it does not seem likely that the wide variety of test articles could be adequately matched or otherwise readily characterized. Furthermore, it is not at all certain that a match or characterization could be assumed constant over the environmental extremes to be encountered and for the duration of the test. A possible resolution of the concern about spectral response might be the inclusion of some sort of spectral recording device within the instrumentation complement in the future in order to add this additional dimension to these resulting data. Measurements are made of total and diffuse components of illumination which may provide at least a qualitative insight into spectral content and its effects. This is done using the Precision Pyranometer and a motor-driven shadow mask. The mask is positioned at the beginning of the test window and is repositioned as necessary throughout the test period.

2.3 System Configuration

The system configuration devised was one which would bring us as close to a fully automated system as possible without making the substantial initial expenditure of funds required to implement computer control. A functional block diagram is shown in Figure 4. Several major decisions were made leading to this particular configuration: (1) All panel measurements were 4 terminal measurements with terminals located physically as close to the solar panels as possible. (2) Transducer scale factors were as large as practical to minimize the need for amplification and its attendant problems between the transducer and the recorders. (3) If possible, all measurement operations were performed in the

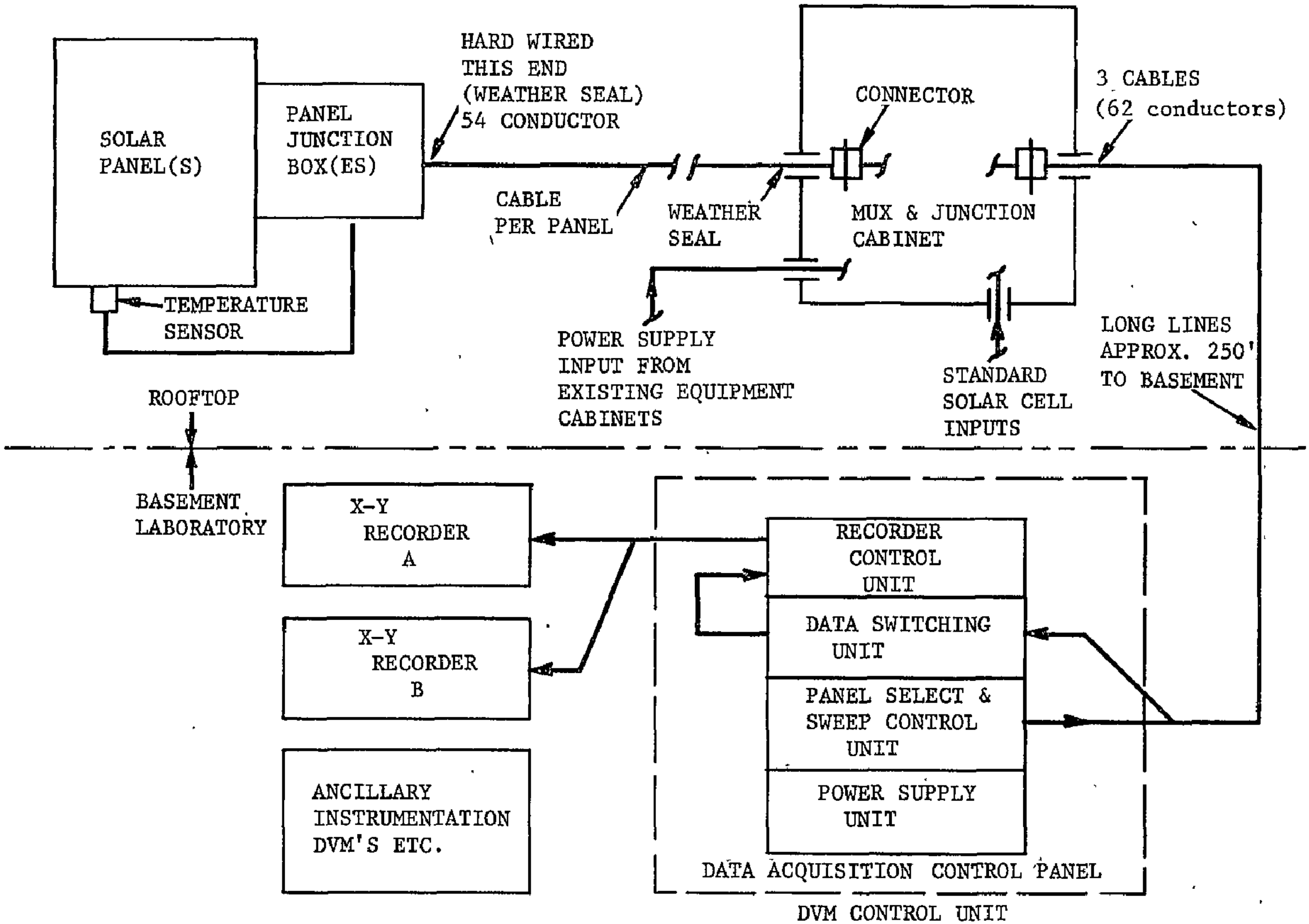

FIGURE 4
FUNCTIONAL BLOCK DIAGRAM
SOLAR PANEL DATA ACQUISITION SYSTEM

sheltered laboratory to avoid the need for deploying laboratory personnel and sensitive recording equipment to the roof in the cold winter weather. (4) The resulting system must be expandable to handle additional solar panels and must be adaptable to computer control.

In addition to serving as test articles, the solar panels must also be a part of the MITRE Photovoltaics Demonstration System when not under test. Therefore, test instrumentation which by our own ground rules may not be applied and removed for each test must offer negligible interference with the normal functioning of the panels.

Parameters to be measured include panel and module voltages, currents, and temperature. Voltage measurements with a high impedance detector offer no interference with normal functions which is also the case for temperature measurement by thermistor. Current measurements on the other hand could significantly interfere with the panel's normal function due to insertion effects of current measuring apparatus. Initially, magnetic current sensing devices offering no insertion effects for normal panel operation were considered. Based upon comparisons of accuracy, cost and size, these were dropped from consideration in favor of manganin meter shunts. Measurements of panel and module currents using meter shunts and their resulting low signal voltages were made over the 250 cable-feet between the roof and the basement laboratory to determine what, if any, noise problems might exist. DC voltages of one millivolt level were transmitted through the roof-lab cables with no apparent difficulties providing normal shielding precautions were taken.

Table II presents a comparison of parameters for these two techniques. The shunt approach will result in an addition of 0.005 ohms equivalent series resistance to an eight module panel with the shunts left in the circuit during normal operation. This is

TABLE II
CURRENT SENSOR COMPARISON

PARAMETER		MANGANIN METER SHUNT	MAGNETIC CURRENT SENSOR
1. Accuracy*:	initial accuracy plus temperature effects for range of $-20^{\circ}C$ to $+50^{\circ}C$	$\pm 0.3\%$	$\pm 3.8\%$
2. Cost:	in the quantity required, 150 current measurement points	\$6-\$7 ea.	\$80.-\$90. ea.
3. Size:	(approx.)	2" x 1¼" x 1.7" ea.	2" x 2½" x 3" ea.
4. Insertion Resistance:	per measurement point	0.01Ω	none
5. Power Requirements:		None other than insertion loss.	0.5 to 1.4 watts per measurement point.

*Calibration requirements over service life must also be considered.

approximately equivalent to less than a 0.005% reduction of voltage at the panel maximum power point. This will be substantially smaller than the uncertainty in measurement of the maximum power point which is expected to be of the order of one-to-two percent. In any event, the criticality of absolute measurement of the panel I-V curve is low for purposes of assessing panel stability overtime. What is required is stability of the insertion effect which will be achieved to a high degree with the manganin shunt.

A single thermistor is specified for measurement of panel temperature. It would be more desirable to use several thermistors per panel and develop some sort of average reading; however, other factors in the system such as existing cable size and cost and availability of additional data switching circuits preclude this. The thermistor is located at a point which will provide a typical indication of temperature.

The thermistor selected will have a value of 30.00 K ohms at 25°C $\pm$ 0.2°C and a resistance of 10.97 K ohms at 50°C $\pm$ 0.2°C. The thermistor resistance will be measured using a digital ohmmeter in the basement laboratory in series with approximately 500 feet of 22 gauge copper wire. The wire will have a 20°C resistance of approximately 8 ohms (15.14 ohms per 1000 ft.) which, at the highest temperature anticipated to be measured (50°C), corresponds with an error of about 0.02°C, this is only ten percent of the thermistor's inherent inaccuracy, at that temperature. About 200 feet of the roof-lab cable is located within the building, thereby tending to stabilize the cable resistance over the seasonal temperature range.

Manufacturer's data for the shunts and thermistors are included in Appendix I. Figure 5 shows a schematic diagram of an eight

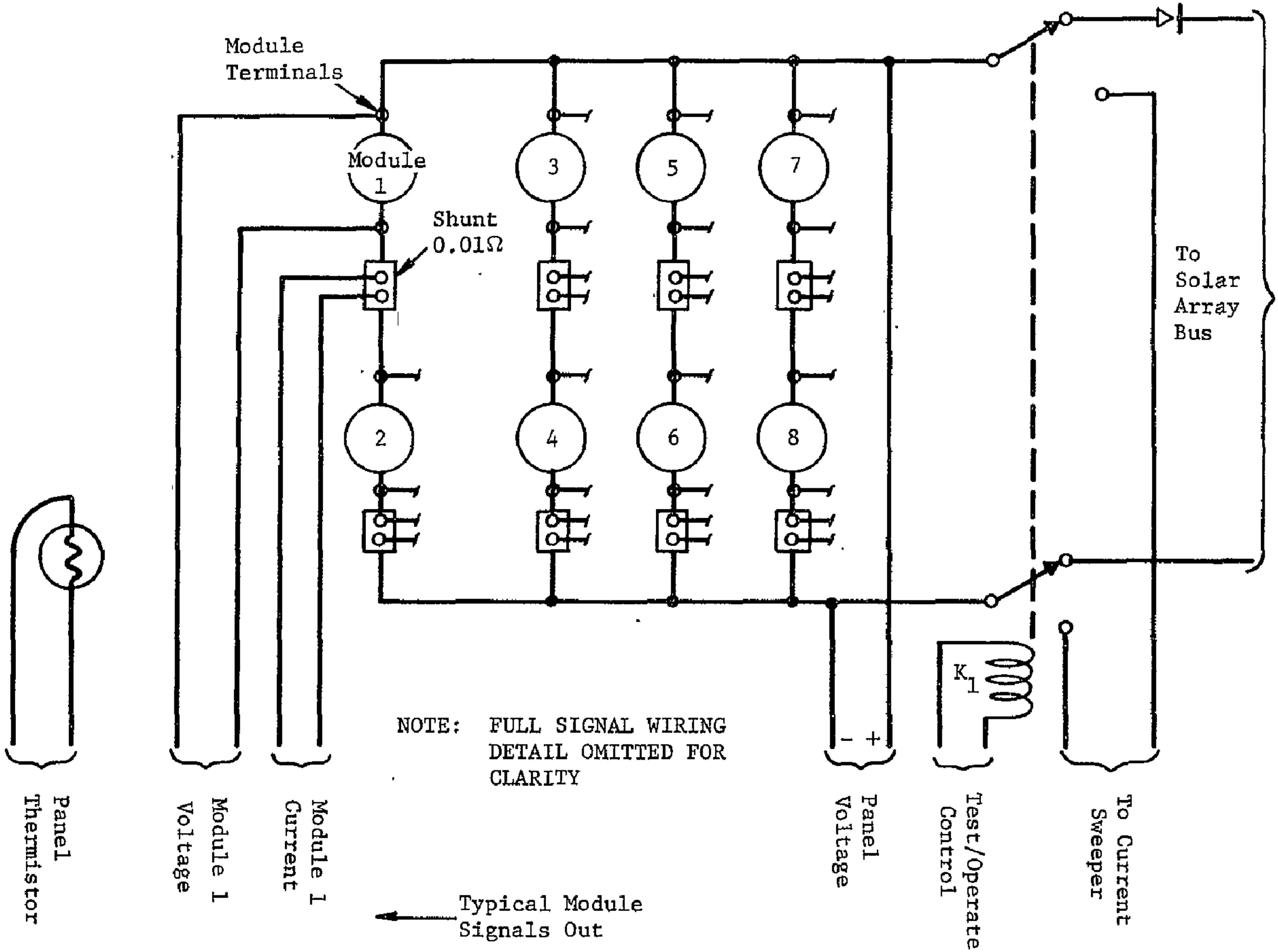

FIGURE 5
SCHEMATIC DIAGRAM OF AN EIGHT-MODULE SOLAR PANEL ASSEMBLY AS INSTRUMENTED

module solar panel as instrumented. Figure 6 shows several photographs of the panel, its associated junction box and the thermistor installation.

All solar panels are connected to the Multiplex (MUX) Junction Cabinet through 54 conductor, #22AWG cables. Thirty-eight conductors are used for signals and control with the remainder paralleled for connection to the panel current sweeper. Within the MUX cabinet, wiring from each panel is connected to one position of a stepping switch bank. The bank is composed of four 26 position by twelve level stepping switches which, together constitute a 48 pole, 26 position, remotely activated switch. Five poles are used for switch position control, 37 poles are used for panel data and control and six poles remain as spares.

Figure 7 shows a functional diagram of the panel selection circuits. The number of the panel to be tested is entered into two thumbwheel switches on the Panel Select and Sweep Control Unit. When this is complete and the ADVANCE switch is depressed (See Figure 8), the panel address in BCD format is transmitted to the selected address decoder and the stepping switch drive circuits in the MUX cabinet on the roof. The drive circuits sense the difference between the panel address delivered from the laboratory and the current stepping switch address and drive the stepping switches until this difference is eliminated for all four switches. When the switch and input addresses agree, a PANEL LOCATED signal is generated which enables transmission of the new switch (panel) address back to the SELECTED PANEL DISPLAY in the laboratory. This address signal is derived independently of the address sent to the roof in order to provide a more reliable indication in the laboratory.

Once a panel or module has been selected for test, it remains to manually record respective data items on a data sheet, load and

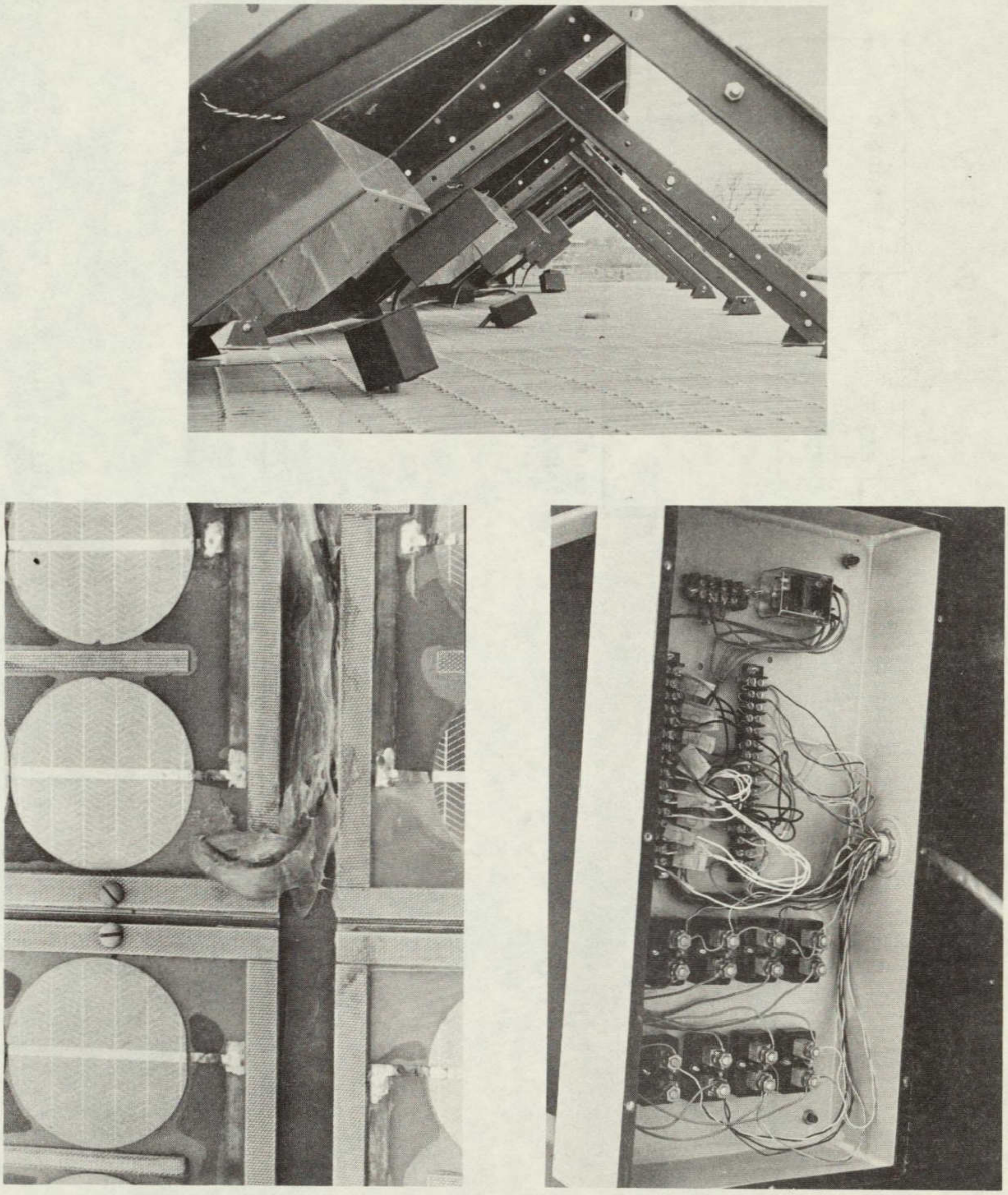

FIGURE 6
PHOTOGRAPHS OF A SOLAREX PANEL, JUNCTION BOX, AND THERMISTOR INSTALLATION

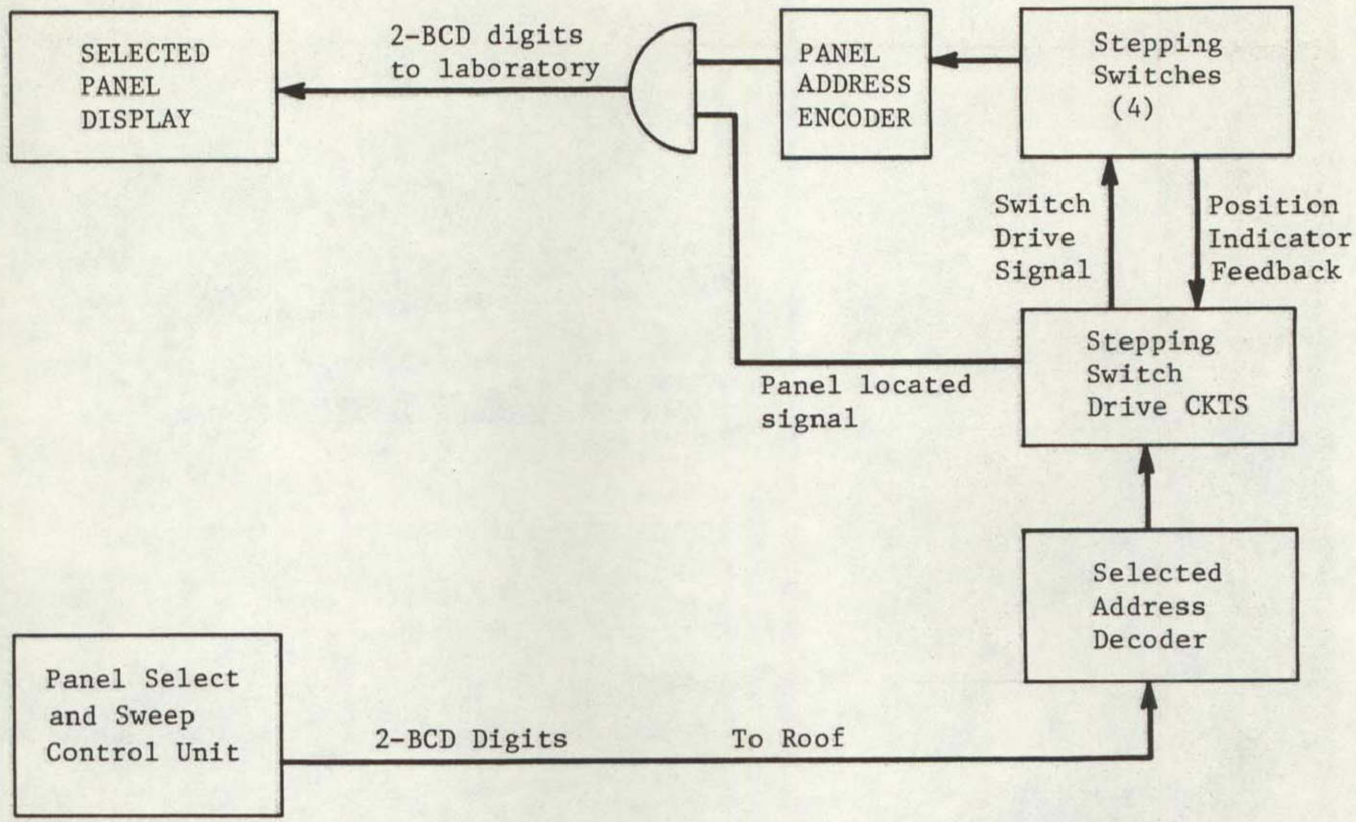

FIGURE 7
FUNCTIONAL DIAGRAM OF PANEL SELECTION CIRCUITS

ORIGINAL PAGE IS
OF POOR QUALITY

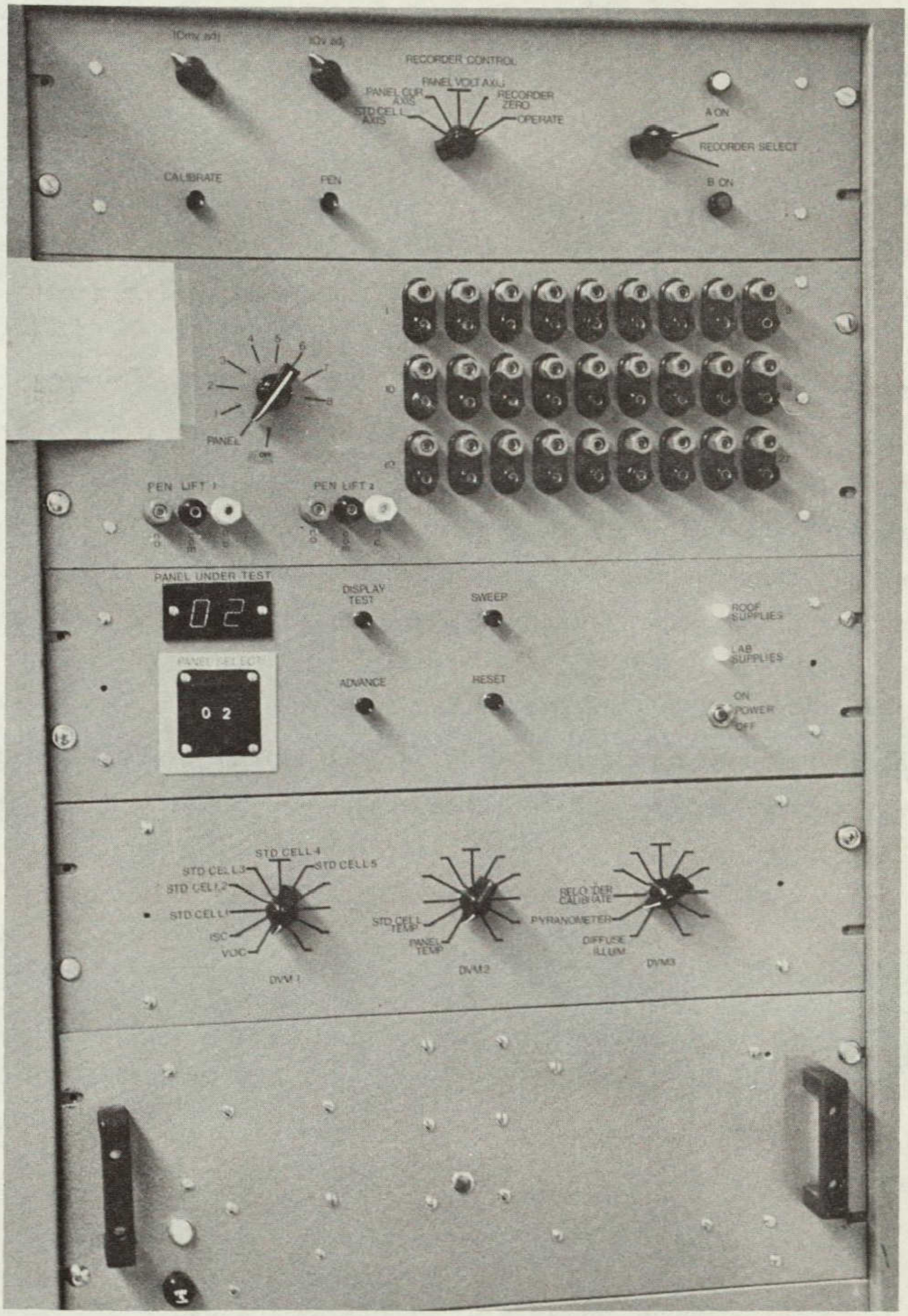

FIGURE 8
PHOTOGRAPH OF DATA ACQUISITION CONTROL PANEL

calibrate the X-Y recorder and sweep the I-V curve by depressing the sweep button (see Figure 8).

The sweeper consists of two assemblies: the ramp generator-recorder pen control located in the laboratory and the power sweep circuit located on the roof. In operation, the sequence of events is as follows: The recorder is poised at the panel open circuit voltage position with pen raised. When the SWEEP switch is depressed, the pen is dropped and a voltage ramp is started. The ramp is delivered to the roof where it is input to the power sweep circuit which follows the ramp sweeping the total panel from open circuit toward short circuit. Panel/module voltage and a voltage proportional to current from the sensing shunts are returned to the laboratory where they drive the X-Y recorder pen. After the panel has been driven to the vicinity of short circuit, the ramp generator saturates, the recorder pen is lifted and the sweep is concluded. A manual ramp reset to zero is included to permit recording short circuit current at the end of the sweep. An automatic reset may be obtained by throwing a switch located behind the panel. The automatic reset feature is not used during normal data taking operations.

2.4 System Error Analysis

This analysis is presented in its entirety in Appendix II. The calculations show a maximum error range of + 3.49 to - 4.68 percent in determining the value of maximum power from a solar panel module.

This error range consists of errors as follows:

(a) Error in determining a maximum power value from an I-V graph: ± 2 percent.

(b) Error due to temperature measurement tolerances:
$\pm$ 3.168 percent.

(c) Error due to illumination measurement tolerances:
$\pm$ 1.637 - 0.596 percent.

Temperature measurement is responsible for the major source of error. Uncertainty in knowledge of temperature distribution over the panel represents 80 percent of that uncertainty.

3.0 TEST PLAN

A test plan was written to organize the testing procedure and to serve as a guide during the actual measurement operations.

Of particular concern in preparing the plan was incorporation of some sort of test to verify that the data acquisition system would faithfully record in the laboratory the parameters of the panel or module being measured. A test was devised whereby two newly calibrated X-Y recorders were employed, one in the laboratory, one on the roof at the panel being measured and an I-V curve was recorded on both recorders simultaneously. The recorder inputs were paralleled using several spare conductors in the roof-laboratory cables and a calibration procedure was performed. The cables were disconnected and the rooftop recorder inputs were connected directly to the module being measured. The I-V curve was then swept from the laboratory as it would be during normal system operation.

Detailed procedures were included as part of the plan for the verification test, recorder calibration and normal data measurement operations. The intent here was to provide a starting point from which we could depart in order to achieve a comfortable operational mode.

Examination of preliminary I-V data from the solar panels to be measured showed that in the majority of cases, the data exhibits low fill factors. In fact, the curve shapes show behavior typical of solar cells with high series resistance. Quantitatively, these characteristics fall outside the range of applicability for the well known techniques for I-V curve manipulation.* As a result, there

---

*See: Harmon and Rasmussen, "Temperature, Illumination Intensity and Degradation Factor Effects on Solar Cell Output Characteristics", IEEE Transactions on Aerospace and Electronic Systems, Vol. AES-2, No. 4, July, 1966.

exist no known, acceptable techniques for making quantitative comparisons of I-V data over time unless, through chance, the illumination and temperature conditions of the data to be compared are identical. In addition, a question must be raised with regard to illumination measurement. Although up to five standard solar cells and a precision pyranometer may be employed for illumination measurement, none of these devices necessarily has the same sensitivity to spectral content or to diffuse illumination as the subject solar panels. Optical performance with regard to direct illumination will also differ between the measurement standards and the panels.

A qualitative approach will be taken in lieu of a more rigorous, quantitative analysis. The primary parameters of interest are the panel/module maximum power point $\left(P_{max}\right)$ and the curve shape in the immediate vicinity of that point. Increasing depression of the current and/or voltage coordinates of the P_{max} point (i_{pmax} and v_{pmax}) away from short circuit current and open circuit voltage, respectively, is symptomatic of increasing series resistance and reduction in available output power. Comparison of I-V curves taken from the same panel at different times will be made on a light table by overlaying the curves and seeking the best fit first in the region of short circuit and then in the region of open circuit voltage. It is necessary that respective graph axis be maintained parallel during this procedure. Graphs to be compared must have been recorded using identical scale calibrations on identical graph sheets. In this manner, changes in the curve shape in the region of P_{max} may be readily observed.

This procedure will mask changes in short circuit current and in open circuit voltage. However, barring large changes in these parameters, it is expected that major effects, if any, will become evident in P_{max} before they appear elsewhere.

4.0 TEST RESULTS

4.1 Data Acquisition Verification Test

As indicated in the Test Plan, simultaneous recordings of an I-V curve were made through the data acquisition system and at the panel location using two X-Y recorders. Figures 9a and 9b show the two I-V curves. These graphs were compared in two ways: first, the graph axes were overlaid to determine the difference in current and voltage coordinates at the maximum power point assuming identical calibration of the two recorders. The curve taken on the roof read 3.3 milliamperes out of 302 and 83.3 millivolts out of 11.75 volts higher than the curve taken in the laboratory. In terms of power, the roof curve read 1.8 percent higher at the maximum power point. The two curves crossed below the maximum power voltage and there were noticeable differences in transient performance between the two recorders leading to a larger percentage difference in the immediate vicinity of open circuit voltage, the starting point for the I-V sweep.

The second comparison was made in the same manner as is to be used to compare solar panel I-V curves measured with the system. The two curves were overlaid on a light table and shifted along the current and voltage axes maintaining parallelism of respective axes. In this manner, the two curves matched exactly except at open circuit voltage and within one volt of open circuit. This is the region of most severe transient performance requirement for the recorders.

4.2 Solar Panel Measurements

The results of the baseline data measurements are presented in Appendix III and represent the raw data

Table III presents the data for each of the panels as extracted from the raw data. Those panels with modules missing are indicated by

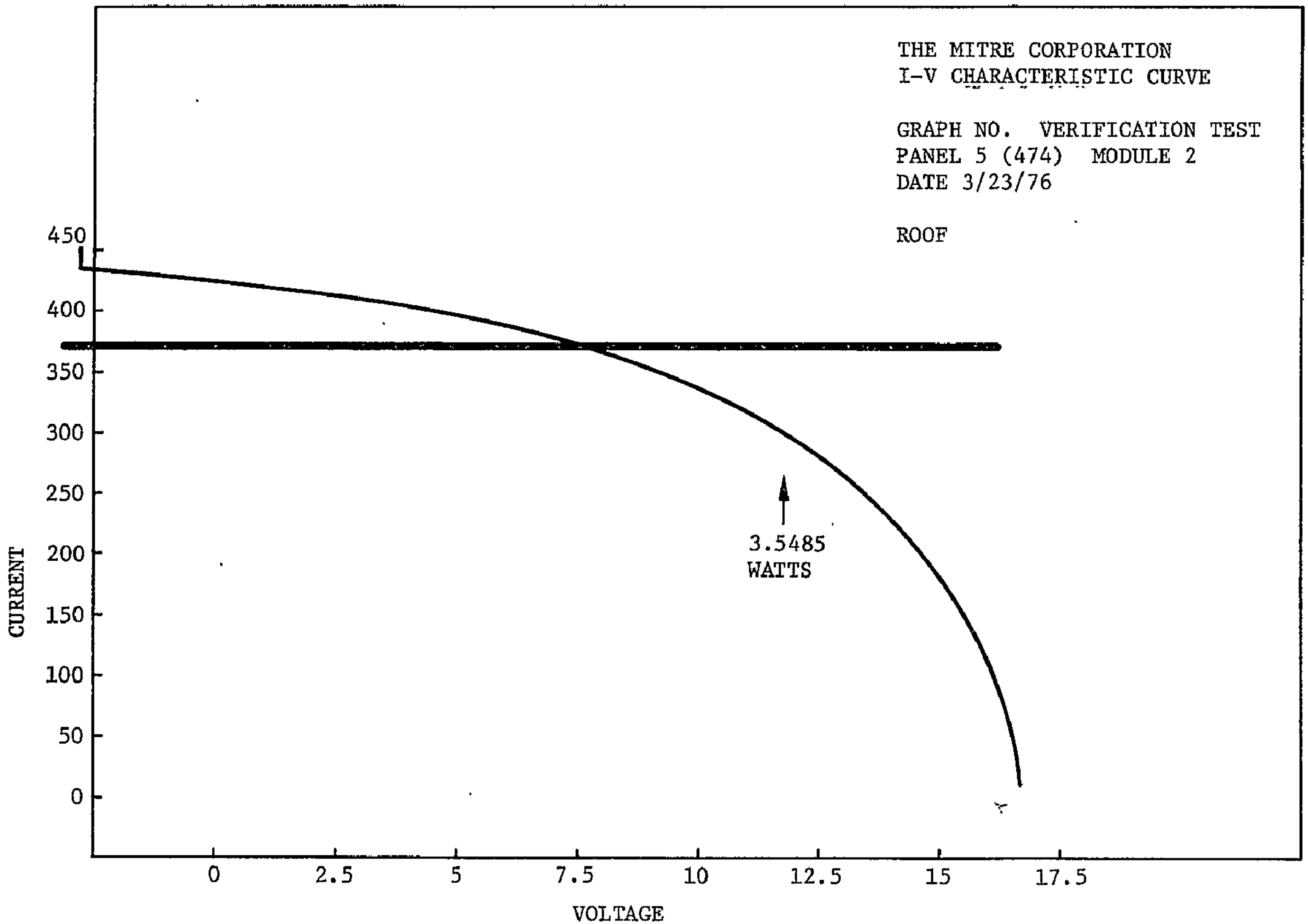

FIGURE 9(a)
VERIFICATION TEST I-V CURVE MEASURED ON ROOF

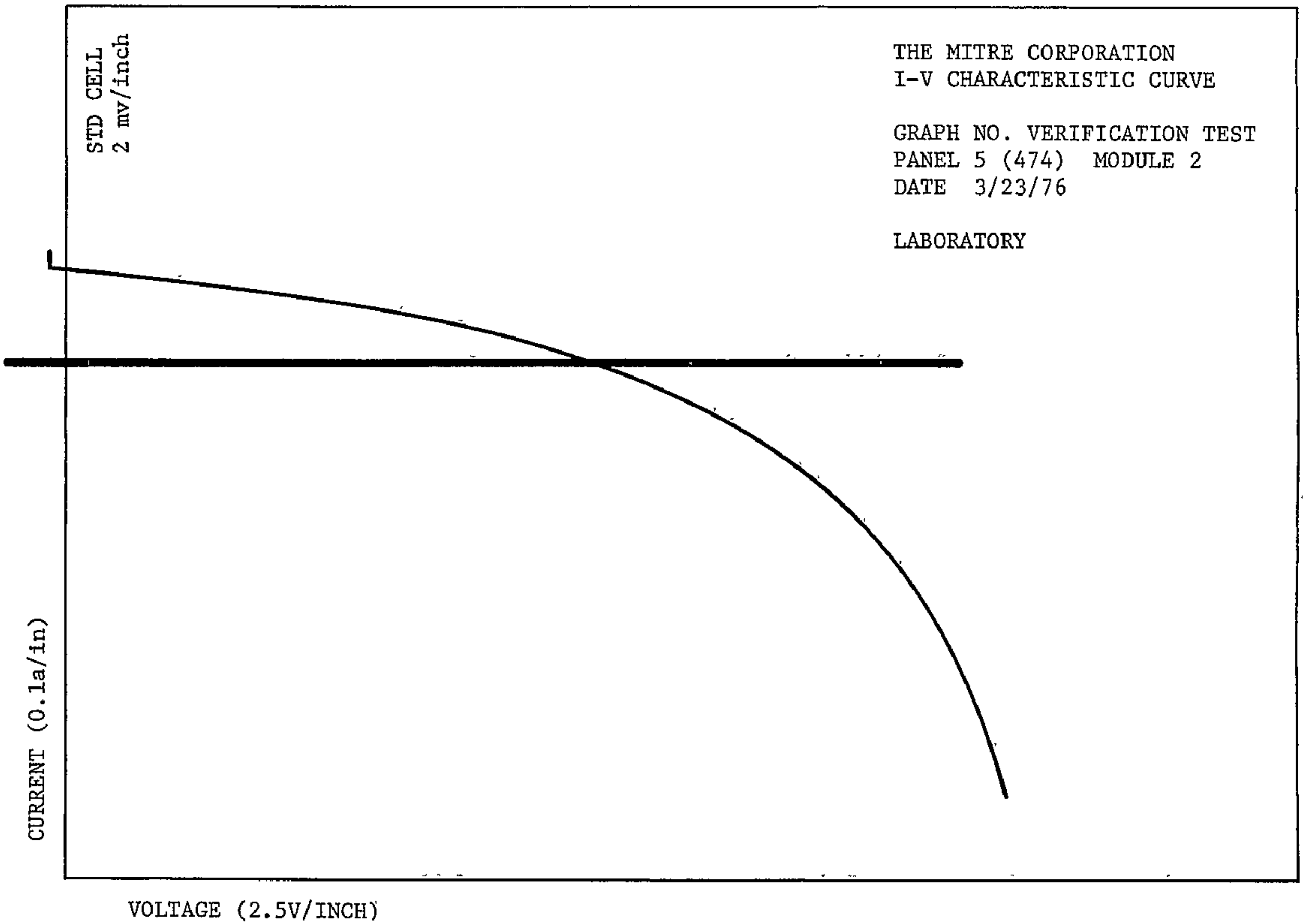

FIGURE 9(b)
VERIFICATION TEST I-V CURVE MEASURED IN LABORATORY

TABLE III
MEASURED DATA FOR THE SOLAR PANELS

PANEL NUMBER		ILLUMINATION (mw/cm^2)	TEMPERATURE (^oC)	V_{oc} (Volts)	I_{sc} (Amps)	P_{max} (Watts)
1	Solarex	101	43	31.39	2.04	29.6
2	Solarex	101	40	32.06	2.01	32.9
3	Solarex	97.4	42	32.36	1.95	29.9
4	Solarex*	97.1	43	32.0	1.45	24.3
5	Solarex	94.6	42	32.23	1.78	26.8
6	Solarex	93.8	42	30.77	1.54	27.9
7	Solarex	87.3	42	32.64	1.22	22.1
8	Solarex*	86.0	40	31.77	1.32	20.2
9	Solarex*	95.2	47	31.77	1.32	18.9
10	Solarex*	94.7	39	32.10	1.34	20.7
11	Solarex*	90.9	45	31.59	1.35	23.5
12	Solarex	89.7	46	31.36	1.69	24.9
13	Solarex	93.2	59	29.94	1.85	25.8
14	Solar Power	92.0	58	34.84	1.42	31.56 with diodes
		98.0	43	37.3	1.40	35.6 w/o diodes
15	Solarex	89.5	61	29.54	1.47	24.6
16	Solarex	89.7	62	29.51	1.68	23.0
17	Solarex*	96.0	28	33.77	1.36	23.3
18	Solarex	112	35	32.93	2.07	33.9
19	OCLI	97	30	31.82	1.75	36.8
20	Spectro-lab	96.9	31	34.99	1.76	43.1

V_{oc} = open circuit voltage

I_{sc} = short circuit current

P_{max} = power at the maximum power point a star, and represents 1/4 of the modules removed, as far as power measurements are concerned. It should be noted that the panels were cleaned on the morning that these data were taken, thereby reducing the effect of accumulated dirt on the results. Because of the poor curve shape, accurate corrections for temperature and illumination can not be made; however, changes in power can be estimated. Because the illumination is close to 100 mw/cm^2, corrections to power for illumination should be proportional to the fractional difference, within a few percent.

Estimates of power corrections for temperature are more difficult, but it is believed that corrections of the order of 0.4 to 0.5 percent per ^{o}C are of the right order of magnitude. In the case of panel 14 where data were taken at two different temperatures the correction was .44%/^{o}C. Thus for purposes of estimation, 0.5%/^{o}C seems reasonable. Using 0.5%/^{o}C, a 30^{o}C temperature change results in a 15% power change, whereas a 0.4%/^{o}C correction results in a 12% power change. Thus an error of 20% in the temperature correction factor will only result in a 3% power correction error.

Of the 17 Solarex panels, 11 were complete. For these 11 using the estimates for corrections stated above, the average peak power at 100 mw/cm^2 and 28^{o}C comes out to be about 31 watts.

The Solar Power panel had an uncorrected maximum power of 35.6 watts. Using the above estimate for correction gives a maximum power of 38 watts.

The OCLI panel had a maximum power of 36.8 watts. Using the above estimate for correction gives a maximum power of 38 watts.

The Spectrolab panel had an uncorrected power of 43.1 watts. Using the estimate for correction gives a maximum power of 45 watts. Table IV gives the performance of the panels as originally specified by the manufacturers.

TABLE IV
PANEL PERFORMANCE AS ORIGINALLY SPECIFIED BY MANUFACTURERS

SOLAREX 3/18/74	50 watts	$28^\circ C$,	$100\ mw/cm^2$
	$-0.4\%/^\circ C$	change of power efficiency in range from $0^\circ C$ to $55^\circ C$	
SOLAR POWER 12/29/75	52.5 watts	$28^\circ C$	$100\ mw/cm^2$
SPECTRO-LAB 1/25/74	47 watts	$43^\circ C$	$100\ mw/cm^2$
	50 watts	$28^\circ C$	$100\ mw/cm^2$
OCLI 1/23/74	46.2 watts	$28^\circ C$	$100\ mw/cm^2$

Several general conclusions can be drawn:

1) Our measurements tend to give results lower than those originally specified by the manufacturers with the difference depending upon the specific manufacturer. This appears to represent a systematic difference and could be due to standard use in establishing illumination levels; in the manner in which temperature was established, or nominal data employed by the manufacturers. It could also indicate some change in all panels due to weathering. Only further tests can establish the nature of the difference.

2) The difference between original specification and results obtained now is much larger for the Solarex panels than for any of the others and is considerably beyond anything that can be accounted for by variations in illumination or temperature effects. One must then conclude that these panels have exhibited substantial electrical performance degradation since their initial installation.

3) The results on the Solar Power panel are surprising, since this panel had only been installed about 2 months prior to measurement. The curve shape appears satisfactory, even though the maximum power is reduced. An I-V curve for this panel is shown in Figure 10. The discontinuities in the curve result from inclusion of bypass diodes within the panel to preclude module voltage reversal during test.

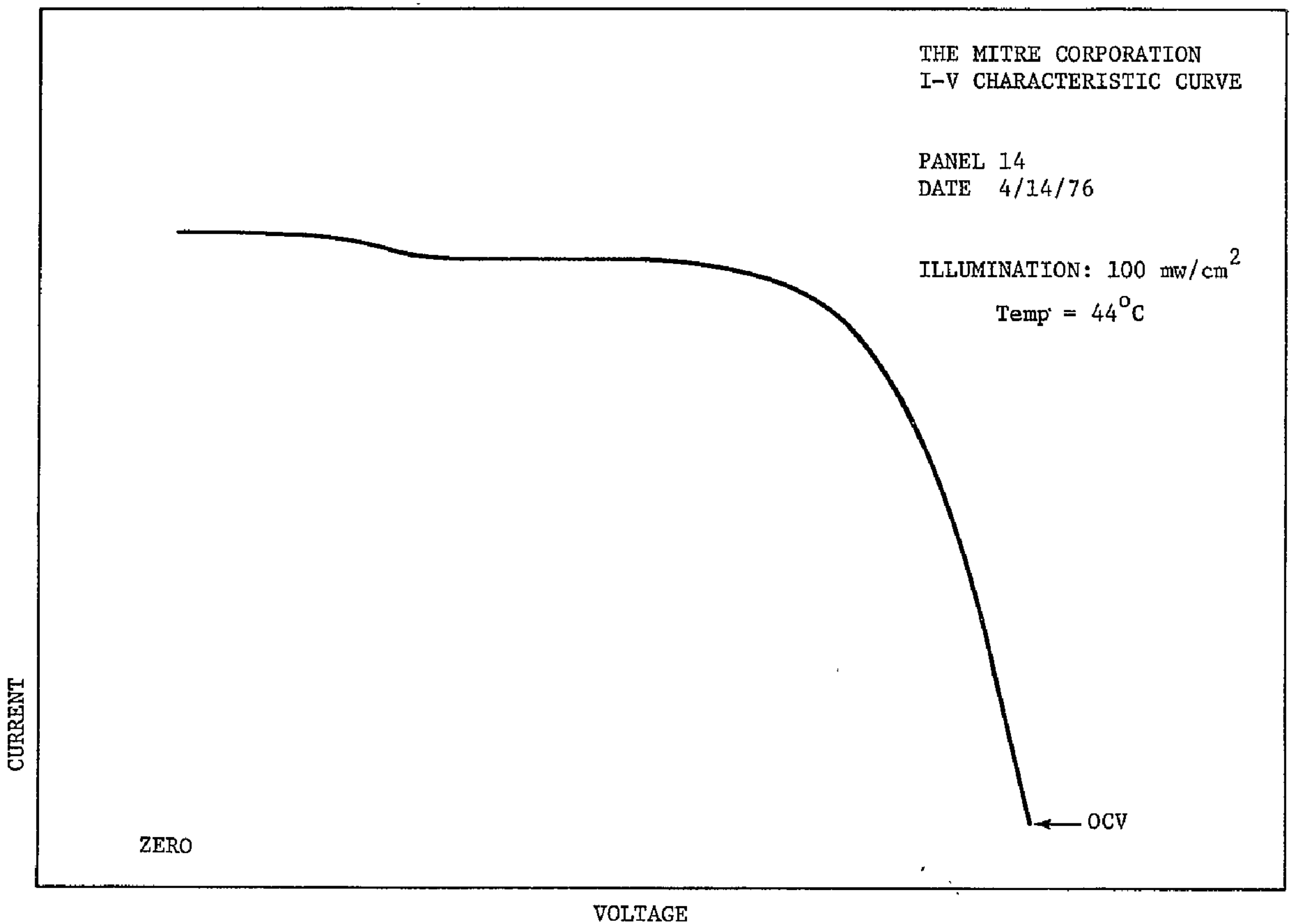

FIGURE 10
I-V CURVE FOR PANEL 14 WITH VOLTAGE REVERSAL PROTECTION DIODES

In general, the terrestrial cell panels which have been exposed to the weather for about two years show significantly lower fill factors than would be desirable. The panels with spacecraft type cells show fill factors which one would expect normally and are consistent with past measurements. Figure 11 shows a typical I-V curve exhibiting a fill factor of 0.409.

We have found that there is a great deal of variability in short circuit currents among similarly rated modules within a panel. To some extent, this is quite understandable since the costs involved in matching as might be done for a spacecraft solar array might well be prohibitive in the commercial-terrestrial application. However, by itself and when coupled with variations in curve shape which we have also observed, this variability could very well lead to significant problems when assembling a large number of these modules into an array and particularly a high voltage array. Operation of mismatched series-connected modules would yield an output power less than the sum of the two module powers. Sweeping an I-V curve of a full panel containing mismatched panels has caused the lower current modules to reverse in voltage. Figure 12 shows two such curves for a pair of series-connected modules. Series-parallel interconnection of a number of modules would, of course, tend to reduce the voltage reversal problem as would inclusion of bypass diodes. However, the curve shape and short circuit current variabilities still exist thereby reducing aggregate output power.

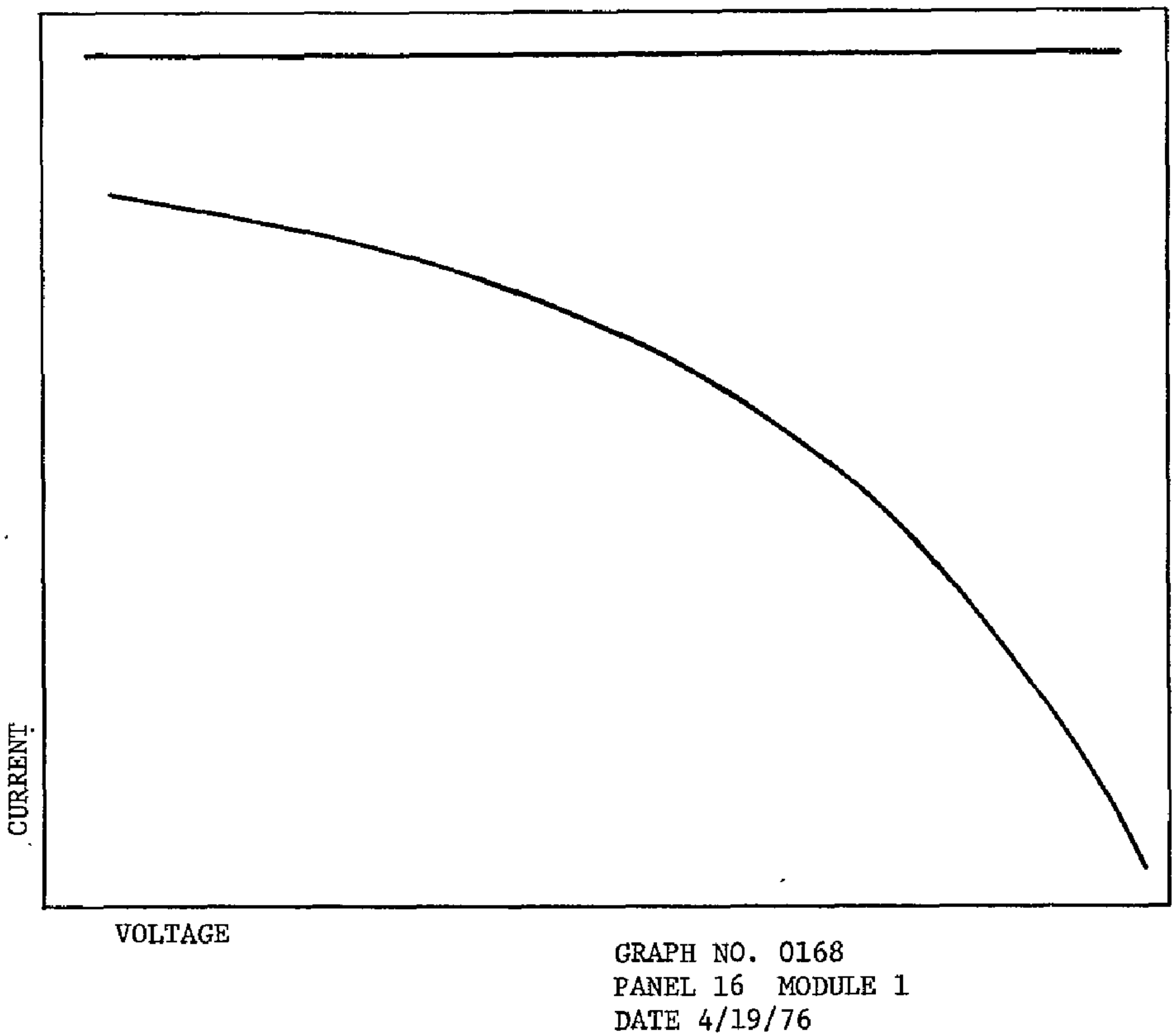

FIGURE 11
TYPICAL I-V CURVE EXHIBITING A FILL FACTOR OF 0.409

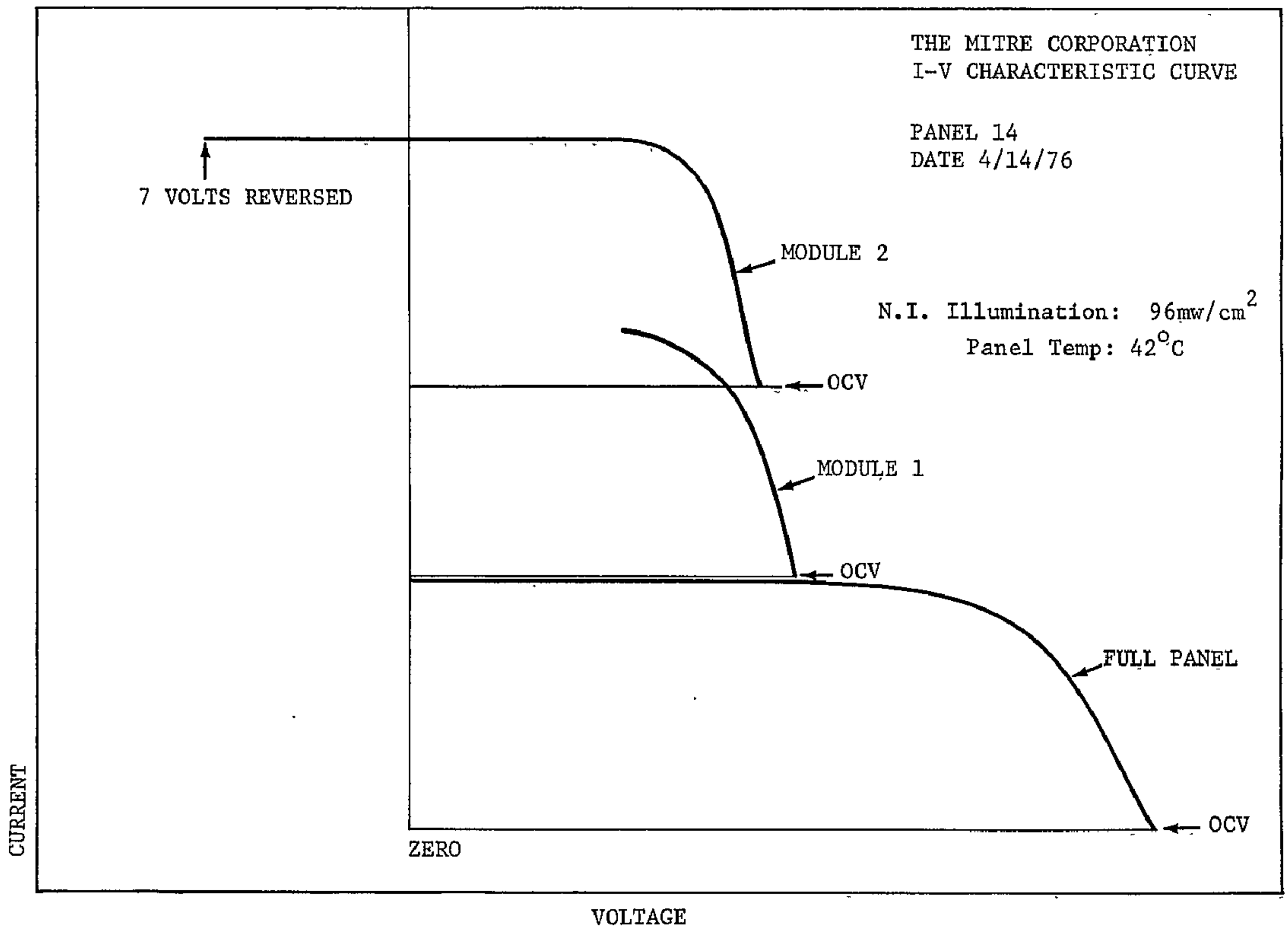

FIGURE 12
I-V CURVES FOR SERIES CONNECTED, MISMATCHED MODULES

We can only speculate at this time as to similar situations at the submodule level -- i.e., at the individual solar cell level. It seems reasonable to assume that if modules exhibit such variability, the individual cells within a module must exhibit at least the same degree of variability. If this is the case, then we must raise questions as to the operating conditions for individual cells and their effect upon the cost effectiveness of not performing a higher degree of selection in manufacture and, in fact, upon the useful operating lifetime of the modules.

4.3 Visual Inspection

It was decided at the beginning of this program to perform a detailed visual inspection of each of the more than 4000 solar cells and associated interconnectors in the MITRE array concurrently with the electrical measurements. This would provide a record of the physical status of the array which could reveal, with each subsequent inspection, any physical deterioration which might be linked to electrical performance changes.

Initially, the inspection was to be performed in the same manner as for spacecraft solar arrays; by an inspector with an eye loupe magnifier, a map of the array and a notebook. For spacecraft solar panels, inspections are generally made in a controlled environment with some concern for the inspector's physical comfort. The inspection task itself can be somewhat subjective and physical discomfort could manifest itself in a less than perfect result.

The MITRE solar array is located on a rooftop open to prevailing winds and, often, extremes of temperature relative to human comfort. The panels are mounted directly to an open steel gridwork which would certainly preclude kneeling to view cells at or near the bottom of the panels. Cells near the middle and top of the panels could only be viewed in a quasi standing-bending position which would be extremely uncomfortable for times longer than a few seconds.

To eliminate the need for subjecting an inspector to this situation, we turned to photography. With adequate photographs of each module, inspection can take place in relative comfort and a record is obtained which is, by far, superior to information subjectively derived and written into a notebook.

A fixture was designed and fabricated to hold a 35mm camera in place and which contained two electronic flash units for consistent illumination. The fixture is shown in Figure 13. Two sides of the fixture were left open to permit sufficient light for focusing. An opaque cloth was placed over the fixture during the exposure to exclude ambient lighting. The remaining interior surfaces of the fixture were painted white to help provide even illumination of the subject module. The fixture is lightweight and is used hand-held against the panel surface straddling the subject module. Figure 14 shows a photograph of a module taken with the fixture and Figure 15 is a section of that photograph showing a single cell.

All modules except the two Solar Power Corporation modules were photographed with the fixture. The Solar Power modules are approximately two feet square and required a significantly greater module-to-camera distance. These modules were photographed, using ambient illumination with the camera placed on a tripod.

In all cases, color slide film was used for the record. The resulting slides may be projected to any size for viewing; up to

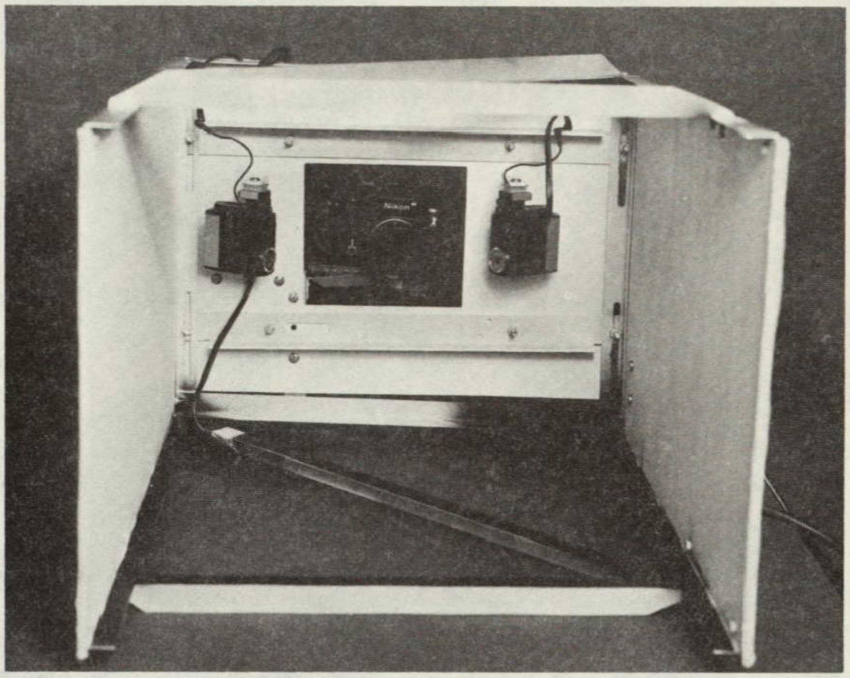

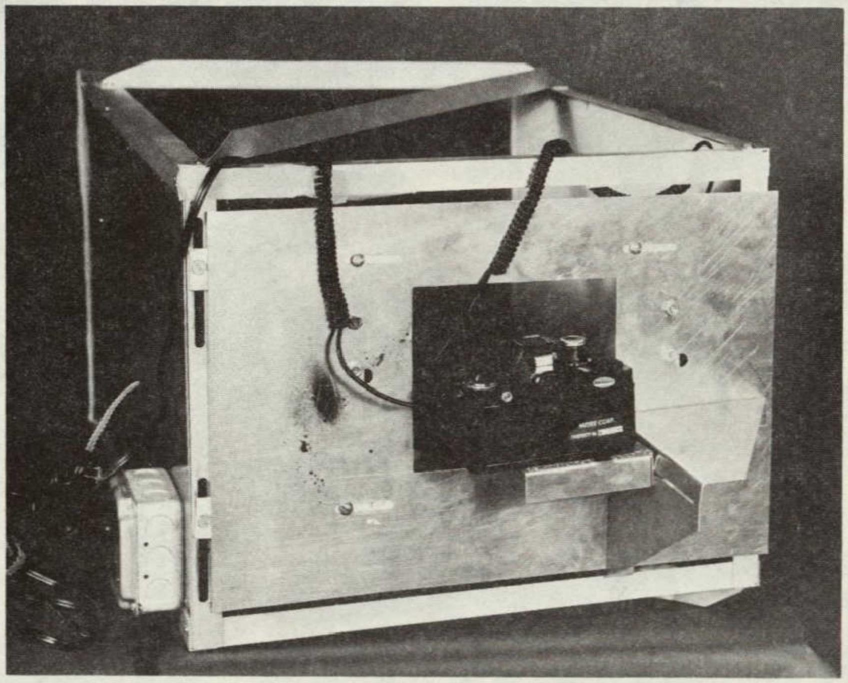

FIGURE 13
PANEL PHOTOGRAPHY FIXTURE

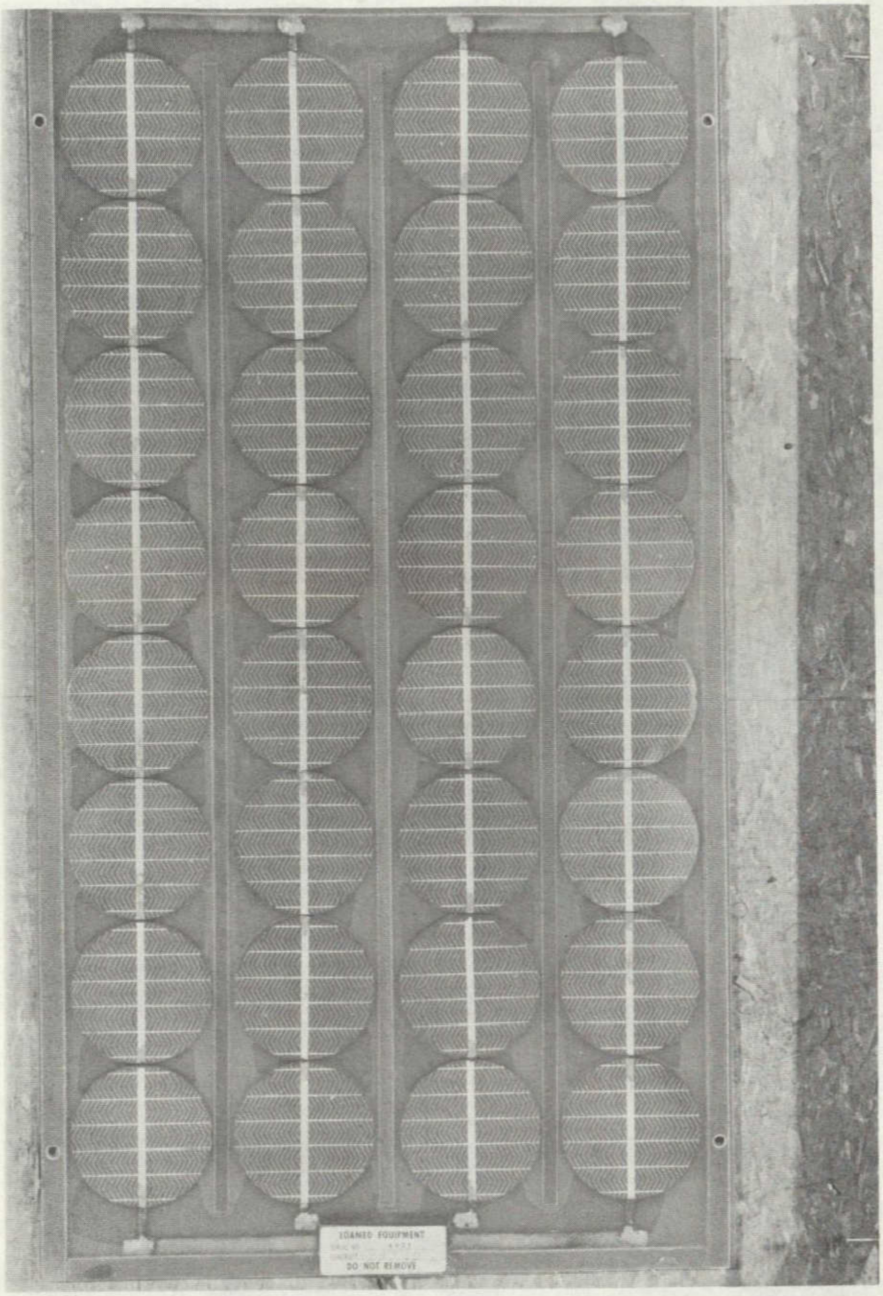

FIGURE 14
MODULE PICTURE TAKEN WITH PHOTOGRAPHY FIXTURE

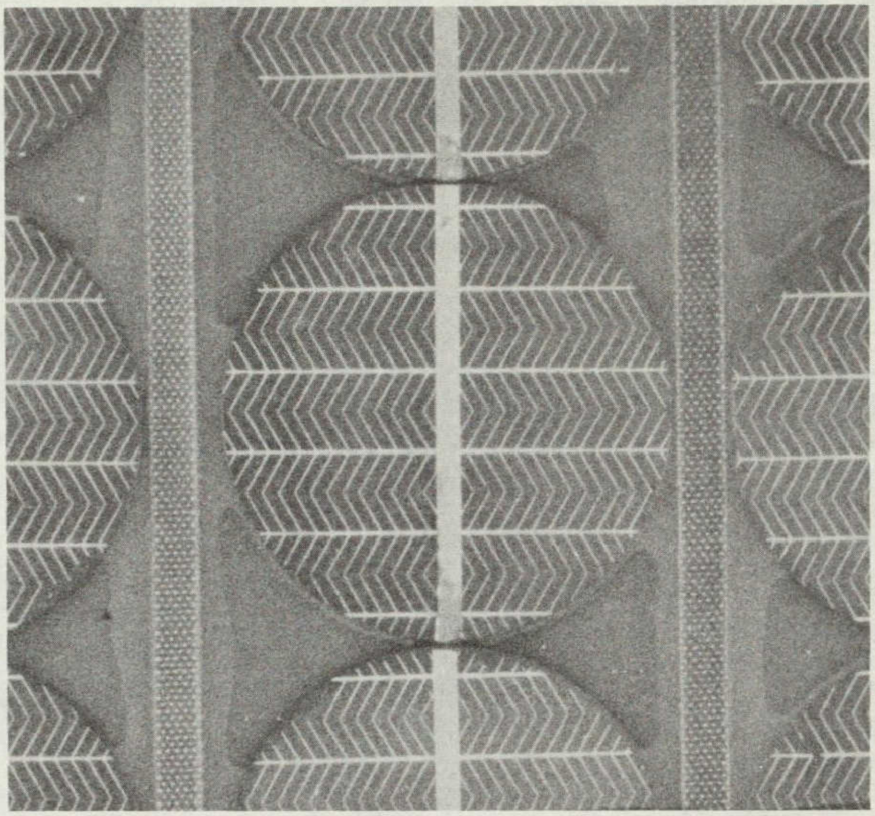

FIGURE 15
SECTION OF MODULE PHOTOGRAPH SHOWING A SINGLE CELL

the resolution capability of the film being employed. Ektachrome-X film was used primarily because we can perform and control processing in the MITRE darkroom. Other films might be just as suitable or even more so depending upon respective priorities.

Several comments are possible after only a cursory visual examination of the panels. For those modules of silicone rubber/glass-epoxy construction which have been on the roof for about two years, there are in almost every case (136 modules), signs of extensive delamination of the silicone material from the glass epoxy. Figure 16 shows a typical case where the lighter, irregularly shaped areas along the edges of the module are areas of delamination. It is not evident from a simple visual inspection that in any case, the delamination has actually exposed the cells. For this particular type of module, it has been claimed that the cells are totally encapsulated in the silicone material. In some cases, it appears that moisture has crept into the space caused by delamination. This is shown in Figure 17. Figure 18 shows moisture entrapment in a different package. Freezing of this moisture could eventually cause cracked cells.

Figure 19 shows a photograph of some cells in the same type of module. The dark area in the center of the cell grid structure appears to be corrosion of some sort. The location of the corroded area, isolated from the soldered cell contact leads to several possibilities. The corrosion could stem from some contaminant inadvertently left on the cell during module assembly. It could be due to an unfavorable combination of potting and cell/cell cleaning materials. It could be due to diffusion of contaminants through the silicone potting material. We suspect that it is not due to solder flux contamination since there is isolation between the soldered joints and the corroded area and the cell contacts were apparently not solder treated. In addition,

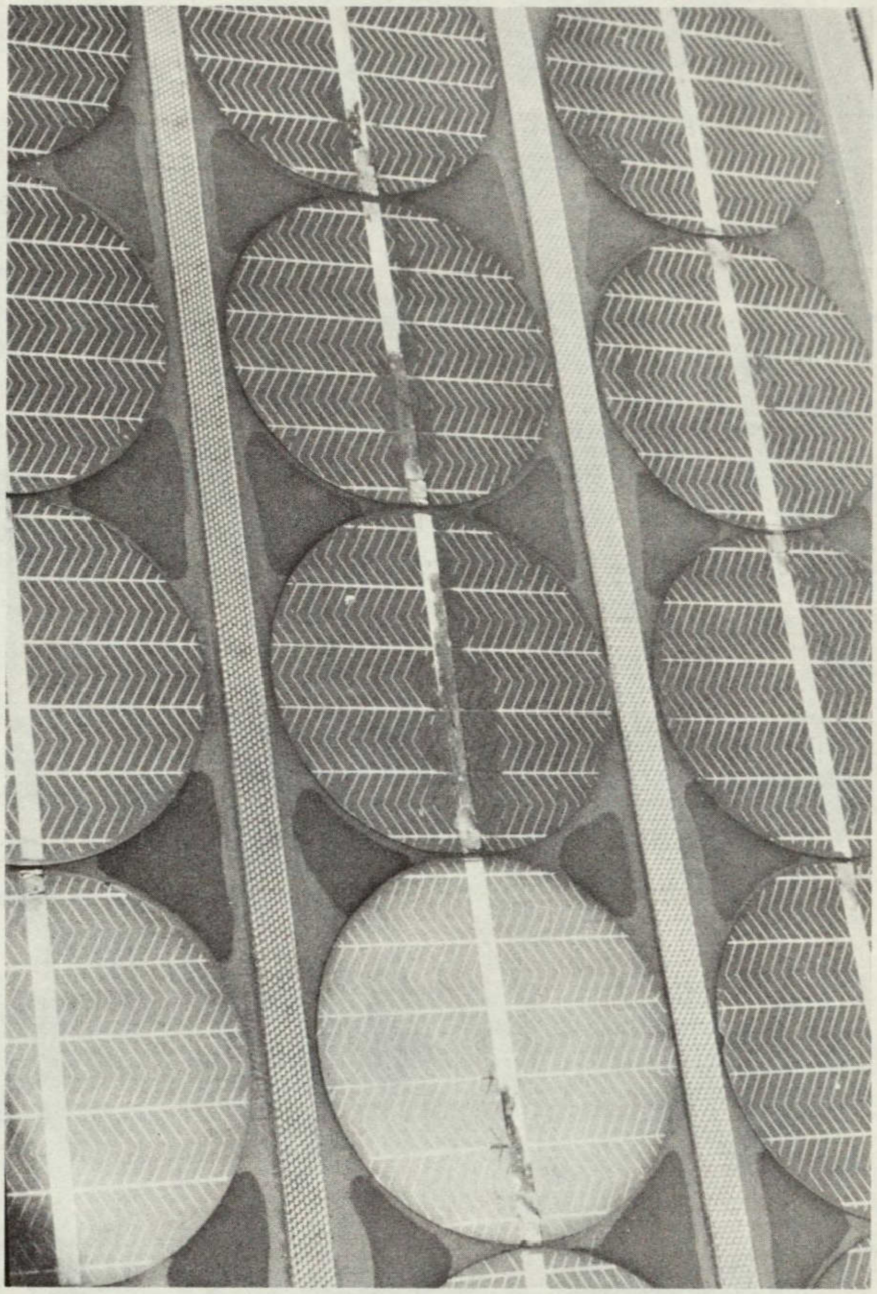

FIGURE 16
PHOTOGRAPH SHOWING EVIDENCE OF DELAMINATION

ORIGINAL PAGE IS
OF POOR QUALITY

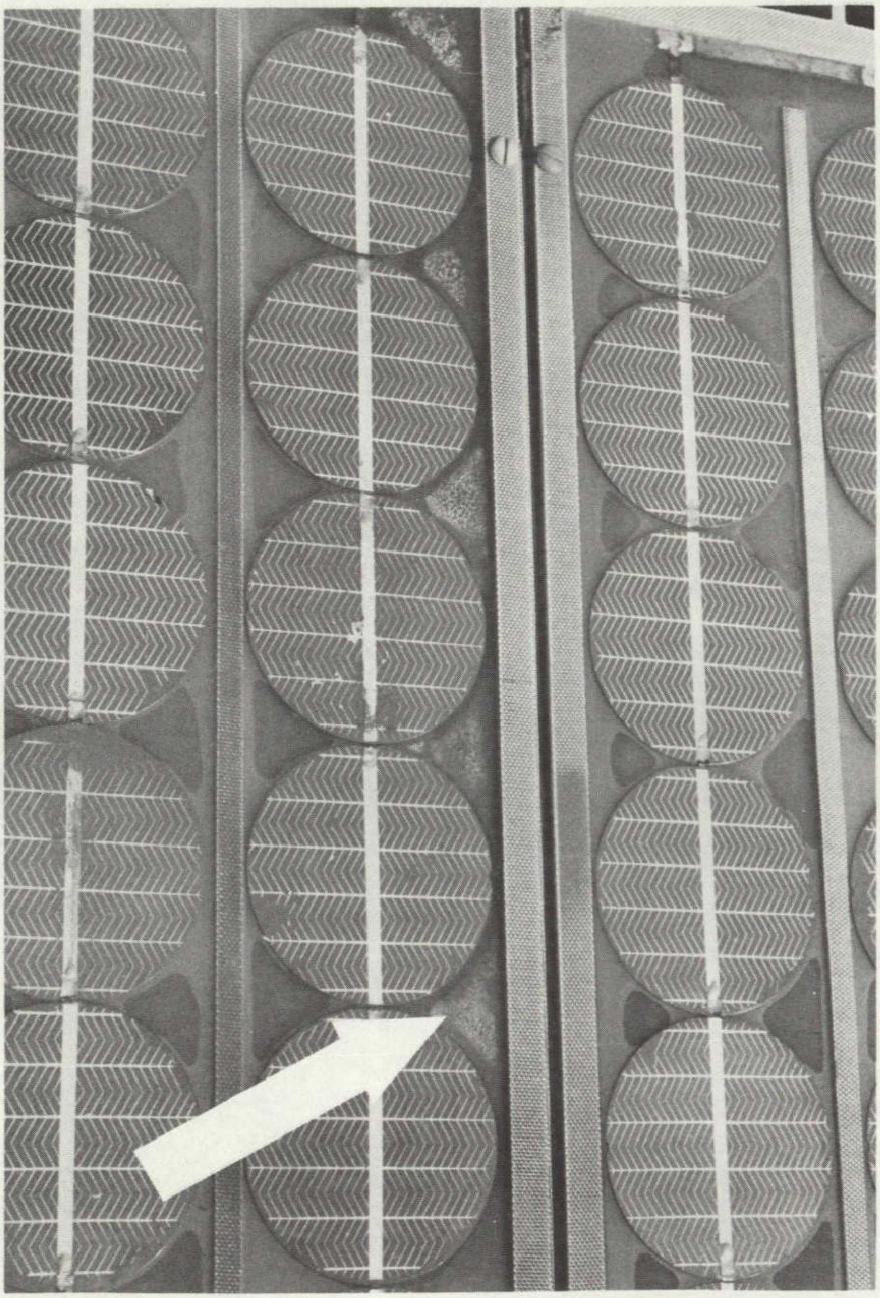

FIGURE 17
MOISTURE ENTRAPMENT IN DELAMINATION VOID

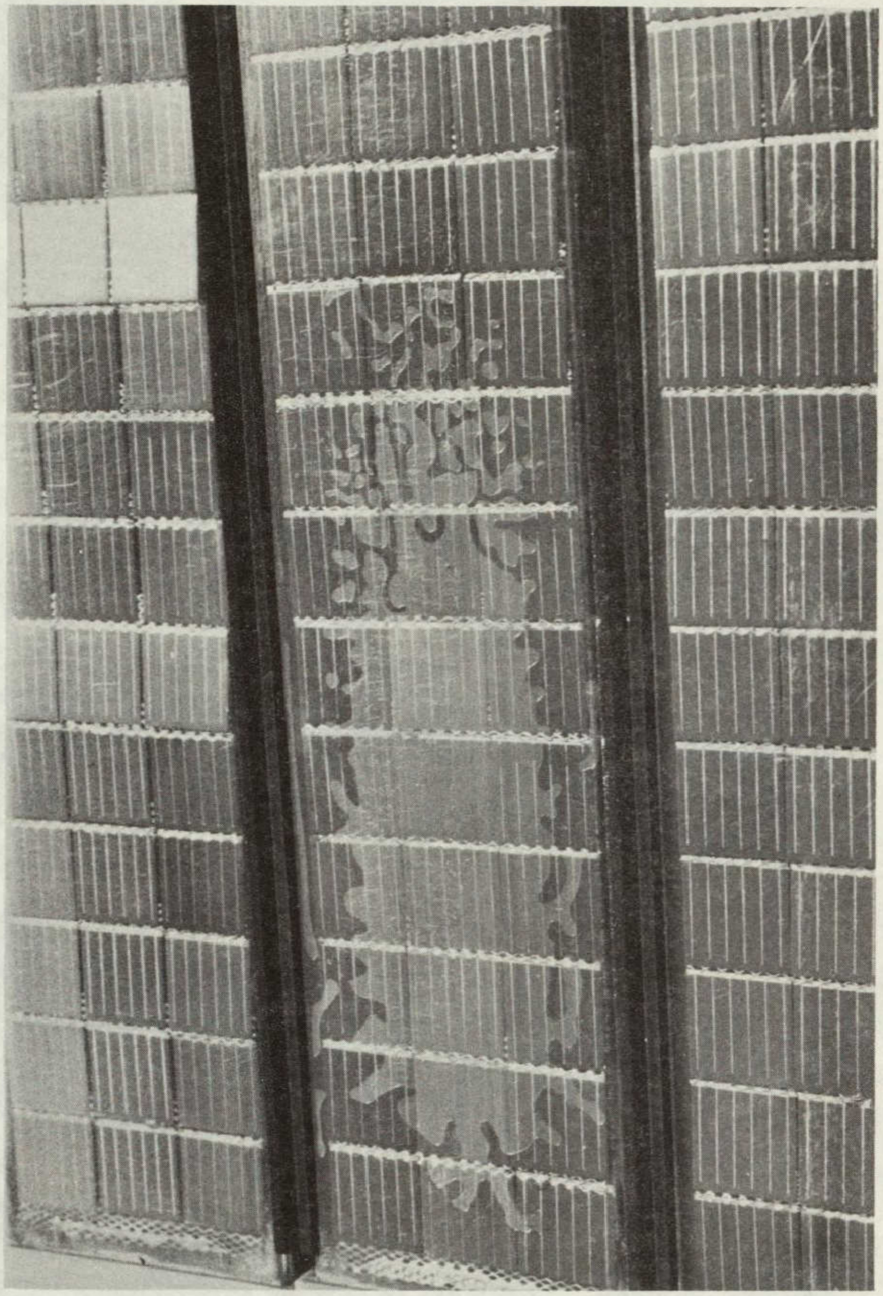

FIGURE 18
LIQUID ENTRAPMENT IN LEXAN SHEATHED MODULE

ORIGINAL PAGE IS
OF POOR QUALITY

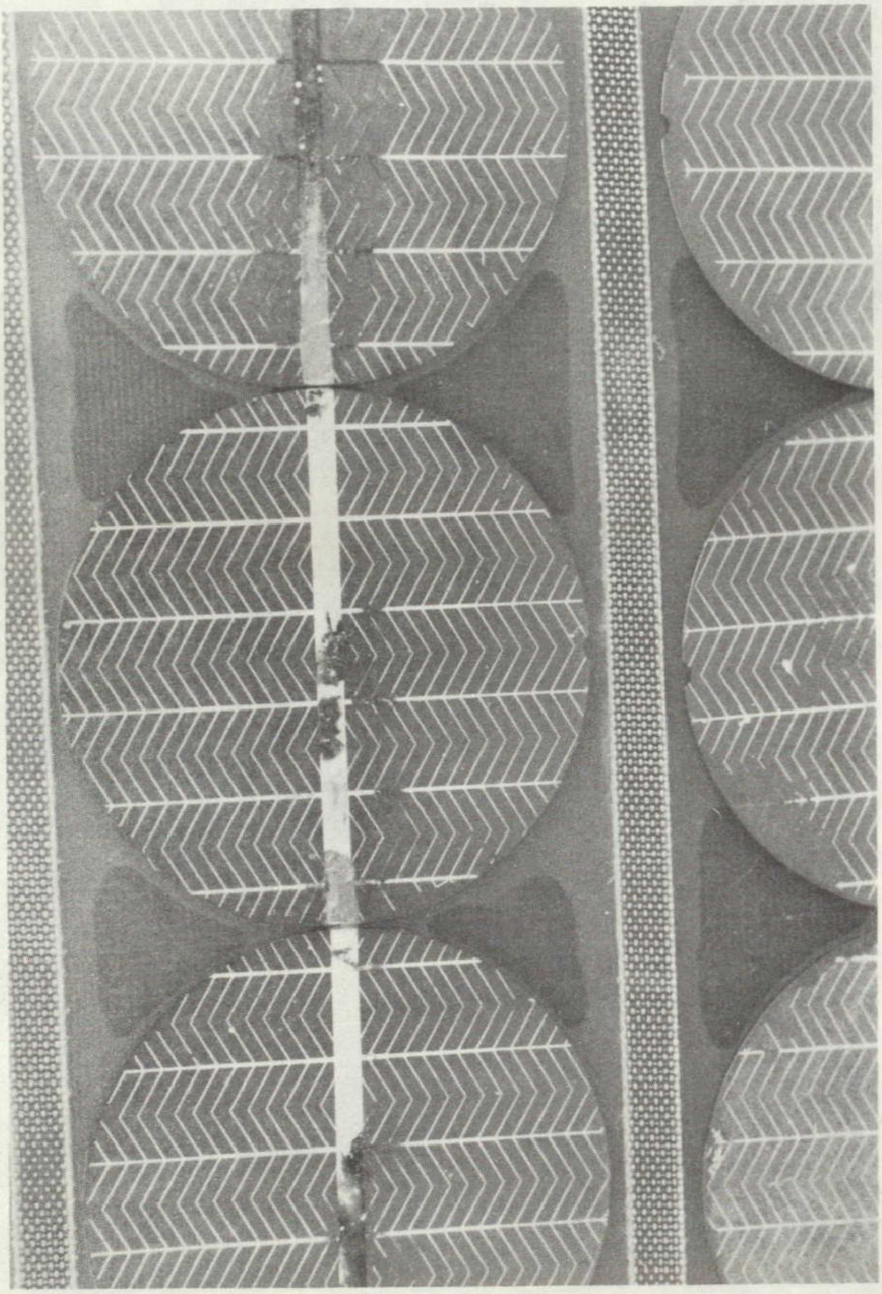

FIGURE 19
CORROSION OF CELL CONTACTS

in a significantly large number of cases, the solder joints do not appear to be corroded either at all or in this particular manner.

In some cases, gas bubbles were included in the potting material during manufacture. These were noted when the panels were received and have been observed periodically since then. When new, these bubbles were intact and in all probability had little effect upon electrical performance. In the course of two years, many of these bubbles have burst probably due to low temperature exposure and thermal cycling of their relatively thin walls. Figure 20 is a photograph of a larger bubble which has burst exposing the surface of the cell beneath to the atmosphere. Figure 21 is a photograph of a cluster of smaller bubbles. In this case, a good deal of dirt has accumulated in the voids left by the burst bubbles and effectively shadows a portion of the cell beneath. This may reduce the cell output by several percent with the ramification that such a situation could lead to a voltage reversal, an overheated cell and eventually an open circuit--particularly in a high voltage string.

In some cases, we have noted what appears to be an erosion of the silicone rubber surface. This is manifested in a dulling of the surface of the potting material after thorough washing to remove accumulated grime.

The glass-epoxy substrate to which the cells are bonded with silicone rubber is also deteriorating. The epoxy binder at the surface of the material appears to have been leached away by the weather. In some places, glass fibers are unravelling due to constant exposure to the wind as illustrated in Figure 22.

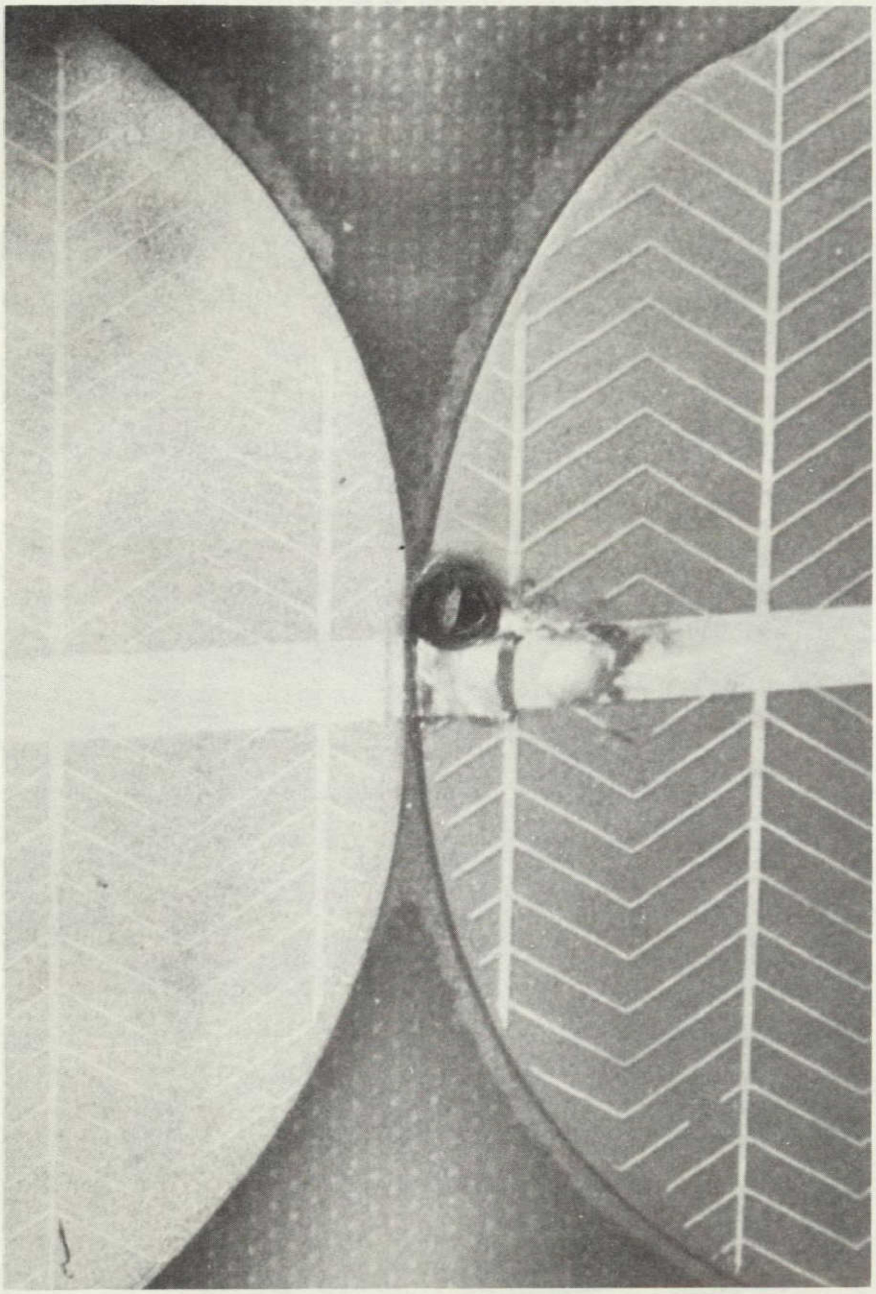

FIGURE 20
LARGE BUBBLE INCLUDED IN ENCAPSULANT

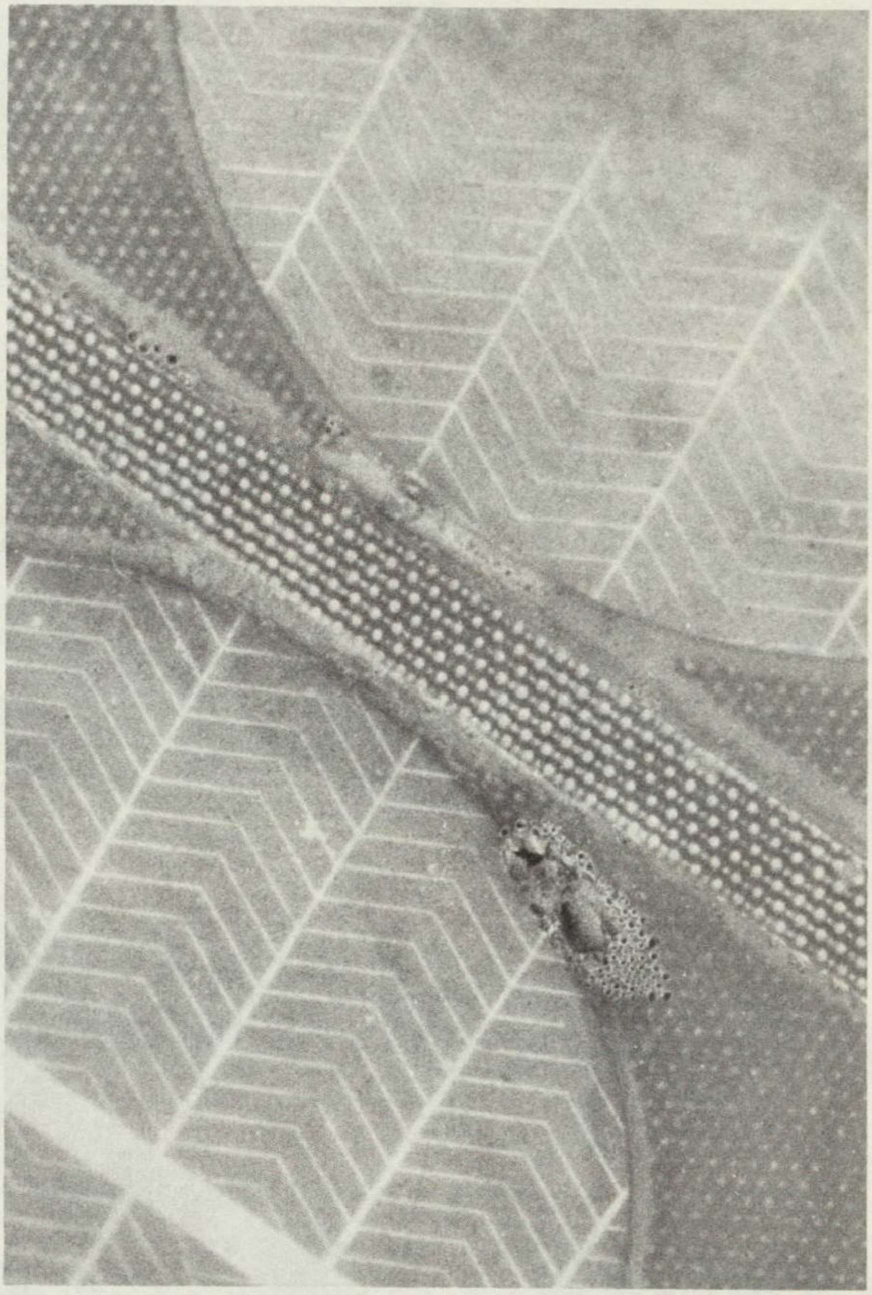

FIGURE 21
BUBBLE CLUSTER INCLUDED IN ENCAPSULANT

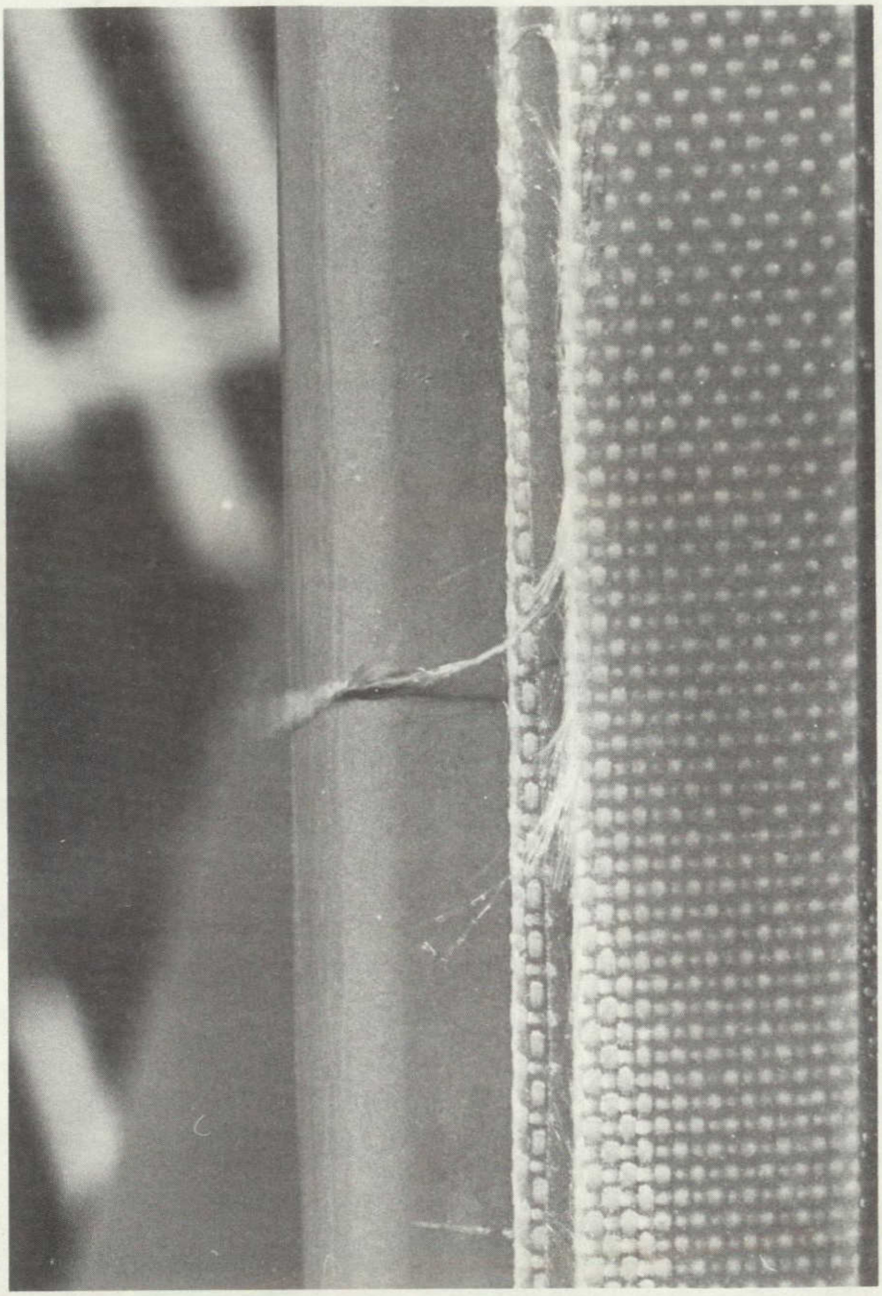

FIGURE 22
UNRAVELLING GLASS FIBERS

4.4 Conclusions to Date

A data acquisition system was built within the economic constraints established at the outset of this program. It is readily apparent that the type of system built has limitations in terms of absolute measurement accuracy as is evident from the results of the Data Acquisition Verification Test. A digital technique properly applied would yield superior results on an absolute basis.

However the method for data comparison which was employed lends itself well to analog recording. Comparison of I-V characteristics visually is much more easily accomplished with continuous trace recordings than with a tabulation of data which might have to be plotted for comparison. In this respect, the verification test results could not have been better.

The poor fill factor (apparently high series resistance) of the majority of panels in the MITRE array has precluded application of well known techniques for I-V curve shifting to correct for temperature and illumination differences. Apparently there has never been a need for manipulation of such characteristics with poor fill factor and, hopefully, the quality levels of coming products will eliminate the need for such tools in the future.

A number of observations may be made concerning the design of data acquisition systems for in situ measurements of terrestrial photovoltaic arrays:

Since the primary purpose of the array is to provide electric power, the instrumentation applied for purposes of performance measurement must interfere as little as possible with that purpose. It is desirable to be able to isolate only the assemblies to be measured leaving the remainder of the array to function normally. In a test or demonstration system this consideration may not be of primary concern as might also be the case for small, isolated systems. However, given the case of a large system - perhaps of several kilowatts or larger size - it may be desirable to make electrical performance measurements periodically for maintenance purposes. Projecting ahead it seems appropriate to disturb this type of system as little as possible for measurements of performance.

The baseline data taken in this program were measured over a period of approximately two months. In terms of actual measurement time, under two minutes (average) per I-V curve were required once a comfortable operating mode was acquired with three people operating the equipment, loading the recorder and writing meter readings on data sheets. The balance of the time was spent in waiting for the test window to open, adjusting equipment, troubleshooting faulty equipment, weekends and evenings, waiting for clouds to pass, correcting human error, and rainy and cloudy days. In the first two weeks of data measurement, there were three "good days" in which some 127 graphs were made. The remaining days were either rainy or cloudy.

The point to be made is that it is certainly technically feasible to make all necessary measurements of the 170 panels and modules in the MITRE array within one test window and several sets of measurements could be made for a more sound statistical approach. The only feasible method for accomplishing this we believe is to employ automated techniques; perhaps a computer controlled data acquisition system. The larger the array system, the greater the difficulty to be encountered in maintenance and the greater the need for rapid, consistent, and cost effective measurements.

Visual inspection of solar panels has an important place in the space program and in experimental situations. It may also turn out to be a useful technique for commercial array systems of the future. For _in situ_ inspections particularly of large arrays, it is inconceivable that the classical eye loupe - record book approach will serve the purpose. The photographic approach seems best at this time providing a permanent, easily used record.

An additional number of observations may be made regarding the data taken and inspections made to date:

Of the solar panels which have been part of the MITRE solar array for approximately two years, those of terrestrial cell composition have displayed very low fill factors of the order of 0.5. Earlier measurements indicate that these fill factors have indeed undergone changes over the two year period. Panels of spacecraft "reject" cells do not appear to have undergone any significant change. Packaging has deteriorated significantly as evidenced by delamination, entrapped moisture, corrosion of cell contacts and apparent erosion of potting material surfaces. To date, six of 136 of these modules have developed open circuits.

Short circuit current and curve shape variability has been observed in most cases, old panels and new. Economics of terrestrial solar panel manufacturing may not, at this time, permit either more careful selection of cells and modules intended for series operation or application of diode bypass techniques to preclude damage - particularly in high voltage circuits.

APPENDIX I

DATA SHEETS

ORIGINAL PAGE IS
OF POOR QUALITY

CATALOG 72

D.C. AMMETER SHUNTS BY EMPRO

Empro
SHUNTS ®

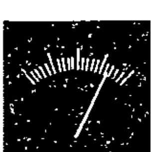

We offer the widest selection of standard model shunts available anywhere. Both switchboard and portable types. With current ratings up to 30,000 amperes. From these many models, you will probably find one to meet your needs exactly. If so, you will enjoy lower cost and faster delivery than possible with special models. If you do need custom-made shunts, we will be happy to develop them for you. Either way, we promise fine craftsmanship and a keen personal interest in your complete satisfaction

EMPRO MANUFACTURING CO., INC.
P O BOX 26064 • INDIANAPOLIS, INDIANA 46226 • 317/823-4478
World's Largest Exclusive Manufacturer of Shunts

STANDARD MODEL
SHUNTS
BY EMPRO

ACCURACY 1/4%

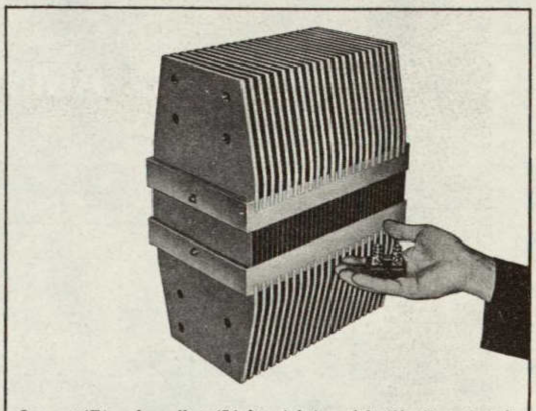

Largest (F) and smallest (Lightweight) models. The Type F style shown here has rated capacities over 10,000 amps.

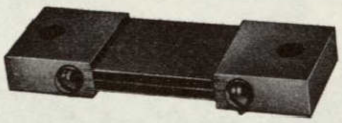

TYPE A

50 MV—15 through 600 amperes
100 MV—50 through 600 amperes

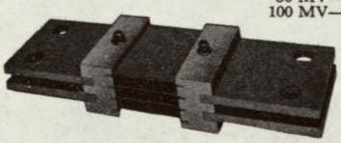

TYPE C

50 MV—1000 through 2000 amperes
100 MV—1000 through 2000 amperes

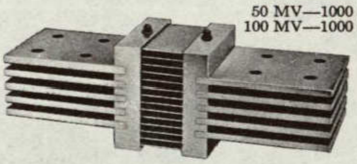

TYPE F

50 MV—2500 through 30000 amperes
100 MV—2500 through 10000 amperes

Note: Style shown here has rated capacities of 10,000 amps and under. Greater capacities are handled by style shown at top right.

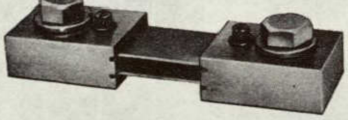

TYPE TRW-50

50 MV—100 through 600 amperes

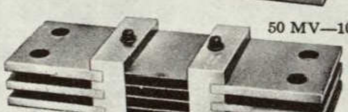

TYPE WT

50 MV—1000 through 10000 amperes
100 MV— 600 through 6000 amperes

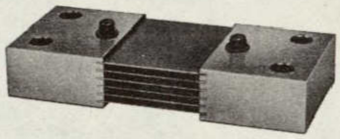

TYPE B

50 MV—300 through 1200 amperes
100 MV—300 through 1200 amperes

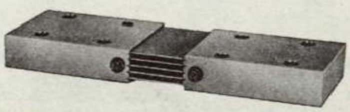

TYPE E

50 MV—1500 through 2000 amperes
100 MV—1500 through 2000 amperes

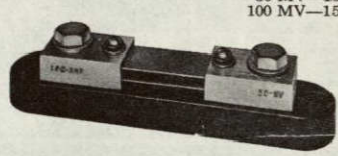

TYPE HA

50 MV—1 through 500 amperes
100 MV—1 through 500 amperes

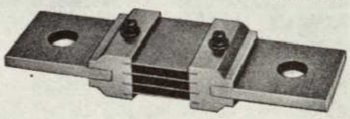

TYPE W

50 MV—300 through 1000 amperes
100 MV—120 through 500 amperes

LIGHTWEIGHT

50 MV—5 through 1200 amperes

ALL TYPES ALSO AVAILABLE IN 25 MV

MSA

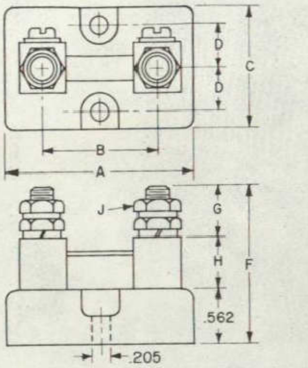

MSB and MSC

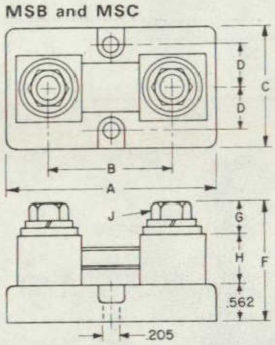

LIGHTWEIGHT TYPES

EMPRO CATALOG NUMBER	TYPE DESIGNATION	MS PART NUMBER	AMP	A	B	C	D	F	G	H	J
MLA-5-50			5	2.00	1.00	1.25	.437	1.688	.625	.500	¼-28
MLA-10-50	MSA100	MS91586-8	10	2.00	1.00	1.25	.437	1.688	.625	.500	¼-28
MLA-15-50	MSA150	MS91586-9	15	2.00	1.00	1.25	.437	1.688	.625	.500	¼-28
MLA-20-50	MSA200	MS91586-10	20	2.00	1.00	1.25	.437	1.688	.625	.500	¼-28
MLA-30-50	MSA300	MS91586-1	30	2.00	1.00	1.25	.437	1.688	.625	.500	¼-28
MLA-50-50	MSA500	MS91586-2	50	2.00	1.00	1.25	.437	1.688	.625	.500	¼-28
MLA-75-50	MSA750	MS91586-3	75	2.00	1.00	1.25	.437	1.688	.625	.500	¼-28
MLA-80-50	MSA800	MS91586-4	80	2.00	1.00	1.25	.437	1.688	.625	.500	¼-28
MLA-85-50	MSA850	MS91586-5	85	2.00	1.00	1.25	.437	1.688	.625	.500	¼-28
MLA-100-50	MSA101	MS91586-6	100	2.00	1.00	1.25	.437	1.688	.625	.500	¼-28
MLA-150-50	MSA151	MS91586-7	150	2.00	1.00	1.25	.437	1.688	.625	.500	¼-28
MLB-170-50	MSB171	MS91587-1	170	3.25	1.625	1.75	.625	1.750	.438	.750	⅜-16 x ⅝
MLB-200-50	MSB201	MS91587-2	200	3.25	1.625	1.75	.625	1.750	.438	.750	⅜-16 x ⅝
MLB-250-50	MSB251	MS91587-3	250	3.25	1.625	1.75	.625	1.750	.438	.750	⅜-16 x ⅝
MLB-300-50	MSB301	MS91587-4	300	3.25	1.625	1.75	.625	1.750	.438	.750	⅜-16 x ⅝
MLB-400-50	MSB401	MS91587-5	400	3.25	1.625	1.75	.625	1.750	.438	.750	⅜-16 x ⅝
MLB-450-50	MSB451	MS91587-6	450	3.25	1.625	1.75	.625	1.750	.438	.750	⅜-16 x ⅝
MLB-500-50	MSB501	MS91587-7	500	3.25	1.625	1.75	.625	1.750	.438	.750	⅜-16 x ⅝
MLB-600-50	MSB601	MS91587-8	600	3.25	1.625	1.75	.625	1.750	.438	.750	⅜-16 x ⅝
MLC-800-50	MSC801	MS91588-1	800	4.50	2.50	2.50	1.00	2.125	.562	1.00	½-13 x ⅞
MLC-1000-50	MSC102	MS91588-2	1000	4.50	2.50	2.50	1.00	2.125	.562	1.00	½-13 x ⅞
MLC-1200-50	MSC122	MS91588-3	1200	4.50	2.50	2.50	1.00	2.125	.562	1.00	½-13 x ⅞

For net prices on lightweight types, see the Empro discount schedule

- Nylon bases are furnished. Bakelite bases are available for MSA on request at no additional cost.

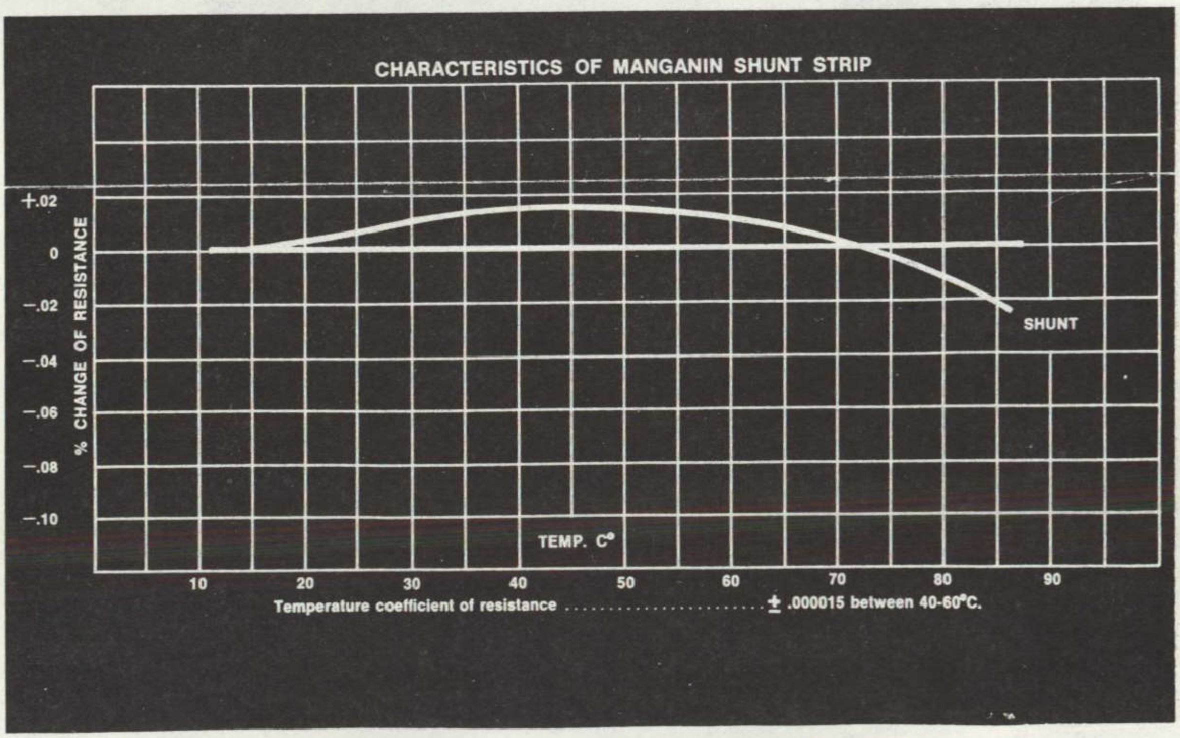

ORIGINAL PAGE IS
OF POOR QUALITY

YSI PRECISION THERMISTOR

Part #44008

RESISTANCE 30,000 OHMS AT 25°C

TIME CONSTANT[1] . 1[2] sec. max., 10[3] sec. max.

DISSIPATION
CONSTANT[4] . . . . 8[2] mw/°C., 1[3] mw/°C.

COLOR CODE . . . Black epoxy on body of thermistor with gray end

MAXIMUM OPERATING TEMPERATURE 150°C

Use heat sinks (needle nose pliers, etc.) when soldering or welding to thermistor leads.

[1] Time constant is the time required for the thermistor to indicate 63% of a new impressed temperature.

[2] Values determined with thermistor suspended by its leads in a "well stirred" oil bath.

[3] Values determined with thermistor suspended by its leads in still air.

[4] The dissipation constant is the amount of power in milliwatts required to raise the thermistor 1°C above the surrounding temperature.

TOLERANCES

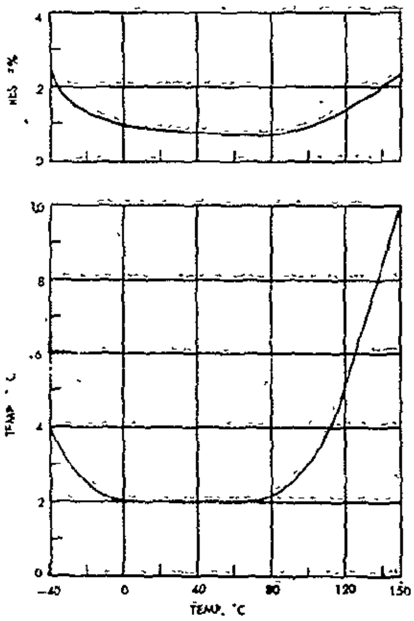

YSI PRECISION THERMISTOR

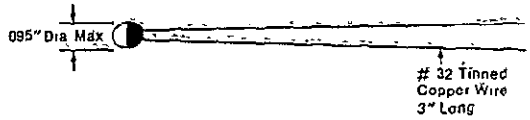

RESISTANCE VERSUS TEMPERATURE -40°C to +150°C

TEMP. °C	RES. Ω	TEMP. °C	RES. Ω	TEMP. °C	RES. Ω	TEMP °C	RES. Ω	TEMP °C	RES. Ω	TEMP. °C	RES. Ω
-40	884.6K	-4	116.0K	32	22.33K	68	5738	104	1840	140	701.2
39	830.9K	3	110.3K	33	21.43K	69	5545	105	1788	141	684.1
38	780.8K	2	104.9K	34	20.57K	70	5359	106	1737	142	667.5
37	733.9K	-1	99.80K	35	19.74K	71	5180	107	1688	143	651.3
36	690.2K	0	94.98K	36	18.96K	72	5007	108	1640	144	635.6
35	649.3K	1	90.41K	37	18.21K	73	4842	109	1594	145	620.3
34	611.0K	2	86.07K	38	17.49K	74	4682	110	1550	146	605.5
33	575.2K	3	81.99K	39	16.80K	75	4529	111	1507	147	591.1
32	541.7K	4	78.11K	40	16.15K	76	4381	112	1465	148	577.1
31	510.6K	5	74.44K	41	15.52K	77	4239	113	1425	149	563.5
30	481.0K	6	70.96K	42	14.92K	78	4102	114	1386	150	550.2
29	453.5K	7	67.66K	43	14.35K	79	3970	115	1348		
28	427.7K	8	64.53K	44	13.80K	80	3843	116	1311		
27	403.5K	9	61.56K	45	13.28K	81	3720	117	1276		
26	380.9K	10	58.75K	46	12.77K	82	3602	118	1241		
25	359.6K	11	56.07K	47	12.29K	83	3489	119	1208		
24	339.6K	12	53.54K	48	11.83K	84	3379	120	1176		
23	320.9K	13	51.13K	49	11.39K	85	3273	121	1145		
22	303.3K	14	48.84K	50	10.97K	86	3172	122	1114		
21	286.7K	15	46.67K	51	10.57K	87	3073	123	1085		
20	271.2K	16	44.60K	52	10.18K	88	2979	124	1057		
19	256.5K	17	42.64K	53	9807	89	2887	125	1029		
18	242.8K	18	40.77K	54	9450	90	2799	126	1002		
17	229.8K	19	38.99K	55	9109	91	2714	127	976.3		
16	217.6K	20	37.30K	56	8781	92	2632	128	951.2		
15	206.2K	21	35.70K	57	8467	93	2552	129	926.7		
14	195.4K	22	34.17K	58	8166	94	2476	130	903.0		
13	185.2K	23	32.71K	59	7876	95	2402	131	880.0		
12	175.6K	24	31.32K	60	7599	96	2331	132	857.7		
11	166.6K	25	30.00K	61	7332	97	2262	133	836.1		
10	158.0K	26	28.74K	62	7076	98	2195	134	815.0		
9	150.0K	27	27.54K	63	6830	99	2131	135	794.6		
8	142.4K	28	26.40K	64	6594	100	2069	136	774.8		
7	135.2K	29	25.31K	65	6367	101	2009	137	755.6		
6	128.5K	30	24.27K	66	6149	102	1950	138	736.9		
-5	122.1K	31	23.28K	67	5940	103	1894	139	718.8		

YSI COMPONENTS DIVISION
P O BOX 279
YELLOW SPRINGS, OHIO 45387

APPENDIX II

DATA ACQUISITION SYSTEM ERROR CALCULATIONS

This analysis is directed toward determining the accuracy with which the maximum power value for any solar panel or module may be determined with the data acquisition system. The constituent elements of the system introduce a variety of errors. These elemental errors are determined and are then combined to develop an overall error value for the system.

There are three types of errors about which we are concerned: Sensing errors or transducer inaccuracies, transmission errors or errors incurred by virtue of having to read system parameters through 250 feet (approximately) of cable and including source and meter impedances and recording/reading error or the inaccuracy of the instruments used to develop numerical data. The latter category includes errors due to calibration inaccuracy and human error in reading and calibrating instruments were applicable. In general, direct reading instruments (i.e.- digital voltmeters and X-Y recorders) have been calibrated using standards traceable to National Reference Standards maintained by the National Bureau of Standards. In all cases, instruments are within manufacturer's specified catalog tolerances. Calibration certificates for this instrumentation are reproduced at the end of this appendix.

(a) Current Sensing

In most cases, current is measured with a combination of an accurate meter shunt and a digital voltmeter. Currents are plotted with an X-Y recorder connected to the sensing terminals of the shunts. All measurements are made through the data transmission network consisting of cables, terminal blocks, stepping switches, and rotary switches.

Shunt Resistance Tolerance

The manufacturer's data for the shunts employed is shown in Appendix I. Shunts are nominally 10 milliohms.

manufacturing tolerance	= ± 0.25%
temperature tolerance	= ± 0.05%*
total worst case	± 0.3%

<u>Transmission Error</u>

The data transmission circuit is shown in Figure II-1 for the case where currents are being recorded on the X-Y plotter. For recording of numerical data, digital voltmeters replace the X-Y recorder in the figure.

Table II-I shows the calculation of circuit resistances. Roundtrip Resistance is taken as 10 ohms for purposes of all calculations and is the same for all parameters except as modified by source resistance differences.

Transmission error is brought about by attenuation of the signal due to the source, cable, and instrumentation input circuit resistances. Figure II-2 shows a circuit diagram of the attenuating network.

Current measurements are made with a Fluke 8800A digital voltmeter set on the 200 mv range in parallel with the Mosely X-Y Recorder model 136A. The voltmeter has an input resistance in this mode of 1000 megohms, minimum, and the recorder has an input resistance of 100K ohms for a net instrumentation input resistance of 100K ohms.

---

*Based upon discussion with manufacturer for the temperature range of -20°C to +50°C.

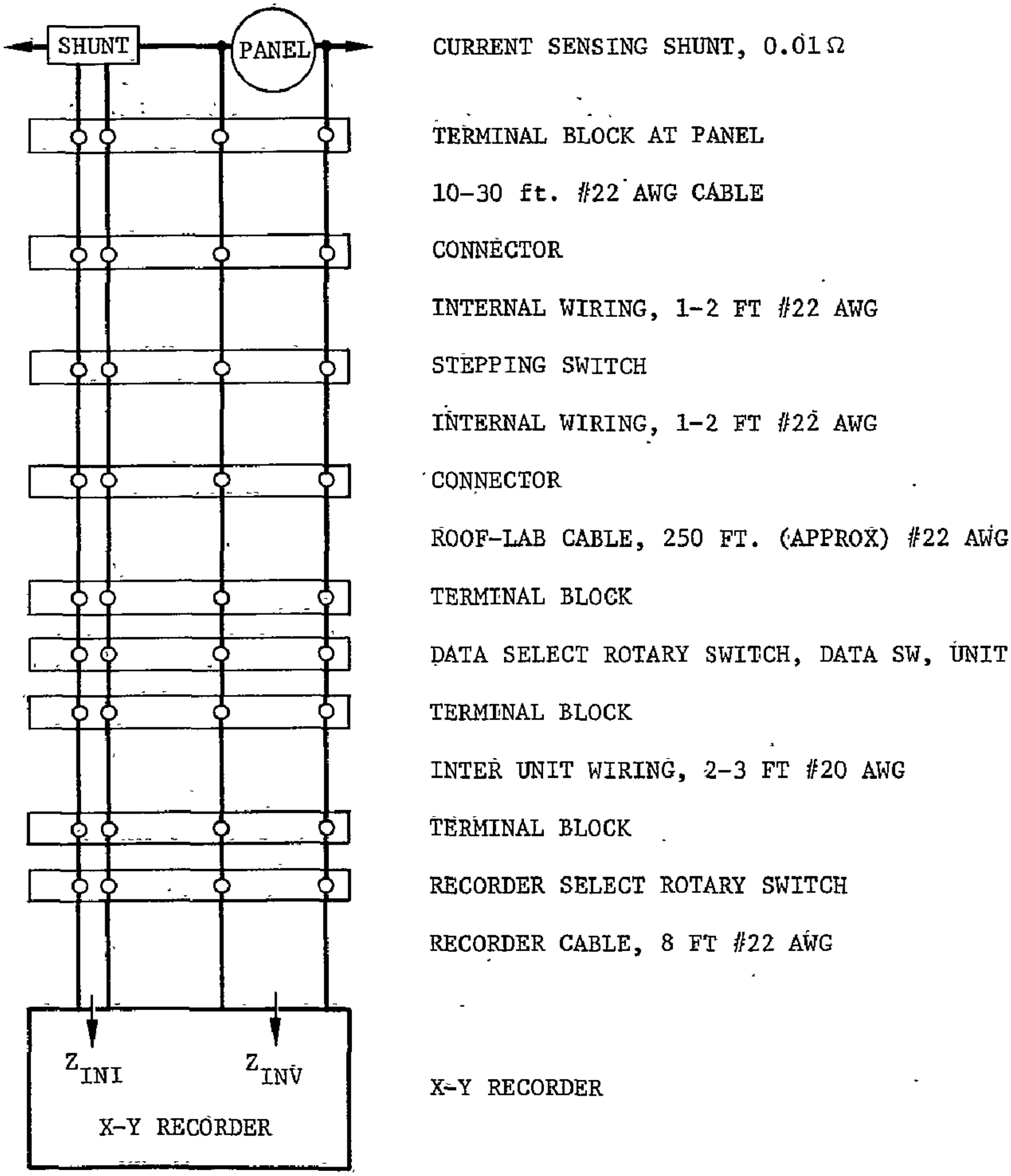

FIGURE II-1
SIGNAL FLOW PATH

TABLE II-1
TRANSMISSION CIRCUIT RESISTANCES

ITEM	RESISTANCE, OHMS	ROUNDTRIP RESISTANCE, OHMS
Source Resistance	0.01	0.01
Terminal Blocks, switches	9@ 0.02 = 0.18	0.36
Panel to MUX Cable	30 ft. AWG 22 30 x 0.01614/ft = 0.484	0.968
Roof-Lab Cable	250 ft. AWG 22 250 x 0.01614/ft = 4.035	8.07
Recorder Cable	8 ft. AWG 22 8 x 0.01614/ft = 0.129	0.258
Misc. cable	7 ft. AWG 22 7 x 0.01614/ft = 0.113	0.226
	Total Roundtrip	9.892 Ω

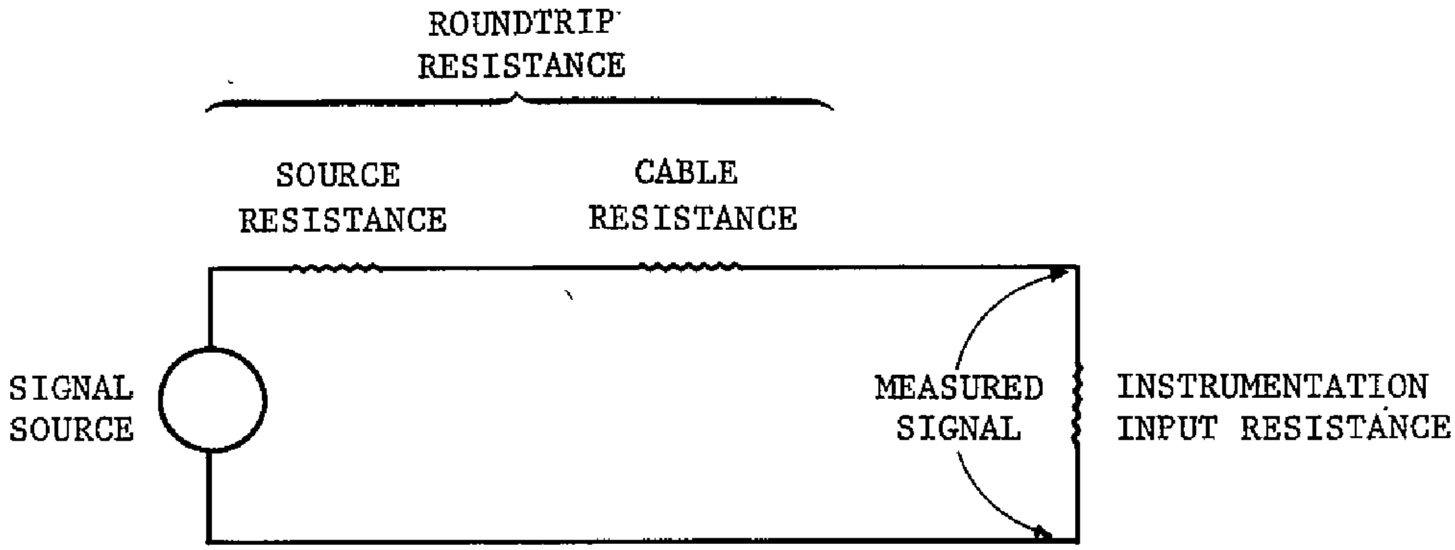

FIGURE II-2
SIGNAL TRANSMISSION ATTENUATION EQUIVALENT CIRCUIT

The measured signal is, then,

$$\frac{R_{input}}{R_{input} + R_{roundtrip}} = \frac{100K}{100K + 10} = 0.999$$

or 99.99 percent of the signal source. This is an error of -0.01 percent due to transmission.

Current Reading Error

The Fluke 8800A digital voltmeter has a specified tolerance on the 200 mv range of

$\pm$(0.01% of input + 0.005% of range)

Current readings are typically at 5 millivolts across the shunt.

$$\text{tolerance} = \pm\left\{0.001 \times 5 + 0.00005 \times 200\right\}$$

$$= \pm\ 0.0105 \text{ millivolts}$$

$$= \pm \frac{0.0105}{5} = \pm\ 0.0021 \quad \text{or } \pm\ 0.21 \text{ percent}$$

(b) Voltage Sensing

Panel/Module voltages are sensed directly without the aid of transducers or voltage divider networks. Therefore, there is no transducer tolerance as there was for current measurements.

Transmission Error

Open circuit voltage measurements are made with a Fluke 8800A digital voltmeter on the 20-volt scale for modules and on the 200-volt scale for full panels. Input resistances are:

$R_{in\ 20} \geq 1000$ meg Ω

$R_{in\ 200} \geq 10$ meg Ω

V_{oc} is measured without the recorder connected. Therefore, transmission errors are assumed to be negligible for open circuit voltage measurements.

Voltage Reading Error

The Fluke 8800A voltmeter has a specified error on 20 and 200 volt ranges of

$\pm$ (0.01% of input + 0.0015% of range)

for module measurement, V_{oc} is typically 16 volts

$$\text{Error} = \pm \left[0.0001 \times 16. + 0.000015 \times 20\right]$$
$$= \pm\ 0.0019 \text{ volts}$$
$$\text{or} \quad \pm\ 0.012 \text{ percent}$$

for panel measurement, V_{oc} is typically 32 volts.

$$\text{Error} = \pm \left[0.0001 \times 32 + 0.000015 \times 200\right]$$
$$= \pm\ 0.0062 \text{ volts}$$
$$\text{or} \quad \pm\ 0.0194 \text{ percent.}$$

(c) Temperature:

Temperature is sensed by a single thermistor located at a point on the panel surface judged to have a temperature typical of all other locations on that panel. A measurement was made of the average module temperature distribution across a randomly selected panel. An infrared sensing device supplied by JPL was employed to make the measurement. A maximum range of 4°C was noted across the panel in still air with insolation varying approximately plus or minus five percent according to pyranometer readings.

The thermistor employed is a YSI model 44008 30K at 25°C (nominal). (See Resistance table in Appendix I.)

max. thermistor resistance tolerance: (-20°C to + 50°C) $\pm$1.3% [at -20°C per mfgr. data]

$\pm$0.7% (at +50°C)

tolerance in ohms at $+50^{o}C = \pm 0.007 \times 10.97K\Omega = 76.8\Omega$

$-20^{o}C = \pm 0.013 \times 271.2K\Omega = 3525.6\Omega$

Thermistor self-heating

thermistor resistance measurement is made with a Fluke 8000A digital multimeter with a sensing current of 1μa.

at $50^{o}C$, dissipation is

$(1\mu a)^2 \times 10.97K\Omega \cong 0.01\ \mu$ watts

for a dissipation constant of $8mw/^{o}C$,

self-heating effect is negligible.

At $-20^{o}C$,

$(1\mu a)^2 \times 271.2K\Omega \cong 0.27\ \mu$ watts

also negligible.

Transmission error

Transmission circuit resistance = 10 Ω

at $50^{o}C$, thermistor will be

$$\frac{10.97 \times 100}{10.97 + 10} = 99.909\% \text{ of meter reading}$$

for an error of -0.091%.

At $-20^{o}C$, thermistor will be

$$\frac{271.2 \times 100}{271.2 + .010} = 99.9963\% \text{ of meter reading}$$

for an error of -0.0037%

Thermistor Resistance Reading Error

Fluke 8000A accuracy is ± (0.2% of reading + 1 digit) on 200KΩ scale and ± (0.5% of reading + 1 digit) on 2000KΩ scale which is used at temperatures below $14^{o}C$.

at $+50^{o}C$,

accuracy is $\pm \left[0.002 \times 10.97K\Omega + 100\Omega\right]$

$= \pm\ 121.9\Omega$

at $-20^{o}C$ $\pm \left[0.005 \times 271.2K\Omega + 1000\Omega\right]$

$= \pm\ 2356.\Omega$

Combined Temperature Reading Errors

Thermistor Placement: $4^{\circ}C$

Thermistor Tolerance $-20^{\circ}C$, 3525.6Ω

$+50^{\circ}C$, 76.8Ω

Self-heating negligible

Transmission 10Ω

Reading $-20^{\circ}C$, 2356Ω

$+50^{\circ}C$, 121.9Ω

Worst case at $-20^{\circ}C$

meter reads $271.2K\Omega + (3525.6 + 10 + 2356)$

$= 271.2K\Omega + 5891.6\Omega$

or $271.2K\Omega + (-3525.6 + 10 - 2356)$

$= 271.2K\Omega - 5871.6\Omega$

Thermistor sensitivity in region of $-20^{\circ}C$:

$-21^{\circ}C$	$286.7K\Omega$
$-19^{\circ}C$	$256.5K\Omega$
$-2^{\circ}C$	$30.2K\Omega$

or slope $= -15.1K\Omega/^{\circ}C$ ave,

error in $^{\circ}C$ is

$$+\frac{5891.6\Omega}{-15.1K\Omega/^{\circ}C} = -0.39\ ^{\circ}C$$

$$-\frac{5871.6\Omega}{-15.1K\Omega/^{\circ}C} = +0.38\ ^{\circ}C.$$

with a placement error of $4^{\circ}C$, the worst case error is

$\pm 4.4^{\circ}C$ at $-20^{\circ}C$.

At $+50^{\circ}C$,

meter reads $10.97K\Omega + (76.8\Omega + 10\Omega + 121.9\Omega)$

$= 10.97K\Omega + 208.7\Omega$

or $10.97K\Omega + (-76.8\Omega + 10\Omega - 121.9\Omega)$

$= 10.97K\Omega - 188.7\Omega$

thermistor sensitivity in region of $+50^{o}C$:

$+ 51^{o}C$	$10.57K\Omega$
$+ 49^{o}C$	$11.39K\Omega$
$+ 2^{o}C$	$-0.82K\Omega$

slope = $-0.41K\ \Omega/^{o}C$

error in ^{o}C is

$$\frac{+208.7\Omega}{-0.41K\Omega/^{o}C} \doteq -0.509\ ^{o}C$$

$$\frac{-188.7\Omega}{-0.41K\Omega/^{o}C} = +0.46\ ^{o}C$$

with placement error of $4^{o}C$

worst case error is

$\pm 4.51\ ^{o}C$ at $+ 50^{o}C$

(d) Illumination (Pyranometer) Measurement

The pyranometer is employed as the illumination measurement standard for the data acquisition system. No attempt will be made in this analysis or in the context of this program to resolve any disparity in spectral response between the pyranometer and the test articles. We do, however, recognize the disparity and the possibility that additional error may in fact exist as a result.

Pyranometer Tolerance

Linearity of the pyranometer is stated by the manufacturers to be $\pm$ 0.5 percent from zero through 1400 watts/meter^2 which corresponds with 1.4 times the nominal value of the solar vector at the earth's surface. In the most recent calibration of our pyranometer, it was found that the calibration constant of the device had changed by 0.476 percent from the previous value, determined approximately one year earlier. We will accept the manufacturer's calibration as absolute and allow the entire 0.5 percent to be accounted for as an illumination measurement error. A temperature dependence of $\pm$ 1.% must be included for a total of $\pm$ 1.5%.

Transmission Error

Pyranometer source resistance at $24^{\circ}C$ is stated by the manufacturer to be 590 ohms. Allowing 10 ohms transmission circuit resistance, the total roundtrip resistance is 600 ohms. The pyranometer output is measured with the HP DY-2401B digital voltmeter on the 0.1 volt range. Input resistance for the voltmeter is 100K ohms.

$$\text{Transmission Error} = \frac{600}{100K + 600} = 0.00596$$

or -0.596 percent

Pyranometer Reading Error

The DY-2401B digital voltmeter is specified to have the following reading tolerances when used to read the pyranometer output voltage on the 100 mv scale.

stability:	$\pm$ 0.06% of full scale
linearity:	$\pm$ 0.005% of full scale
attenuation:	$\pm$ 0.005% of reading

worst case combination of the above yields

$$\text{Error} = \pm (0.065\% \text{ f.s.} + 0.005\% \text{ of reading})$$

for pyranometer measurements on the 100 mv scale - typical readings are 10 mv.

$$\text{Error} = \pm (0.00065 \times 100 + 0.00005 \times 10)$$

$$= \pm (0.065 \text{ mv} + 0.0005 \text{ mv})$$

$$= \pm (0.0655 \text{ mv})$$

or

$$\pm \frac{0.0655}{10} \times 100 = \pm 0.655\%$$

(e) X-Y Recorder Error

Of primary concern in determining errors due to the X-Y Recorder are errors in determining the maximum power value from the recorded I-V characteristic curves. Of importance here are errors in calibration of the recorder, transmission, recorder linearity and reading from the graph.

Recorder Calibration Error

Figure II-3 shows a schematic diagram of the calibration circuit. Calibration of voltage and current axes are made using this circuit. A calibration voltage of 15 volts as read on the DY-2401B digital voltmeter is used for the voltage axis. Depending upon the panel or module to be measured, combinations of three and six inch deflections are used to calibrate voltage and current axes for the stated calibration voltages. Assuming the error due to measuring the calibration voltages is independent of recorder deflection, the worst case for transmitting this error to the recorder would occur for the smaller calibration deflections. This situation occurs when calibrating for a full panel I-V curve.

This error breaks down into voltage and current axis calibration voltage measurement error and operator error in zeroing and deflecting the pen. Recorder gain control resolution does not seem to have been a significant contributor to this error and will not be considered.

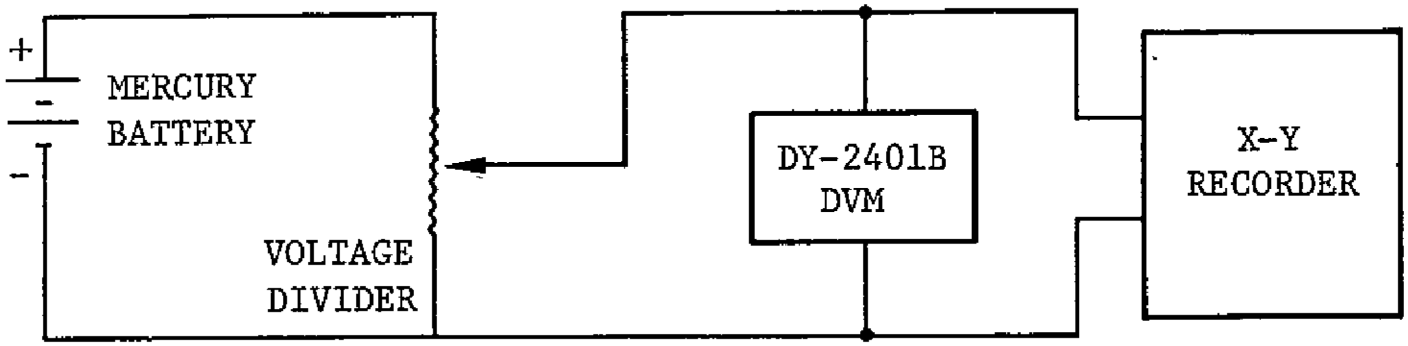

FIGURE II-3
RECORDER CALIBRATION CIRCUIT DIAGRAM

Recorder drift has been a problem. However, the operating mode which has evolved includes recalibration no less frequently than every sixteen curves. This seems to have eliminated all drift effects from the primary voltage and current measurement axes. The pyranometer axis (second Y axis) does drift a great deal but does so slowly and certainly not a consequential amount during an I-V sweep. Since the absolute calibration of this scale is not critical, this factor will not enter into this analysis.

Calibration voltages are measured with the DY-2401B digital voltmeter. As for pyranometer reading error, the current axis calibration voltage measurement error is

$$\text{Error} = \pm (0.065\% \text{ f.s.} + 0.005\% \text{ of reading})$$

Calibration voltage for recorder current axis is 6.0 millivolts measured on the 100 mv scale.

$$\text{Error} = \pm (0.00065 \times 100 + 0.00005 \times 6)$$

$$= \pm (0.065 + 0.0003) \text{ mv} = \pm 0.0653 \text{ mv}$$

or

$$\pm \frac{0.0653}{6} \times 100 = \pm 1.09\%$$

For the voltage axis, the calibration voltage is 15.0 volts measured on the 10 volt range. The DY-2401B is specified to have the following tolerances on the 10 volt range when used at 50% overrange.

Stability: $\pm$ 0.02% of full scale

Linearity: $\pm$ 0.01% of full scale

Attenuator: $\pm$ 0.005% of reading

Worst case combination of the above yields

$$\text{Error} = \pm (0.03\% \text{ f.s.} + 0.005\% \text{ of reading})$$

$$= \pm (0.0003 \times 10.0 + 0.00005 \times 15.0)$$

$$= \pm \ 0.00375 \text{ volts}$$

Or

$$\pm \frac{0.00375 \times 100}{15} = \pm \ 0.025\%$$

Operator error in performing calibration occurs in setting the recorder pen at zero and at the deflection point. The graph sheets used are ruled in tenths of inches with accented lines at one inch intervals. The recorder pen trace is approximately one tenth of a small division or 0.01 inch wide (optimistically). Allowing 0.01 inch pen placement error at zero and at calibration deflection yields a $\pm$ 0.02 inch operator error in both current and voltage. For calibration deflections of three inches, this corresponds with

$$\frac{\pm 0.02}{3.0} \times 100 = \pm 0.667\%$$

<u>Transmission Errors</u>

In the vicinity of the maximum power point, voltage transmission error is due to array internal impedance, cable roundtrip resistance (10 ohms) and recorder input resistance. Array impedance is taken as the slope of the I-V curve around the P_{max} point. For a randomly selected panel (panel 4), the average slope of the I-V curve in the vicinity of P_{max} is found to be 21.93 ohms. Recorder input resistance is 1 megohm.

Transmission

$$\text{Error} = \frac{-(21.93 + 10)}{10^6 + 21.93 + 10} \times 100$$

$$= -0.0032\%$$

Current transmission error is determined by Roundtrip Resistance and recorder input resistance which is 100K ohms

Transmission

$$\text{Error} = \frac{-10}{10^5 + 10} \times 100 = -0.009999\%$$

$$\approx -0.01\%$$

<u>Recorder Linearity Error</u>

Recorder linearity is specified as ±0.1 percent of full scale. This is assumed to be ±0.1 percent in X and Y directions, independently.

<u>Graph Reading Error</u>

As for calibration, error in reading the I-V graph is assumed to be 0.01 inch. For a typical 6 inch deflection, this corresponds with an error of

$$\pm \frac{0.01}{6} \times 100 = \pm 0.1667\%$$ for current and voltage.

(f) <u>Combined Errors in Determining P_{max}</u>

Maximum power is determined by locating the point on the I-V graph which has the highest product of its coordinates.

Assuming negligible error in detecting this maximum other than graph reading error, the resulting number is subject to error from the following:

(1) current sensing and transmission error

(2) voltage sensing and transmission error

(3) recorder calibration error in current and voltage

(4) recorder linearity error in current and voltage

An error summary is shown in Table II-II.

The combined error in voltages and currents are taken as the root-sum-squared (RSS) of the random error factors plus the non-random error factors. Only transmission error is non-random and for current,

$$\text{Error} = \pm\sqrt{(0.3)^2 + (1.09)^2 + (0.667)^2 + (0.1)^2 + (0.167)^2} - 0.01$$

$$= (\pm 1.33 - 0.01) \text{ percent}$$

$$= {}^{+1.32}_{-1.34} \text{ percent}$$

for voltage,

$$\text{Error} = \pm\sqrt{(0.0)^2 + (0.025)^2 + (0.667)^2 + (0.1)^2 + (0.167)^2} - 0.0032$$

$$= (\pm 0.695 - 0.0032) \text{ percent}$$

$$= {}^{+0.692}_{-0.698} \text{ percent.}$$

Power P, is the product of V and I as measured from the graph:

$$P = V(1 + \text{tolerance}_V) \quad I\ (1 + \text{tolerance}_I)$$

$$P = VI\ (1 + \text{tol}_V)\ (1 + \text{tol}_I)$$

TABLE II-II
ERROR SUMMARY

	SENSOR	TRANS-MISSION DVM	TRANS-MISSION RECORDER	READING—DVM	OTHER
CURRENT	± 0.3	-0-	-0.01	± 0.21	
VOLTAGE	-0-	-0-	-.0032	± .0194	
TEMPERATURE					
ILLUMINATION	± 1.5	-.596		± .655	
RECORDER					
Calib. voltage current axis				± 1.09	
Calib. voltage voltage axis				± .025	
Calib. voltage operator error					± 0.667
Linearity, current					± 0.1
Linearity, voltage					± 0.1
Graph reading, current					± 0.167
Graph reading, voltage					± 0.167

$$P = VI\ (1 + tol_V + tol_I + tol_V\ Tol_I)$$

In most cases where tolerances are small as they are here, the the cross product is negligible and,

$$P \cong VI\ (1 + tol_V + tol_I)$$

The error, then, in the power value read from the graph is

$$\text{Error} = tol_V + tol_I$$

$$= {}^{+\,1.32}_{-\,1.34} \quad {}^{+\,0.692}_{-\,0.698}$$

$$= {}^{+\,2.012}_{-\,2.038} \text{ percent}$$

There is additional error to be considered in interpreting the power value. Errors in temperature and illumination measurement will cause effective shifts in the I-V curve.

Temperature error was determined to be $\pm$ 4.5°C. For a typical solar panel with 64 series cells, this corresponds with

-2.2 mv/°C/cell x 64 series cells/ panel x 4.5°C.

or $\pm$ 0.6336 volts tolerance at open circuit voltage.

Assuming the same voltage tolerance at the maximum power voltage,* the error in V_{pmax} due to temperature error is

$$\text{Error} = \frac{\pm \Delta V_{oc} \times 100}{V_{pmax}}$$

Maximum power voltages have been found to be of the order of 20 volts at elevated panel temperatures and,

$$\text{Error} \pm \frac{\pm\ 0.6336 \times 100}{20} = \pm\ 3.168 \text{ percent}$$

---

*We recognize that this is not strictly correct because of curve shape changes with temperature. However, these changes are expected to be small compared with the open circuit voltage shift.

Illumination Error was determined to be due to several factors which are combined as errors were in the graph reading analysis, above. From Table II-II, random type errors are RSS'ed

$$\text{Error} = \pm\sqrt{(1.5)^2 + (0.655)^2} - 0.596$$

$$= \pm 1.637 - 0.596 \text{ percent}$$

Variation in illumination is translated to the I-V curve directly as current changes. The above error numbers will, therefore, directly reflect error in the current at the P_{max} point.

Temperature and illumination based error values must now be combined with P_{max} errors from the graph analysis. Allowing $\pm 2\%$ for graph based errors,

$$\text{Error} = \pm\sqrt{(2)^2 + (1.637)^2 + (3.168)^2} - 0.596 \text{ percent}$$

$$= \pm 4.086 - 0.596 \text{ percent}$$

$$= {}^{+\,3.49}_{-\,4.68} \text{ percent}$$

for total error in determining maximum power value.

2-2

Certificate of Conformance

For

Instrument John Fluke Digital Multimeter

Model No. 8800A Serial No. 97079

Submitted by: The Mitre Corporation

McLean, Virginia

This instrument has been calibrated in terms of the standards maintained at this laboratory, and was found to be within manufacturers catalog specified tolerance

The following standards were used as references for this calibration. Their calibration is traceable to the National Reference Standards maintained by the National Bureau of Standards.

Honeywell Thomas ohm mod 1190 s/n M2644 NBS # 211723
Guildline Instrument mod 9152T4 s/n 35353 NBS# 212530
Holt 6A s/n 180 AC Voltage Test No. 201944

Calibration date: 12-11-75 Calibration Data Enclosed Yes ☐ No ☐

Temperature: 73 °F.

Humidity: 40 % R.H.

By: __________

Approved: __________
Metrology Service Manager

Springfield, Virginia Branch

Metrology Services Group
Test Instruments Division
Honeywell Inc.

Certificate of Conformance

For

Instrument Fluke DVM

Model No. 8000A Serial No. 05526

Submitted by: Mitre

McLean, Virginia

This instrument has been calibrated in terms of the standards maintained at this laboratory, and was found to be within manufacturer's catalog specified tolerance.

The following standards were used as references for this calibration. Their calibration is traceable to the National Reference Standards maintained by the National Bureau of Standards.

Honeywell Thomas ohm mod 1190 s/n M2644 NBS# 211723
Guildline Instrument mod 9152T4 s/n 35353 NBS# 212530
Holt 6A s/n 180 AC Voltage Test No. 201944
Fluke 207-5B s/n 454 Test No. NAA Frequency Emissions

Calibration date: 1-12-76 Calibration Data Enclosed Yes ☐ No ☐

Temperature: 73 °F.

Humidity: 35 % R.H.

By: [signature]

Approved: [signature]
Metrology Service Manager

Springfield, Virginia Branch

ORIGINAL PAGE IS
OF POOR QUALITY

Metrology Services Group
Test Instruments Division
Honeywell Inc.

ORIGINAL PAGE IS
OF POOR QUALITY

Certificate of Conformance

For

Instrument Dymec Digital Voltmeter

Model No. 2401-B Serial No. 444-01627

Submitted by: Mitre Corporation

McLean, Virginia

This instrument has been calibrated in terms of the standards maintained at this laboratory, and was found to be within manufacturers specified catalog tolerance.

The following standards were used as references for this calibration. Their calibration is traceable to the National Reference Standards maintained by the National Bureau of Standards.

Guildline Instrument mod 9152T4 s/n 35353 NBS# 212530
Holt 6A s/n 180 AC Voltage Test No. 201944
Fluke 207-5B s/n 454 Test No. NAA Frequency Emissions

Calibration date: 1-8-76

Calibration Data Enclosed Yes ☐ No ☐

Temperature: 73 °F.

Humidity: 40 % R.H.

By: [illegible]

Approved: [illegible]
Metrology Service Manager

Springfield, Virginia Branch

Metrology Services Group
Test Instruments Division
Honeywell Inc.

Certificate of Conformance

For

Instrument Mosley X Y Recorder

Model No. 136 Serial No. 17

Submitted by: Mitre Corporation

McLean, Virginia

This instrument has been calibrated in terms of the standards maintained at this laboratory, and was found to be within manufacturers catalog specified tolerance

The following standards were used as references for this calibration. Their calibration is traceable to the National Reference Standards maintained by the National Bureau of Standards.

Guildline Instrument mod 1952T4 s/n 35353 NBS # 212530
Holt 6A s/n 180 AC Voltage Test No. 201944
Fluke 207-5B s/n 454 Test No. NAA Frequency Emissions

Calibration date: 1-8-76

Calibration Data Enclosed Yes ☐ No ☒

Temperature: 73 °F.

Humidity: 30 % R.H.

By: ____________

Approved: ____________
Metrology Service Manager

Springfield, Virginia Branch

Metrology Services Group
Test Instruments Division
Honeywell Inc.

Certificate of Conformance

For

Instrument: Hewlett-Packard X-Y-Y Recorder

Model No. 136A Serial No. 162

Submitted by: Mitre

McLean, Virginia

This instrument has been calibrated in terms of the standards maintained at this laboratory, and was found to be within manufacturers catalog specified tolerance.

The following standards were used as references for this calibration. Their calibration is traceable to the National Reference Standards maintained by the National Bureau of Standards.

Guildline Instrument mod 9152T4 s/n 35353 NBS# 212530
Holt 6A s/n 180 AC Voltage Test No. 201944
Fluke 207-5B s/n 454 Test No. NAA Frequency Emissions

Calibration date: 1-19-76 Calibration Data Enclosed Yes ☐ No ☐

Temperature: 73 °F.

Humidity: 40 % R.H.

By: [signature]

Approved: [signature]
Metrology Service Manager

Springfield, Virginia Branch

Metrology Services Group
Test Instruments Division
Honeywell Inc.

Certificate of Conformance

For

Instrument Cimron Digital Voltmeter

Model No. 7200A Serial No. 4143

Submitted by: Mitre Corporation

McLean, Virginia

This instrument has been calibrated in terms of the standards maintained at this laboratory, and was found to be within manufacturers specified catalog tolerance.

The following standards were used as references for this calibration. Their calibration is traceable to the National Reference Standards maintained by the National Bureau of Standards.

Guildline Instrument mod 9152T4 s/n 35353 NBS# 212530

Calibration date: 1-8-76

Calibration Data Enclosed Yes ☐ No ☒

Temperature: 73 °F.

Humidity: 40 % R.H.

By: [signature]

Approved: [signature]
Metrology Service Manager

Springfield, Virginia Branch

Metrology Services Group
Test Instruments Division
Honeywell Inc.

Certificate of Conformance

For

Instrument John Fluke Portable Calibrator

Model No. 515A Serial No. 6017

Submitted by: The Mitre Corporation

McLean, Virginia

This instrument has been calibrated in terms of the standards maintained at this laboratory, and was found to be within manufacturers catalog specified tolerance.

The following standards were used as references for this calibration. Their calibration is traceable to the National Reference Standards maintained by the National Bureau of Standards.

Honeywell Thomas ohm mod 1190 s/n M2644 NBS# 211723
Guildline Instrument mod 9152T4 s/n 35353 NBS# 212530
Holt 6A s/n 180 AC Voltage Test No. 201944
Fluke 207-5B s/n 454 Test No. NAA Frequency Emissions
Fluke A-50 s/n 2122 Test No. 3087-969

Calibration date: 12-11-75 Calibration Data Enclosed Yes ☐ No ☐

Temperature: 73 °F.

Humidity: 40 % R.H.

By: [signature]

Approved: ____________
Metrology Service Manager

Springfield, Virginia Branch

Metrology Services Group
Test Instruments Division
Honeywell Inc.

EPLAB

THE EPPLEY LABORATORY, INC.
SCIENTIFIC INSTRUMENTS
NEWPORT, R I. 02840 U.S A.

STANDARDIZATION
OF
EPPLEY PRECISION PYRANOMETER

(horizontal surface receiver-180° twin hemisphere)

Model PSP Serial Number 13433F3 Resistance 590 ohm at 24 °C

Temperature Compensation

Range -20 to + 40 °C

This radiometer has been compared with the Eppley group of reference standards. under radiation intensities of about 700 watts $meter^{-2}$ (roughly one-half a solar constant), the adopted calibration temperature is 25 °C.

As a result of a series of comparisons, it has been found to develop an emf of.

10.56×10^{-6} volts/watt $meter^{-2}$

7.36 millivolts/cal cm^{-2} min^{-1}

The calculation of this constant is based on the fact that the relationship between radiation intensity and emf is rectilinear to intensities of 1400 watts . $meter^{-2}$. This pyranometer is linear to within ± 0.5 percent up to this intensity.

The calibration was made with both hemispheres of Schott WG295 (clear) glass. This value should be *increased* for other Schott hemispheres as follows: GG400 = 0.0 %, OG530 = 0.5%, RG610 = 1.5% and RG695 = 2 0%

According to present accepted practice. this Eppley Pyranometer has been standardized with reference to the International Pyrheliometric Scale 1956.

Useful conversion facts: 1 cal-cm^{-2} min^{-1} = 697.3 watts/$meter^2$
1 BTU/ft^2-hr^{-1} = 3.153 watts/$meter^2$

Date of Test: March 17, 1976

IN CHARGE OF TEST
Richard H. Hatch

The Eppley Laboratory, Inc.

By: [signature]

S. O. 33068

Newport, R. I.

Date March 19, 1976

Shipped to: Mitre Corporation
McLean, Virginia

Remarks:

APPENDIX III

SOLAR PANEL/MODULE

ORIGINAL DATA AND CURVES

More than 200 Solar Panel and Module I-V curves were recorded in the course of this program. Only one set of curves for a full panel and its eight constituent modules is shown here.

SOLAR PANEL/MODULE DATA SHEET

DATE 7/19/76 GRAPH NO. 0158

PANEL NO. 15 MODULE NO. 1

RECORDER ZERO SET: HORIZ. [✓] VERT. [ ] (CHECK ✓)

CALIBRATE SCALE: HORIZ. [✓] VERT. [ ] (CHECK ✓)

PYRANOMETER READING: 9.65 mv.

VOC: 14.82 volts

PANEL TEMP: 7.59 K-ohms

TIME OF DAY: 11:51 hours

ISC: 4.45 mv.

PYRANOMETER READING: 9.73 mv.

STD. CELL 1 : 53.9 mv.

STD. CELL 2: 53.1 mv.

STD. CELL 3: 53.2 mv.

STD. CELL 4: ______ mv.

STD. CELL 5: ______ mv.

STD. CELL TEMP: 19.30 K-ohms

DIFFUSE ILLUM: 1.97 mv.

REMARKS: ______

OPERATOR: [signature]

OBSERVER: ______ AGENCY: ______

HEWLETT-PACKARD 9270-1006

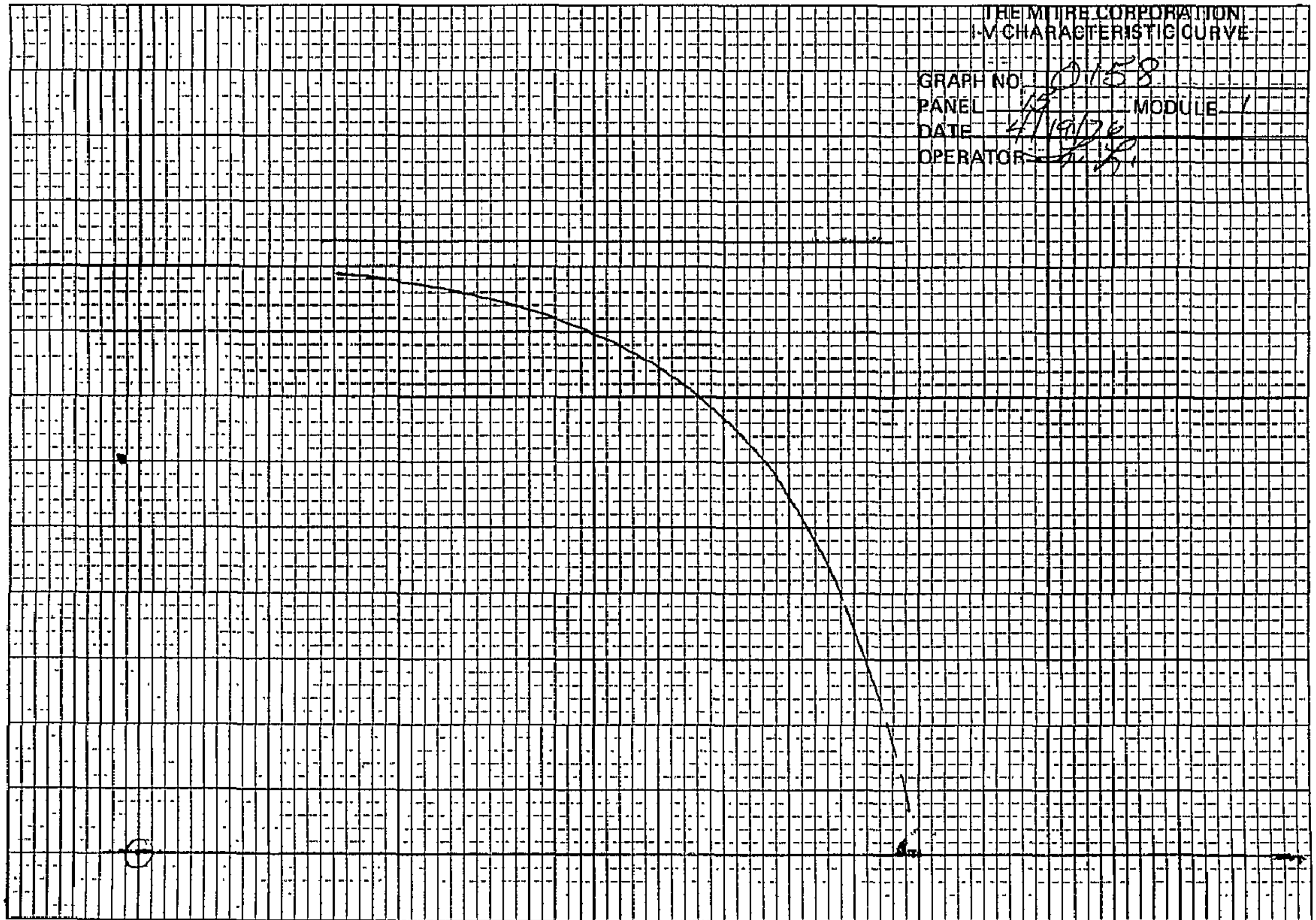

CURRENT (0.1A. /INCH)

VOLTAGE (2.5V. /INCH)

SOLAR PANEL/MODULE DATA SHEET

DATE 4/19/76 GRAPH NO. 0159

PANEL NO. 15 MODULE NO. 2

RECORDER ZERO SET: HORIZ. [✓] VERT. [✓] (CHECK ✓)

CALIBRATE SCALE: HORIZ. [ ] VERT. [✓] (CHECK ✓)

PYRANOMETER READING: 9.63 mv.

VOC: 14.90 volts

PANEL TEMP: 7.50 K-ohms

TIME OF DAY: 11.53 hours

ISC: 4.44 mv.

PYRANOMETER READING: 9.70 mv.

STD. CELL 1 : 53.7 mv.

STD. CELL 2: 52.9 mv.

STD. CELL 3: 53.0 mv.

STD. CELL 4: ______ mv.

STD. CELL 5: ______ mv.

STD. CELL TEMP: 14.93 K-ohms

DIFFUSE ILLUM: 1.98 mv.

REMARKS: ______

OPERATOR: DMH

OBSERVER: ______ AGENCY: ______

HEWLETT-PACKARD 9270 1006

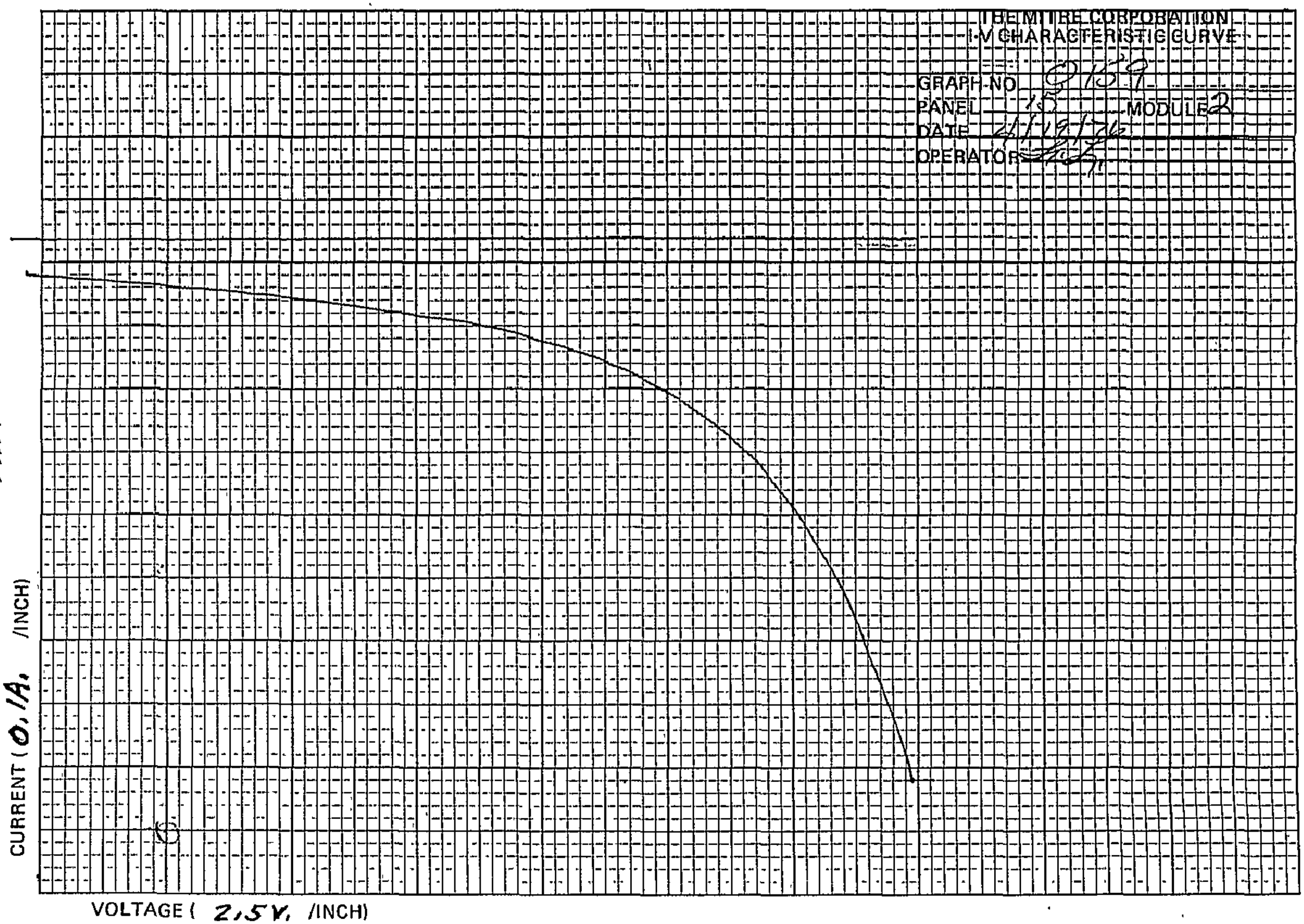

SOLAR PANEL/MODULE DATA SHEET

DATE 9/19/76 GRAPH NO. 0160

PANEL NO. 15 MODULE NO. 3

RECORDER ZERO SET: HORIZ. [✓] VERT. [ ] (CHECK ✓)

CALIBRATE SCALE: HORIZ. [ ] VERT. [ ] (CHECK ✓)

PYRANOMETER READING: 9.62 mv.

VOC: 14.87 volts

PANEL TEMP: 7.50 K-ohms

TIME OF DAY: 11.54 hours

ISC: 4.47 mv.

PYRANOMETER READING: 9.66 mv.

STD. CELL 1 : 54.0 mv.

STD. CELL 2: 53.1 mv.

STD. CELL 3: 53.3 mv.

STD. CELL 4: mv.

STD. CELL 5: mv.

STD. CELL TEMP: 19.0 K-ohms

DIFFUSE ILLUM: 1.99 mv.

REMARKS:

OPERATOR: [signature]

OBSERVER: AGENCY:

HEWLETT-PACKARD 9270 1006

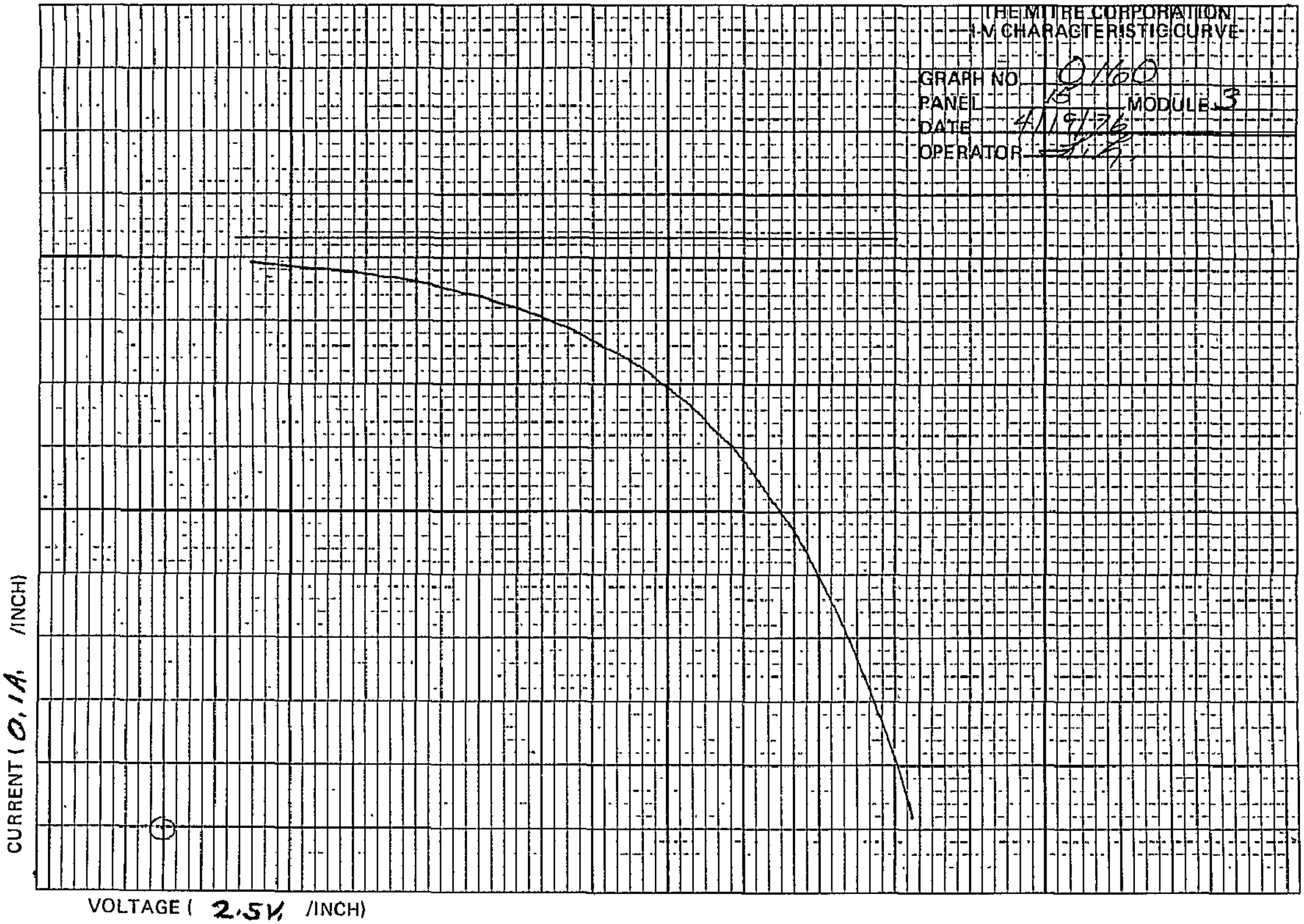

SOLAR PANEL/MODULE DATA SHEET

DATE 4/19/76 GRAPH NO. 0161

PANEL NO. 15 MODULE NO. 4

RECORDER ZERO SET: HORIZ. [✓] VERT. [✓] (CHECK ✓)

CALIBRATE SCALE: HORIZ. [ ] VERT. [✓] (CHECK ✓)

PYRANOMETER READING: 9.65 mv.

VOC: 14.9 volts

PANEL TEMP: 7.42 K-ohms

TIME OF DAY: 11:55 hours

ISC: 4.49 mv.

PYRANOMETER READING: 9.69 mv.

STD. CELL 1 : 54.1 mv.

STD. CELL 2: 53.2 mv.

STD. CELL 3: 53.4 mv.

STD. CELL 4: ______ mv.

STD. CELL 5: ______ mv.

STD. CELL TEMP: 18.1 K-ohms

DIFFUSE ILLUM: 1.99 mv.

REMARKS: ______

OPERATOR: [signature]

OBSERVER: ______ AGENCY: ______

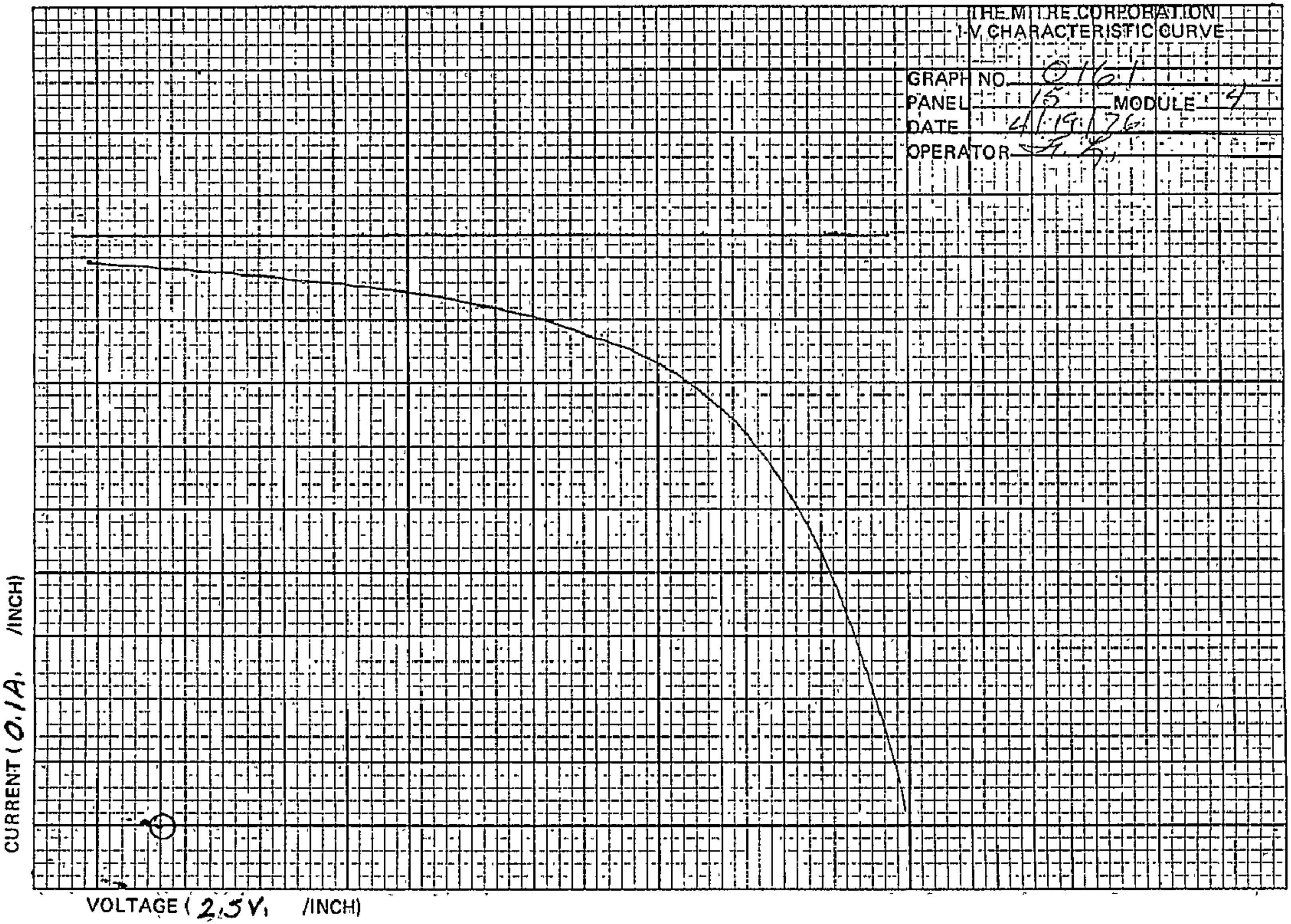
THE MITRE CORPORATION
I-V CHARACTERISTIC CURVE
GRAPH NO. 0161
PANEL 15
MODULE 4
DATE 4/19/76
OPERATOR
CURRENT (0.1A. /INCH)
VOLTAGE (2.5V. /INCH)

SOLAR PANEL/MODULE DATA SHEET

DATE 4/19/76 GRAPH NO. 0162

PANEL NO. 15 MODULE NO. 5

RECORDER ZERO SET: HORIZ. ✓ VERT. ✓ (CHECK ✓)

CALIBRATE SCALE: HORIZ. ☐ VERT. ✓ (CHECK ✓)

PYRANOMETER READING: 9.68 mv.

VOC: 14.9 volts

PANEL TEMP: 7.28 K-ohms

TIME OF DAY: 11.56 hours

ISC: 4.35 mv.

PYRANOMETER READING: 9.70 mv.

STD. CELL 1 : 54.2 mv.

STD. CELL 2: 53.4 mv.

STD. CELL 3: 53.5 mv.

STD. CELL 4: ______ mv.

STD. CELL 5: ______ mv.

STD. CELL TEMP: 18.7 K-ohms

DIFFUSE ILLUM: 1.99 mv.

REMARKS: ______

OPERATOR: TMH

OBSERVER: ______ AGENCY: ______

HEWLETT-PACKARD 9270 1006

A-III.12

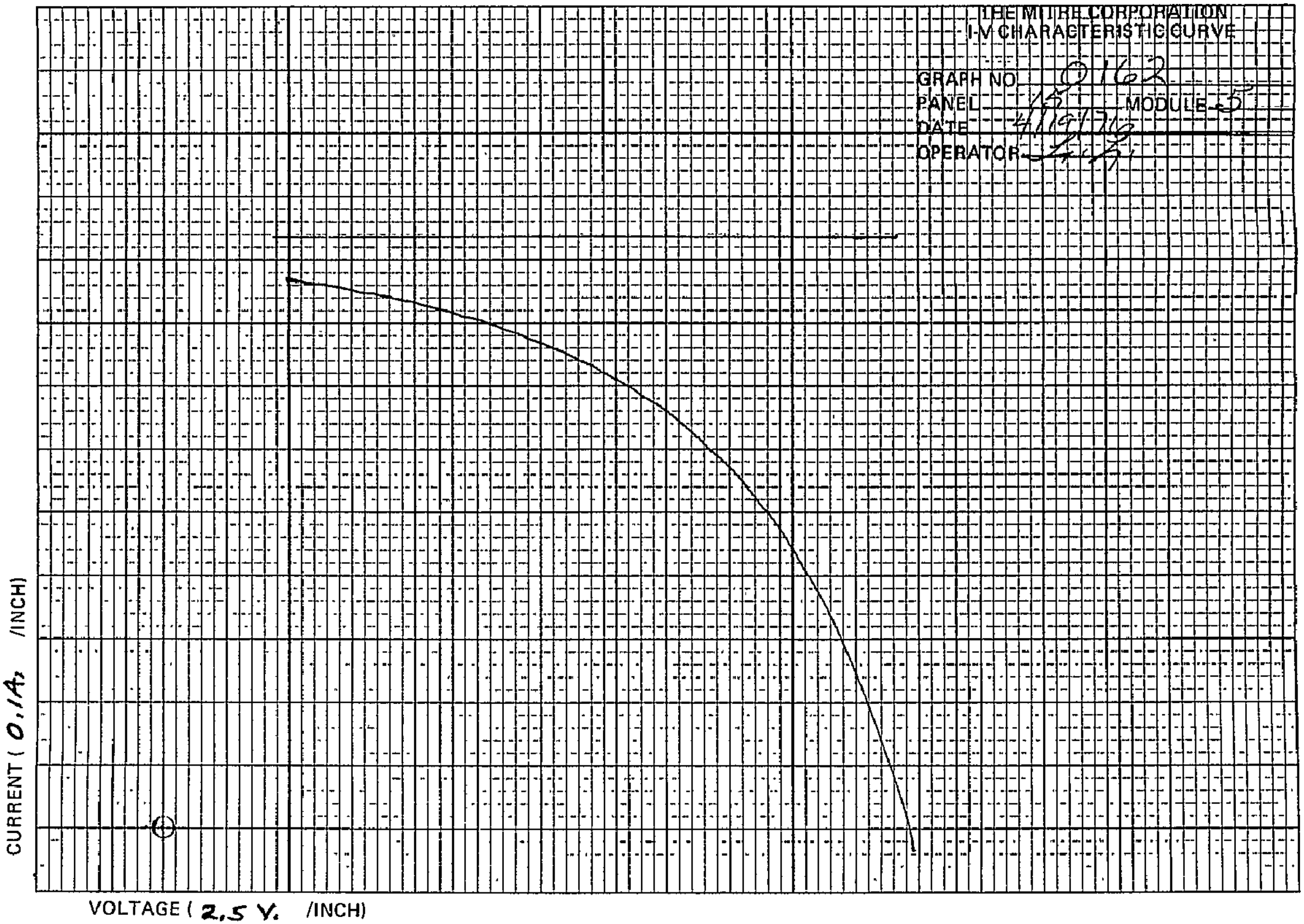

SOLAR PANEL/MODULE DATA SHEET

DATE 4/19/76 GRAPH NO. 0163

PANEL NO. 15 MODULE NO. 6

RECORDER ZERO SET: HORIZ. [✓] VERT. [✓] (CHECK ✓)

CALIBRATE SCALE: HORIZ. [ ] VERT. [/] (CHECK ✓)

PYRANOMETER READING: 9.63 mv.

VOC: 14.77 volts

PANEL TEMP: 7.21 K-ohms

TIME OF DAY: 11.58 hours

ISC: 4.32 mv.

PYRANOMETER READING: 9.62 mv.

STD. CELL 1 : 53.8 mv.

STD. CELL 2: 52.9 mv.

STD. CELL 3: 53.0 mv.

STD. CELL 4: ______ mv.

STD. CELL 5: ______ mv.

STD. CELL TEMP: 18.4 K-ohms

DIFFUSE ILLUM: 1.99 mv.

REMARKS: ______

OPERATOR: Jm H

OBSERVER: ______ AGENCY: ______

HEWLETT-PACKARD 9270 1006

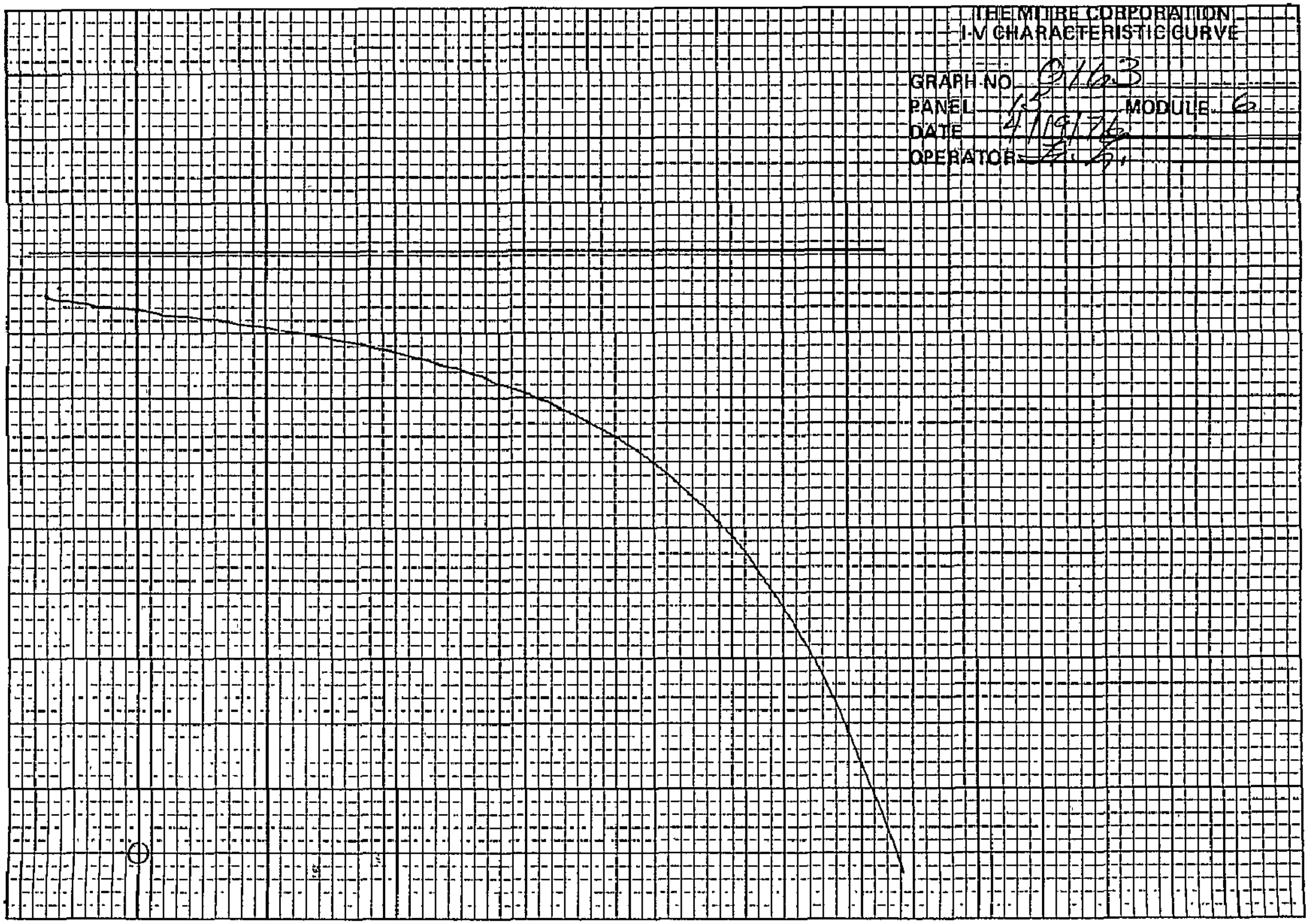

CURRENT (0.1A. /INCH)

VOLTAGE (2.5 V. /INCH)

SOLAR PANEL/MODULE DATA SHEET

DATE 4/19/76 GRAPH NO. 0164

PANEL NO. 15 MODULE NO. 2

RECORDER ZERO SET: HORIZ. ✓ VERT. ✓ (CHECK ✓)

CALIBRATE SCALE: HORIZ. ☐ VERT. ☐ (CHECK ✓)

PYRANOMETER READING: 9.57 mv.

VOC: 14.58 volts

PANEL TEMP: 7.32 K-ohms

TIME OF DAY: 11.59 hours

ISC: 3.95 mv.

PYRANOMETER READING: 9.56 mv.

STD. CELL 1 : 53.5 mv.

STD. CELL 2: 52.7 mv.

STD. CELL 3: 52.7 mv.

STD. CELL 4: ______ mv.

STD. CELL 5: ______ mv.

STD. CELL TEMP: 18.3 K-ohms

DIFFUSE ILLUM: 1.99 mv.

REMARKS: ______

OPERATOR: [signature]

OBSERVER: ______ AGENCY: ______

HEWLETT-PACKARD 9270-1006

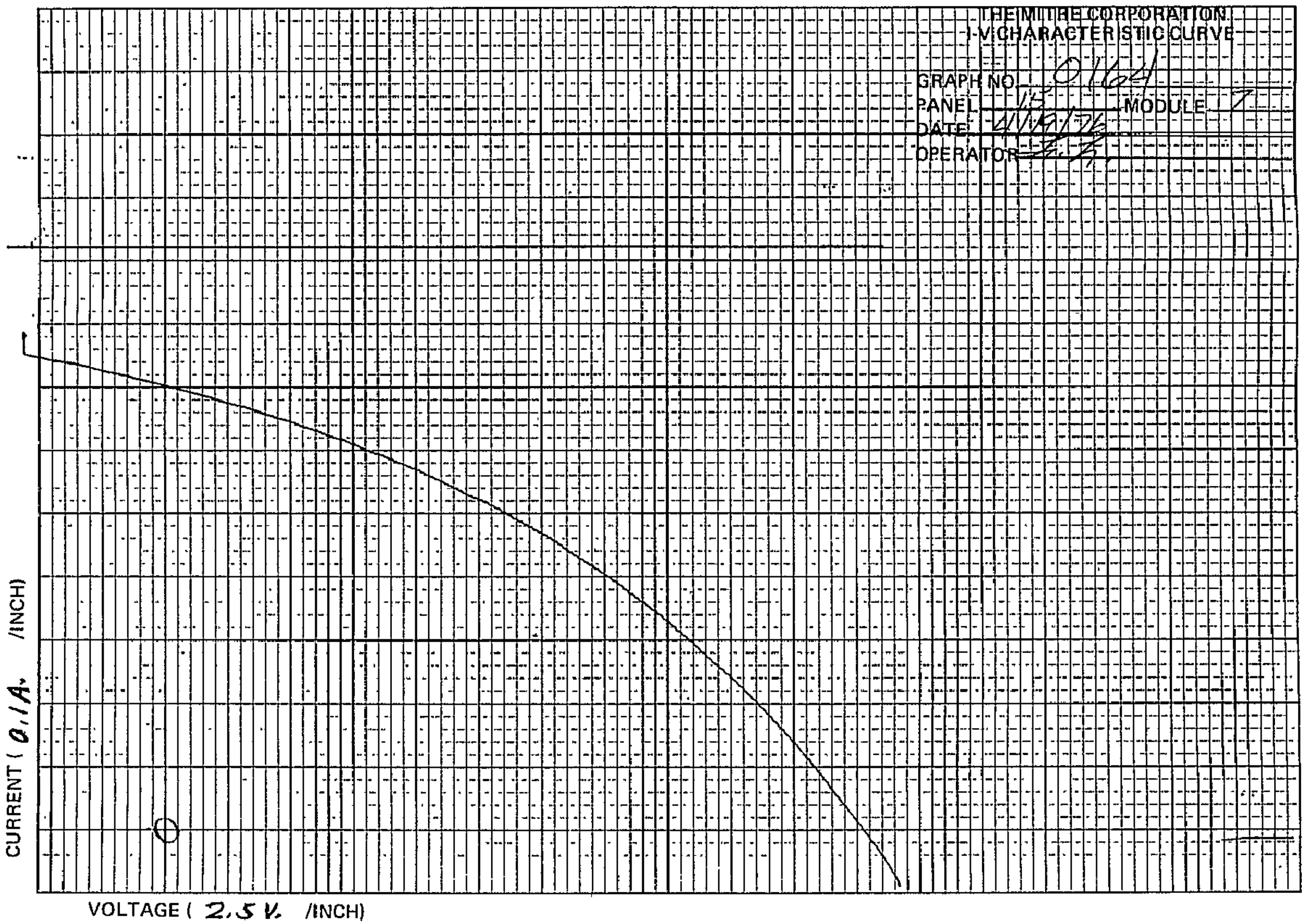

SOLAR PANEL/MODULE DATA SHEET

DATE 4/19/76 GRAPH NO. 0165

PANEL NO. 15 MODULE NO. 8

RECORDER ZERO SET: HORIZ. [✓] VERT. [✓] (CHECK ✓)

CALIBRATE SCALE: HORIZ. [ ] VERT. [ ] (CHECK ✓)

PYRANOMETER READING: 9.51 mv.

VOC: 15.02 volts

PANEL TEMP: 7.39 K-ohms

TIME OF DAY: 12:00 hours

ISC: 3.94 mv.

PYRANOMETER READING: 9.50 mv.

STD. CELL 1 : 53.8 mv.

STD. CELL 2: 53.2 mv.

STD. CELL 3: 53.5 mv.

STD. CELL 4: ______ mv.

STD. CELL 5: ______ mv.

STD. CELL TEMP: 18.3 K-ohms

DIFFUSE ILLUM: 2.00 mv.

REMARKS: ______

OPERATOR: [signature]

OBSERVER: ______ AGENCY: ______

HEWLETT-PACKARD 9270 1006

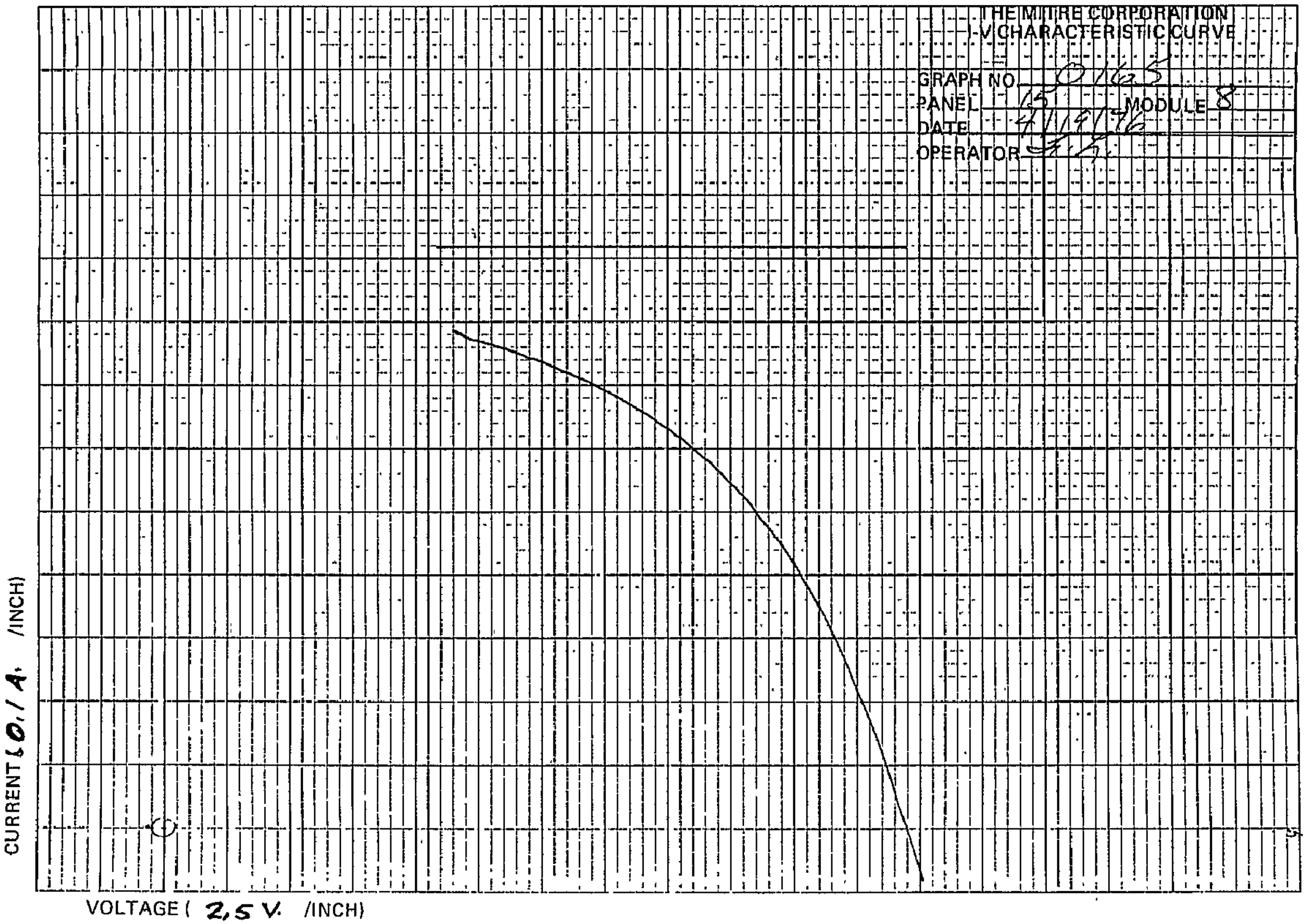

SOLAR PANEL/MODULE DATA SHEET

DATE 4/19/76 GRAPH NO. 0166

PANEL NO. 15 MODULE NO. Full

RECORDER ZERO SET: HORIZ. ✓ VERT. ✓ (CHECK ✓)

CALIBRATE SCALE: HORIZ. ✓ VERT. ✓ (CHECK ✓)

PYRANOMETER READING: 9.41 mv.

VOC: 29.54 volts

PANEL TEMP: 2.34 K-ohms

TIME OF DAY: 12:03 hours

ISC: 8.45 mv.

PYRANOMETER READING: 9.43 mv.

STD. CELL 1 : 52.9 mv.

STD. CELL 2: 52.2 mv.

STD. CELL 3: 52.2 mv.

STD. CELL 4: ____ mv.

STD. CELL 5: - — mv.

STD. CELL TEMP: 18.2 K-ohms

DIFFUSE ILLUM: 1.99 mv.

REMARKS:

OPERATOR: [signature]

OBSERVER: AGENCY:

HEWLETT PACKARD 9270-1006

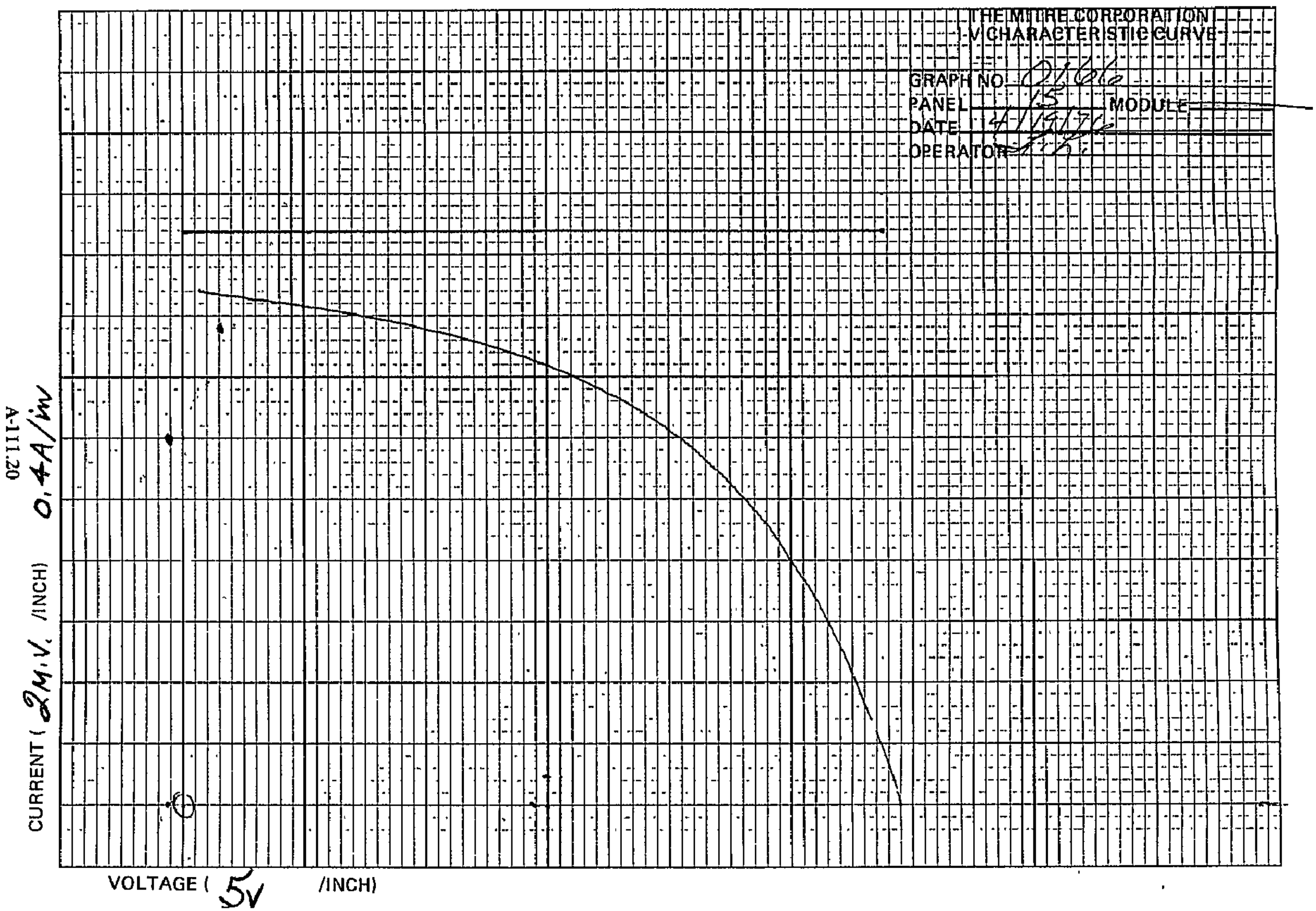

DISTRIBUTION

D-10

C. A. Zraket

D-12

H. D. Benington
C. C. Grandy
S. Keeny
A. Tachmindji

W-50

F. Eldridge
R. S. Greeley
G. M. Haas
R. P. Ouellette
K. Stetten

W-51

R. Pikul
J. Pfeffer

W-52

G. Bennington
D. Blake
A. Cherdak
E. Friedman
S. Goldstein
R. Inman
A. Johnson
M. Scholl
E. Ward

W-53

G. Erskine
J. W. Overbey III
V. Wenk

W-54

J. Golden
S. Lubore
L. Thomas

W-55

E. G. Sharp
J. T. Stone
N. Coates

W-33

F. Lempicki

Document Control
Washington Library
Bedford Library
W-50 Library (10)

EXTERNAL DISTRIBUTION

Mr. Lloyd V. Risley
Vice-President-Engineering
ECO-ENERGY SYSTEMS, INC.
415 South Main Street
Box 852
Clarendon, Texas 79226

Commander/USAMERDC
Attn: S.T.S. FB-EA (Dr. Faehn
Fort Belvoir, Va. 22060

Ms. Leona Laughlin
MIT
Lincoln Laboratory
244 Wood Street
Lexington, Mass. 02173

H. J. Speikers
2416 East 15th Avenue
North St. Paul, Minnesota 55109

Dr. Nicolas A. Carbel
UNIVERSIDAD PROVINCIAL DE LA RIOJA
Instituto De Zonas Aridas (IZA)
Chamical
La Rioja-Republica Argentina

Lockheed/Huntsville
Attn: Mr. Sears
Box 1103
Hunt, Alabama 35807

Roger Little
SIMULATION PHYSICS, INC.
41 B Street
Burlington, Mass. 01803

Anthony Eden, Captain, USAF
Project Officer,
USAFA Solar Energy Program
Department of the Air Force
Department of Civil Engineering
Engineering Mechanics, and Materials
USAF Academy, Colorado 80840

Mr. E. L. Hamm
(P.C.D.E.)
Gneral Services Administration
Washington, D. C. 20405

Mr. J. W. Yerkes
Solar Technology Inc.,
9701 Lurline Street
Chatsworth, California 91311

Dr. John Kolyer
Autonetics Division
Rockwell International
P. O. Box 4192 GA 25
Anaheim, California 92803

Ft. Belvoir
Electrochemical Division
Building 327
MERDC
Ft. Belvoir, Va. 22060

Robert Schacher
8 Harding Drive
Rye, New York 10580

Mr. John E. Lawrence
SILICON MATERIAL, INC.
341 Moffell Blvd.,
Mountain View, CA 94043

Mr. N. Steere
HOST SYSTEM, INC.
4105 Duke Street
Alexandria, Va. 22304

Mr. Larry A. Mertens
Communications Engineer
DEPARTMENT OF GENERAL SERVICES
Communications Division
2025 19th Street
Sacramento, California 95818

Dr. John D. Meakin
Associate Director
UNIVERSITY OF DELAWARE
Newark, Delaware 19711

Mr. Earl W. Kazis
General Solar Power Company
99 Park Avenue
New York, N. Y. 10016

Mr. Kenneth Williams
U. S. Coast Guard
Research and Development Center
Avery Point
Groton, Connecticut 06340

Dr. R. Minder
% ELECTROWATT ENGINEERING SERVICES, LTD.
Zurich Bellerivestrasse 36
Switzerland

Mr. E. J. Rattin
Staff Engineer
Energy Programs
The Aerospace Corporation
Post Office Bovd 92957
Los Angeles, California 90009

Mr. Milton Meckler, P. E.
President
THE ENERGY GROUP CONSULTANTS
10000 Santa Monica Blvd.,
Suite 300
Los Angeles, California 90067

Professor T. L. Chu
Southern Methodist University
Institute of Technology
Electrical Engineering Department
Dallas, Texas 75275

Mr. Jack Eckert
EXXON RESEARCH
ERC-1-3008
Linden Avenue
Linden, New Jersey 07036

Mr. Richard Forman
National Bureau of Standards
Solid State Materials Section
A259 Materials Building
Washington, D. C. 20234

Mr. Ales F. Fort
National Research Council of Canada
Division of Physics
Montreal Road, Ottawa
Ontario, Canada KIA OR 6

Mr. Neal F. Shepard, Jr.
General Electric Co.,
Space Division
528 Elliott Drive
King of Prussia, Pa. 19406

Mr. E. A. Shirland
Westinghouse Research Lab
Churchill Boro
Pittsburgh, PA 15235

Mr. Richard L. Statler
Naval Research Lab
Code 6623
Washington, D. C. 20375

Mr. E. L. Ralph
SPECTROLAB, INC.
12484 Gladstone
Sylmar, CA 91342

P.V.S. Rao
Motorola, Inc.
Mail Drop A112
5005 E. McDowell Road
Phoenix, AZ 85062

Mr. Hans S. Rauschenbach
TRW Systems
3620 Michelle Drive
Torrance, CA 90503

Mr. Robert K. Riel
Westinghouse Research Labs
Pittsburgh, Pa. 15235

Mr. Allen Rothwarf
Institute of Energy Conversion
University of Delaware
Newark, DE 19711

Mr. Ray S. Miller
Rockwell International
Space Division, Mail Code SL10
12214 Lakewood Blvd.,
Downey, CA 90241

Dr. A. I. Mlavsky
Mobil-Tyco Solar Energy Corp.,
16 Hickory Drive
Waltham, MA 02154

Dr. Tapan Mukherjee
National Science Foundation
Rann/Aert
1800 G Street, N. W.
Washington, D. C. 20550

Mr. Harry (Don) Nelson
US Coast Guard
R&D
US Coast Guard (G=EDE-4/61)
Washington, D. C. 20590

Dr. W. Palz
CNES
129 Rue De L'Universite
Paris, France

Mr. Stanley L. Leonard
The Aerospace Corp.
P. O. Box 92957
Los Angeles, CA 90009

I. A. Lesk
Motorola, Inc.
Corporate Research Lab
4039 E. Raymond Street
Phoenix, AZ 85040

Dr. M. A. Lind
National Bureau of Standards
Washington, D. C. 20234

Dr. Joseph J. Loferski
Division of Engineering
Brown University
Providence, RI 02912

Cdr. Lloyd R. Lomer
U. S. Coast Guard
Commandant USCG
(G-DET-2)
USCG Headquarters
Washington, D. C. 20590

Mr. Dan R. Lott
Lockheed Missiles & Space
Company
978 Pinewood Drive
San Jose, CA 95129

Mr. Werner Luft
TRW Systems
One Space Park
Redondo Beach, CA 90278

Mr. John McCristall
Optical Coast
Laboratory, Inc.
Photoelectronics Group
15251 East Don Julian Road
City of Industry, CA 91746

Mr. Harold Weinstein
Sensor Technology
21012 Lassen Street
Chatsworth, CA 91311

Dr. Ronald Wichner
Lawrence Livermore Lab
7000 East Avenue
Livermore, CA 94707

Dr. Martin Wolf
Univ. of PA
260 Towne Bldg.,
Philadelphia, PA 19174

Mr. J. M. Woulbroun
Owens-Illinois, Inc.
P. O. Box 1035
Toledo, OH 43666

Dr. Solomon Zwerdling
Director of Solar Energy
Programs
Argonne National Lab
Bldg., 362-C185
9700 South Cass Avenue
Argonne, Illinois 60439

Mr. Edward L. Burgess
SANDIA LABS
Albuquerque, N. M. 87115

Mr. Marshall Cannady
TRW Systems
One Space Park, MI/1406
Redondo Beach, CA 90278

Mr. Ernst M. Cohn
NASA
Code RPP
Washington, D. C. 20546

Mr. Donald A. Corbett
TRW Systems Group
One Space Park
Redondo Beach, CA 90278

Steven F. Di Zio
SES, Inc.
70 S. Chapel St.,
Newark, DEL. 19711

Mr. Alfred E. Austin
Battelle Columbus Laboratories
505 King Avenue
Columbus, Ohio 43201

Mr. Terry L. Babineaux
Optical Coating Laboratory, Inc.
P. O. Box 1599
Santa Rosa, CA 95403

<u>EXTERNAL DISTRIBUTION CONTINUED</u>

Mr. Douglas Rusta
TRW, INC.
1 Space Park
Redondo Beach, California

Mr. Leo Pessin
Fairchild Industries
Germantown, Md.

Mr. Frank Hornbuckle
Fairchild Industries
Germantown, Md.

Mr. Albert Smith
CML Satellite
1750 K St., N. W.
Washington, D. C. 20006

Dr. John F. Halldane
Senior Physical Scientist
Federal Energy Administration
Federal Building
Room 7413
Washington, D. C. 20461

Mr. Scott Peters
Atomic Industrial Forum
1747 Pennsylvania Ave., N.W.
Washington, D. C. 20006

Mr. David Fox
103 West 75th Street
New York, New York 10023

Mr. R. Williams
USAMERDC
Building 399
Room 133
Fort Belvoir, Va.

Dr. J. Bond
USAMERDC
Building 326
Room 4
Fort Belvoir, Va.

Mr. Leonard Wojton
Apartment #B1
University of Pittsburgh at Johnstown
Johnstown, Pa. 15907

Ms. Peggy Maas
Electronics
1221 Avenue of Americas
New York, N. Y. 10020

Mr. S. Derman
% Electronic Design Magazine
50 Essex
Rochelle Park, New Jersey 07662

Energy, Research Development
Administration
Attn: Dr. L. Magid
Washington, D. C. 20545

Commander/USA MERDC
Attn: S. T. S. FB-EA (Dr. Jokl)
Fort Belvoir, Va. 22060

Dr. J. Lindmeyer
President
THE SOLAREX CORPORATION
1335 Piccard Drive
Rockville, Maryland 20850

Energy Research & Development
Administration
Attn: Dr. M. Prince
Washington, D. C. 20545

Congressman Mike Gravel
Senate Office Building
Room 33
17 Dirkson
Washington, D. C. 20510

Congressman Mike McCormick
House Office Building
1503 Longworth
Washington, D. C. 20515

Mr. Arthur B. Greenberg
Aerospace Corporation
P. O. Box 92957
Los Angeles, California 90009

Mr. John F. Jordan
D. H. Baldwin Co.,
1820 Mills Avenue
El Paso, Texas 79901

EXTERNAL DISTRIBUTION CONCLUDED

Mr. Charles E. Backus
Arizona State University
Tempe, Arizona 85281

Mr. Bill Bailey
MOTOROLA
10234 N. 59th Place
Scottsdale, Arizona 85253

F. T. C. Bartels
Spectrolab
12500 Gladstone Avenue
Sylmar, CA 91342

Mr. John R. Barton
BOEING
14666 S. E. 173rd
Renton, WASH 98055

Mr. John Vincent
1917 North Hills Drive
Raleigh, N. C. 27612

Mr. S. Bloom
6433 King Louis Drive
Alexandria, VA 22312